UNIVERSIDAD POLITÉCNICA DE MADRID

ESCUELA TÉCNICA SUPERIOR DE INGENIEROS AGRÓNOMOS

DEPARTAMENTO DE BIOTECNOLOGÍA-BIOLOGÍA VEGETAL

TESIS DOCTORAL

PATRONES Y PROCESOS ESPACIALES EN POBLACIONES Y COMUNIDADES VEGETALES: NUEVAS HERRAMIENTAS E HIPÓTESIS

Autor: Pablo Ancelmo Ramón Contento[1].

Directores: **Dr. Marcelino De la Cruz Rot[2].** Doctor en Ciencias Biológicas

Dr. Miguel Ángel de Zavala Gironés[3]. Doctor en Ecología y Biología Evolutiva

[1]Departamento de Ciencias Naturales, Universidad Técnica Particular de Loja. Ecuador.

[2]Departamento de Biotecnología-Biología. Universidad Politécnica de Madrid. España.

[3]Departamento de Ciencias de la Vida. Universidad de Alcalá de Henares. España.

Madrid, 2015

Marcelino de la Cruz Rot, Profesor titular de Universidad del Departamento de Biotecnología-Biología Vegetal de la Universidad Politécnica de Madrid y Miguel Ángel de Zavala Gironés, Profesor Titular de Universidad del Departamento de Ciencias de la Vida de la Universidad de Alcalá de Henares

CERTIFICAN:

Que los trabajos de investigación desarrollados en la memoria de la tesis doctoral: **"Patrones y procesos espaciales en poblaciones y comunidades vegetales: nuevas herramientas e hipótesis",** son aptos para ser presentados por el Matemático Pablo Ancelmo Ramón Contento ante el tribunal que en su dia se consigne, para aspirar al Grado de Doctor por la Universidad Politécnica de Madrid.

Vo.Bo. Director de Tesis

Dr. Marcelino de la Cruz Rot

VoBo Co-Director de Tesis

Dr. Miguel Ángel de Zavala Gironés

UNIVERSIDAD POLITECNICA DE MADRID

Tribunal nombrado por el Mgfco. y Exmo. Sr. Rector de la Universidad Politécnica de Madrid, el día ……. de …….2013.

Presidente: ……..

Secretario: ……..

Vocal: ……

Vocal: ……

Vocal: ……

Suplente: ……

Suplente: ……

Realizado el acto de defensa y lectura de Tesis el día …….……de ……...de 2013 en la E.T.S.I. Ingenieros Agrónomos.

Calificación ……..

……..
EL PRESIDENTE

……..
LOS VOCALES

…….

EL SECRETARIO

A mi esposa y a mis hijos.

AGRADECIMIENTOS

Primero me gustaría agradecer a Dios por permitirme alcanzar los proyectos que me he propuesto en la vida. A Cecilia mi esposa y mis queridos hijos Pablo, Andrés, Ma. Daniela, Ma. Cecilia, José Ignacio y Ana Paula, así como a mi madre Inés por el apoyo incondicional e invaluable, y por los sacrificios que han hecho para que yo realice mis estudios; y otros familiares que han sido soporte importantísimo para conseguir esta meta.

Mi agradecimiento especial al Dr. Marcelino de la Cruz y al Dr. Miguel Angel de Zavala, director y co-director de tesis respectivamente; quienes me han dado el apoyo académico necesario para llevar a cabo este trabajo, ya sea de forma presencial como a distancia. Gracias Marcelino por tanta paciencia para responder las innumerables preguntas sobre R.

A las personas que me ayudaron a obtener los datos para realizar esta investigación. A Miguel Angel e Ignacio Zavala por facilitarme los datos utilizados para el desarrollo del Capítulo 1; a Omar Cabrera, Ana Arévalo, Israel Guitierrez y Ronny Luzuriaga por el arduo trabajo de campo realizado en el matorral seco, datos que se utilizaron en el Capítulo 2; al soporte otorgado por Center for Tropical Forest Science of the Smithsonian Tropical Research Institute y los servicios de agencias primarias que han otorgado el apoyo para la conceción de la parcela permanente BCI, quienes me facilitaron los datos del cuarto censo, que han servido para el desarrollo de los Capítulos 3 y 4.

Al P. Dr. Luis Miguel Romero, ex-rector de la Universidad Técnica Particular de Loja, y al Dr. César Pérez, coordinador del programa de doctorado en la UPM, que gracias a su proyecto de formación de doctores en tiempo compartido, se hizo realidad este sueño.

A mis compañeros del Departamento de Ciencias Naturales, sección de Ecología y Sistemática, quienes me brindaron el apoyo oportuno fundamentalmente durante mis estancias en la Universidad Politécnica de Madrid.

La realización de esta tesis fue apoyada parcialmente por los proyectos A/024796/09 y A/030244/10 de la Agencia Española de Cooperación Internacional y para el Desarrollo

(AECID) y el proyecto Islas-Espacio CGL2009-13190-C03-02 del Ministerio de Ciencia e Innovación.

Pablo Ramón C.

INDICE GENERAL

RESUMEN

Generalmente los patrones espaciales de puntos en ecología, se definen en el espacio bi-dimensional, donde cada punto representado por el par ordenado (x,y), resume la ubicación espacial de una planta. La importancia de los patrones espaciales de plantas radica en que proceden como respuesta ante importantes procesos ecológicos asociados a la estructura de una población o comunidad. Tales procesos incluyen fenómenos como la dispersión de semillas, la competencia por recursos, la facilitación, respuesta de las plantas ante algún tipo de estrés, entre otros.

En esta tesis se evalúan los factores y potenciales procesos subyacentes, que explican los patrones de distribución espacial de la biodiversidad vegetal en diferentes ecosistemas como bosque mediterráneo, bosque tropical y matorral seco tropical; haciendo uso de nuevas metodologías para comprobar hipótesis relacionadas a los procesos espaciales. En este trabajo se utilizaron dos niveles ecológicos para analizar los procesos espaciales, el nivel de población y el nivel de comunidad, con el fin de evaluar la importancia relativa de las interacciones intraespecíficas e interespecíficas.

Me centré en el uso de funciones estadísticas que resumen los patrones de puntos para explorar y hacer inferencias a partir de datos espaciales, empezando con la construcción de un nuevo modelo nulo para inferir variantes del síndrome de dispersión de una planta parásita en España central. Se analizó la dependencia de los patrones espaciales tanto de los hospedantes afectados como de los no-afectados y se observó fuerte dependencia a pequeña y mediana distancia. Se utilizaron dos funciones (kernel) para simular la dispersión de la especie parásita y se identificó consistencia de estos modelos con otros síndromes de dispersión adicionalmente a la autodispersión. Un segundo tema consistió en desarrollar un método ANOVA de dos vías? para patrones de puntos replicados donde el interés se concentró en evaluar la interacción de dos factores. Este método se aplicó a un caso de estudio que consitió en analizar la influencia de la topografía y la altitud sobre el patrón espacial de un arbusto dominante en matorral seco al sur del Ecuador, cuyos datos provienen de patrones de puntos replicados basados en diseño. Partiendo de una metodología desarrollada para procesos uni-factoriales, se construyó el método para procesos bi-factoriales y así poder evaluar el efecto de interacción. Se observó que la topografía por sí sola así como la interacción con la altitud presentaron efecto significativo sobre la formación del patrón espacial. Un tercer tema fue identificar la relación entre el patrón espacial y el síndrome de dispersión de la comunidad vegetal en el bosque tropical de la Isla de Barro Colorado (BCI), Panamá. Muchos estudios se han desarrollado en este bosque tropical y algunos han analizado la relación síndrome-patrón espacial, sin embargo lo novedoso de nuestro estudio es que se evaluaron un conjunto amplio de modelos (114 modelos)

basados en procesos que incorporan la limitación de la dispersión y la heterogeneidad ambiental, y evalúan el efecto único y el efecto conjunto, para posteriormente seleccionar el modelo de mejor ajuste para cada especie. Más de la mitad de las especies presentaron patrón espacial consistente con el efecto conjutno de la limitación de la dispersión y heterogeneidad ambiental y el porcentaje restante de especies reveló en forma equitativa el efecto único de la heterogeneidad ambiental y efecto único de limitación de la dispersión. Finalmente, con la misma información del bosque tropical de BCI, y para entender las relaciones que subyacen para mantener el equilibrio de la biodiversidad, se desarrolló un índice de dispersión funcional local a nivel de individuo, que permita relacionar el patrón espacial con cuatro rasgos funcionales clave de las especies. Pese a que muchos estudios realizados involucran esta comunidad con la teoría neutral, se encontró que el ensamble de la comunidad de BCI está afectado por limitaciones de similaridad y de hábitat a diferentes escalas.

ABSTRACT

Overall the spatial point patterns in ecology are defined in two-dimensional space, where each point denoted by the (x,y) ordered pair, summarizes the spatial location of a plant. The spatial point patterns are essential because they arise in response to important ecological processes, associated with the structure of a population or community. Such processes include phenomena as seed dispersal, competition for resources, facilitation, and plant response to some type of stress, among others.

In this thesis, some factors and potential underlying processes were evaluated in order to explain the spatial distribution patterns of plant biodiversity. It was done in different ecosystems such as Mediterranean forest, tropical forest and dry scrubland. For this purpose new methodologies were used to test hypothesis related to spatial processes. Two ecological levels were used to analyze the spatial processes, at population and community levels, in order to assess the relative importance of intraspecific and interspecific interactions.

I focused on the use of spatial statistical functions to summarize point patterns to explore and make inferences from spatial data, starting with the construction of a new null model to infer variations about the dispersal syndrome of a parasitic plant in central Spain. Spatial dependence between point patterns in a multivariate point process of affected and unaffected hosts were analyzed and strong dependence was observed at small and medium distance. Two kernel functions were used to simulate the dispersion of parasitic plant and consistency of these models with other syndromes was identified, in addition to ballistic dispersion. A second issue was to analyze altitude and topography effects on the spatial population structure of a dominant shrub in the dry ecosystem in southern Ecuador, whose data come from replicated point patterns design-based. Based on a methodology developed for uni-factorial process, a method for bi-factorial processes was built to assess the interaction effect. The topography alone and interacting with altitude showed significant effect on the spatial pattern of shrub. A third issue was to identify the relationship between the spatial pattern and dispersal syndromes of plant community in the tropical forest of Barro Colorado Island (BCI), Panamá.

Several studies have been developed in this tropical forest and some focused on the spatial pattern-syndrome relationship; however the novelty of our study is that a large set of models (114 models) including dispersal limitation and environmental heterogeneity were evaluated, used to identify the only and joint effect to subsequently select the best fit model for each species. Slightly more than

fifty percent of the species showed spatial pattern consistent with only the dispersal limitation, and the remaining percentage of species revealed the only effect of environmental heterogeneity and habitat-dispersal limitation joined effect, equitably. Finally, with the same information from the tropical forest of BCI, and to understand the relationships underlying for balance of biodiversity, an index of the local functional dispersion was developed at the individual level, to relate the spatial pattern with four key functional traits of species. Although many studies involve this community with neutral theory, the assembly of the community is affected by similarity and habitat limitations at different scales.

INTRODUCCIÓN GENERAL Y OBJETIVOS

1. Ecología y espacio

Los patrones espaciales aleatorios de las plantas en comunidades naturales, son la excepción más que la regla; es decir se encuentran más lejos o más cerca unas de otras, que lo esperado por el azar (Maestre et al. 2005; Maestre & Escudero 2009; Rayburn et al. 2011). El estudio de las causas y las consecuencias de estos patrones espaciales constituye un temas importante de la ecología vegetal actual (Raventós *et al.*, 2010). Las distribuciones espaciales de los organismos, factores abióticos e interacciones ecológicas juegan un papel fundamental en el mantenimiento de la estructura, funcionamiento y dinámica de los ecosistemas (Maestre & Escudero 2009).

¿Por qué es importante el análisis espacial en ecología? El análisis de patrones espaciales de puntos es de vital importancia en el campo de la ecología, porque procesos ecológicos pueden dar lugar a estructuras espaciales predecibles? (Legendre & Legendre 1998), permitiendo comprender los mecanismos que controlan la distribución de las especies. Las características del patrón espacial se asocian con procesos ecológicos, así por ejemplo, patrones regulares se interpretan como indicadores de fuerte competencia entre plantas por limitación de recursos (Kenkel 1998), mientras que patrones agrupados son evidencia de interacciones neutras o positivas entre las plantas, en ecosistemas áridos (Kéfi *et al.*, 2008), distribuciones en forma de parches (Schenk et al. 2003, Perry et al. 2008) ¿¿qué sigue aquí?. Con el desarrollo de nuevas metodologías de inferencia a partir de procesos ecológicos (McIntire & Fajardo 2009; Rayburn et al. 2011), y análisis (Wiegand & Moloney 2004; Wiegand et al. 2007; Raventós et al. 2010), la cantidad de estudios basados en procesos espaciales de puntos, que han modelado el efecto de la estructura espacial sobre la comunidad vegetal (Bolker et al. 2003; Turnbull et al. 2007), se ha incrementado considerablemente; sin descuidar la complejidad que puede representar la relación entre el patrón de plantas y los procesos ecológicos (Turnbull et al., 2007; Law et al., 2009). Bajo el nombre de análisis espacial se engloba a un conjunto de técnicas encaminadas a analizar cuantitativamente datos espacialmente explícitos (Legendre y Fortin 1989).

2. Patrones de puntos

Aproximaciones clásicas

La literatura menciona algunos enfoques básicos relacionados con el surgimiento de la teoría de los procesos de puntos, entre ellos podemos mencionar tablas de vida, problemas de conteo, ingeniería

de la comunicación, física de partículas entre otros (Daley and Vere-Jones 2003). De los mencionados, el enfoque que prevalece en espacios de alta dimensión, es el conteo de eventos en intervalos o regiones de varios tipos, relacionado con las distribuciones discretas. El proceso de puntos es uno de los procesos en el cual los puntos ocurren totalmente al azar en un sentido definido, un caso particular en el proceso de Poisson (Cox and Isham 1980). El uso de las distancias como medidad de las relaciones espaciales entre individuos de una población (Dice 1952, Clark and Evans 1954, Moore 1954), fueron importantes aportes en el desarrollo de la metodología estadística para analizar procesos de puntos. Uno de los trabajos pioneros sobre aplicación de los porcesos de puntos a la ecología de plantas fue el uso de distancias punto-planta en el estudio de los patrones de poblaciones de plantas (Pielou 1959). Sin embargo las aplicaciones se orientaron también hacia otras áreas como la epidemiología y neurofisiología (Gani 1972, Brillinger 1975).

Si bien el proceso de Poisson homogéneo, fue uno de los primeros modelos empleados para resolver problemas relacionados con procesos de puntos, pronto se descubrió que era factible construir otra clase de modelos, sobre todo para explicar agrupamiento espacial. La primera aplicación de los procesos agrupados se le atribuye a Neyman en 1939 (Gelfand et al. 2010). Posteriores intentos de un análisis comprensivo de los patrones de puntos fueron hechos por Bartlett en los años 60s, quien propuso el uso de un espectro bidimensional de todas las distancias inter-puntos de un patrón espacial, permitiendo el desarrollo de pruebas a diferentes escalas (Getis, 1983). Quizá de aquí surgió la necesidad que condujo a Brian D. Ripley a introducir técnicas de segundo orden (Ripley 1976, 1977), entre ellas la principal medida reducida de segundo momento, o función K; posteriormente modificada y extendida (Ripley 1979, 1981; Diggle 1979). En esta línea, un modelo de agrupamiento basado en distancias inter-puntos fue desarrollado por Strauss (1975). La definición de la función K de Ripley ha sido extendida hacia procesos no estacionarios (Baddeley *et al*. 2000).

En 1978, Arthur Getis y Barry Boots publicaron un importante texto sobre Modelos de Procesos Espaciales, el cual proponía un análisis formal de patrones de puntos con características específicas como agrupamiento e inhibición y pruebas estadísticas (Anselin & Rey 2009). La motivación para desarrollar teoría de segundo orden es que una o varias medidas singulares desde un punto a otro punto no es suficiente para resumir un conjunto de datos en forma de patrones de puntos (Ripley, 1976, 1977, 1979). El objeto era encontrar una función de distribución acumulativa basada en todas las distancias entre los pares de puntos, este enfoque es conocido como segundo momento o análisis de segundo orden (Getis 1983). Este conjunto de métodos basados en distancias al vecino más

cercano, fue desarrollado para el análisis de datos provenientes de mapas exhaustivos que representan ubicaciones de todos los individuos (Ripley 1979, 1981).

Aproximaciones actuales

Uno de los trabajos que cubre la mayor cantidad de temas metodológicos relacionados con análisis estadístico de patrones espaciales de puntos, y sus aplicaciones a datos que proceden de las ciencias biológicas, corresponde a Diggle (2003, 2014). El enfoque adoptado por Diggle (2003) se basa en modelos estocásticos, asumiendo que los eventos son generados por algún mecanismo aleatorio subyacente. Los procesos de puntos son considerados como modelos matemáticos para patrones de puntos irregulares o aleatorios (Stoyan 2006). En algunos estudios, el análisis de patrones espaciales es utilizado para evaluar hipótesis sobre los procesos responsables de los patrones observados (Liebhold & Gurevitch 2002). Para comprender estos procesos funcionales es necesario identificar las escalas espaciales y temporales a las cuales ellos ocurren (Fortín & Dale 2005); y pese a ser inherentes a los procesos, su inclusión explícita se ha realizado en las tres últimas décadas (Ripley 1981; Legendre & Legendre 1998; Getis & Franklin 1987). A escalas suficientemente grandes, el ambiente natural exhibe heterogeneidad la cual tiende a producir patrones agregados (Diggle 2003). Tales características espaciales y temporales nos permiten relacionar con el proceso subyacente como establecimiento, crecimiento, competencia, reproducción, senescenciay mortalidad (Dale 2004).

Desde hace algunas décadas, los ecólogos se han planteado la pregunta: ¿Qué determina la combinación particular de especies encontradas en comunidades biológicas, el número de especies y la abundancia relativa?. La respuesta más ampliamente aceptada incluye la influencia de factores bióticos y ambientales (Harvey et al. 1983). Una metodología eficaz es mediante la comprobación de las hipótesis mediante el empleo de procedimientos estadísticos lo que provee de una explicación pausible de las observaciones. Esto conlleva la necesidad de evaluar la potencia o significancia del patrón observado, frente un modelo nulo (teórico) planteado de forma apropiada, permitiendo pruebas de aleatorización de datos ecológicos (Gotelli 2001).

El análisis estadístico de patrones espaciales puede presentarse en tres formas básicas (Wiegand and Moloney 2014): (1) datos cuantitativos analizables mediante técnicas de geoestadística, (2) datos categóricos representados por mapas segmentados en áreas y utilizados en el campo de la ecología de paisaje, y (3) patrones espaciales de puntos relacionados con la ubicación de objetos en el espacio. La presente tesis está orientada al análisis de información presentada en forma de patrones de puntos.

El fin principal para la elaboración de esta tesis, fue la construcción de nuevas herramientas de análisis espacial, basado en patrones de puntos, para comprobar hipótesis innovadoras en ecología de poblaciones y comunidades. En el primer capítulo, y conscientes de la limitación de los modelos nulos existentes para comprobar hipótesis ecológicas (Goreaud & Pélissier 2003, Wiegand & Moloney 2004), nos hemos propuesto desarrollar modelos nulos con mayor sentido biológico basados en curvas de dispersión y de capacidad de contagio a partir de modelos de control epidemiológico (Diggle 2003). Mediante el empleo de funciones de densidad basadas en distancias de dispersión (Cousens *et al.* 2008 , Cap. 5), hemos construido un modelo nulo para la dispersión de una especie vegetal parásita de bosque mediterráneo, y para poder inferir un vector de dispersión secundario.

En el segundo capítulo, realicé un análisis de patrones espaciales de puntos basados en un diseño replicado, empleando metodología estadística para inferencia del tipo análisis de la Varianza de dos vías ("two-way ANOVA"), para comprobar el efecto de dos factores abióticos sobre el patrón espacial de la población estudiada. La potencia de las pruebas fue evaluada mediante randomización ("bootstrap"). Utilicé el enfoque desarrollado por Diggle *et al*. (1991), para construir y testar esta herramienta en un contexto ecológico (distribución espacial de una especie de arbusto dominante en matorral seco al sur del Ecuador), lo que permitió probar el efecto de la interacción entre factores. Se observó un efecto de interacción significativo entre la latitud y topografía del terreno, frente al efecto individual de cada factor.

El tercer capítulo, lo he orientado a re-examinar los datos estudiados por Seidler y Plotkin (2006), un estudio referente sobre la relación entre síndromes de dispersión y agregación espacial en una comunidad de plantas de bosque tropical. Considerando que en las comunidades ecológicas la heterogeneidad ambiental juega un papel importante en la estructuración del patrón espacial (Wiegand & Moloney 2004), se ajustó y evaluó la bondad de ajuste de un conjunto amplio de modelos de procesos de puntos (Poisson homogéneo, Poisson heterogéneo, Poisson cluster homogéneo y Poisson cluster heterogéneo), llegando a comprobar que para un poco más de la mitad de las especies se mantiene la misma relación establecida por Seidler & Plotkin (2006) con los síndromes de dispersión. Ssin embargo el porcentaje restante de las especies presentó patrón espacial que se explica mejor con la inclusión de la heterogeneidad ambiental. Mediante el modelo de mejor ajuste, hemos visto que las especies dispersadas por animales son las menos agrupadas, mientras que las especies de dispersión balística y viento son las más agrupadas, de acuerdo al tamaño medio del

grupo (sigma). Esta relación está en sintonía con la observada por Seidler & Plotkin (2006), quienes usaron modelo Poisson cluster homogéneo.

En el capítulo final, hemos construido un índice para cuantificar la dispersión funcional local en una comunidad de especies vegetales del bosque tropical de la isla de Barro Colorado. Aunque la perspectiva individualista es prevalente en la moderna teoría ecológica de comunidades, la variedad de herramientas existentes actualmente para analizar patrones espaciales de diversidad desde el punto de vista de las especies individuales es escasa. Uno de mis objetivos ha sido el de avanzar en esta línea desarrollando funciones que permitan describir la estructuración de la diversidad funcional de la comunidad alrededor de especies individuales. Encontramos que la dispersión funcional varió dependiendo de la escala, a pequeña escala ($r<10$) el valor del índice KFDisp de la mayoría de especies (80%) no resultó significativo, es decir la proximidad funcional de cada especie respecto a la comunidad fue similar a lo esperado por azar, como indicador de un efecto significativo de asociación de hábitat en especies equivalentes, o co-existentes a corta distancia. Mientras que a distancias más grandes (>20m), la dispersión funcional individual de la mayoría de especies es mayor que lo esperado por azar. Estos resultados revelaron que el ensamble de la comunidad está afectado por las limitaciones de similaridad y de hábitat que afectan a diferentes escalas.

3. Objetivos de la tesis

Esta disertación doctoral ha sido estructurada en cuatro capítulos que cubren diferentes aspectos y etapas de la investigación. El objetivo principal es:

- Construir nuevas herramientas de análisis espacial, basadas en patrones de puntos, para comprobar hipótesis innovadoras en ecología de poblaciones y comunidades.

Los objetivos específicos de la tesis se han agrupado en orden al nivel ecológico de organización, empezando con problemas relacionados a población y terminando con la comunidad.

A nivel poblacional

- Construir y evaluar un nuevo modelo nulo para poblaciones de parásitos forestales

A pesar que desde hace tiempo en la literatura ecológica se reconoce la limitación de los modelos nulos existentes para testar hipótesis ecológicas no se han desarrollado actualmente modelos nulos válidos para estudiar las relaciones de dependencia entre epifitos y forofitos. Nos proponemos

desarrollar modelos nulos con alto sentido biológico basados en kernels de dispersión y capacidad de contagio.

- Desarrollar y testar herramientas para el análisis de patrones de puntos replicados basado en diseño análisis de varianza de dos vías.

Hoy en día, una gran cantidad de investigaciones en ecología implican replicación de parcelas de estudio incluidas aquellas donde se recogen datos en forma de patrones espaciales de puntos; sin embargo la disponibilidad de herramientas para el análisis de este trabajo es muy limitada. El desarrollo de este tipo de herramientas, a más de contribuir con metodología novedosa en el contexto ecológico, permitiría testar el efecto de diferentes factores bióticos o ambientales sobre el patrón espacial de la población o comunidad estudiada.

A nivel de comunidad

- Aplicar nuevas herramientas para describir la relación entre síndrome de dispersión y patrón espacial

Existen algunos trabajos que son un referente en el estudio de la relación entre síndromes de dispersión y agregación espacial en comunidades de plantas; sin embargo, considerando que en las comunidades ecológicas la heterogeneidad ambiental y la dispersión juegan un papel importante en la estructuración del patrón espacial, es pertinente re-examinar aquellos resultados, ajustando y evaluando la bondad de ajuste de un conjunto de modelos, y comprobar si se mantienen las misma relación establecidas.

- Desarrollar un índice local de diversidad funcional, que incluya el patrón espacial de distribución de la comunidad

A pesar de que la perspectiva individualista es prevalente en la moderna teoría ecológica de comunidades, la variedad de herramientas existentes actualmente para analizar patrones espaciales de diversidad desde el punto de vista de las especies individuales es escasa. Aunque recientemente se han realizado algunas aportaciones en este tema, es imperioso avanzar en esta línea desarrollando indicadores que permitan describir la estructuración de la diversidad funcional de la comunidad alrededor de especies individuales.

Referencias

Anselin, L. and Rey, S. 2009. "Perspectives on Spatial Data Analysis". En: Anselin, L., Rey, S. J. (Eds). *Perspectives on Spatial Data Analysis. Advances in Spatial Science*. Springer, New York. pp 1-20.

Baddeley, A. J., Moller, J. and Waagepetersen, R. 2000. Non- and semi –parametric estimation of interaction in inhomogeneous point patterns. *Statistica Neerlandica* 54(3): 329-350.

Bolker, B. M.; Pacala, S. W.; Neuhauser, C. 2003. Spatial dynamics in model plant communities: What do we really know? *The American naturalist* 162(2): 135-148.

Brillinger, D. R. 1975. The identification of point process systems. *Annals of Probability* 3(6): 909-924.

Clark, P. J. and Evans, F. C. 1954. Distance to nearest neighbour as a measure of spatial relationship in populations. *Ecology* 35, 445.

Cousens, R., Dytham, C. and Law, R. 2008. *Dispersal in plants: A population perspective*. Oxford. New York.

Dale, M. R. T. 2004. *Spatial Pattern Analysis in Plant Ecology*. Cambridge University Press. New York.

Dice, L. R. 1952. Measure of the spacing between individuals within a population. *Contr. Lab. Vertebr. Biol. Univ. Mich*. 55, 1.

Diggle, P. J. 1979. On parameter estimation and goodness-of-fit testing for spatial point patterns. *Biometrics* 35(1): 87-101.

Diggle, P. J.; Lange, N.; Benes, F. M. 1991. Analysis of Variance for Replicated Spatial Point Patterns in Clinical Neuroanatomy. – *Journal of American Statistical Association* 86(415): 618-625.

Diggle, P.J., 2003: *Statistical analysis of spatial point patterns*. Second edition. Arnold. London. UK.

Diggle, P. 2010. "Historical Introduction". En: Gelfand, A.E.; Diggle, P.J.; Fuentes, M.; Guttorp, P. (Eds.). Handbook of Spatial Statistics. CRC Press. A Chapman & Hall Book. New York. pp. 3-14.

Diggle, P. J. 2014: *Statistical Analysis of Spatial and Spatio-Temporal Point Patterns*. Third edition. CRC Press. A Chapman & Hall Book. Boca Raton.

Fortin, M-J.; Dale, M. R. T. 2005. *Spatial Analysis*. Cambridge University Press, Cambridge.

Gani, J. 1973. Point processes in epidemiology. Technical report Nro 203. Department of Statistics. Stanford University.

Gelfand, A.E., Diggle, P.J., Fuentes, M. and Guttorp, P. 2010. *Handbook of Spatial Statistics*. CRC Press. A Chapman & Hall Book. New York.

Getis, A. 1983. Second-Order Analysis of Point Patterns: The Case of Chicago as a Multi-Center Urban Region. *The Professional Geographer* 35: 73-80.

Getis, A. and Franklin, J. 1987. Second-Order neighborhood analysis of mapped point patterns. *Ecology* 68(3): 473-477.

Gotelli, N. J. 2001. Research frontiers in null model analysis. *Global Ecology & Biogeography* 10: 337-343.

Goreaud, F. and Pélissier, R. 2003. Avoiding misinterpretation of biotic interactions with the intertype K_{12}-function: population independence vs. random labelling hypotheses. *Journal of Vegetation Science* 14: 681-692.

Harvey, P. H., Colwell, R. K., Silvertown, J. W. and May, R. M. 1983. Null Models in Ecology. *Annals Review of Ecological Systematics* 14: 189-211.

Kéfi, S., van Baalen, M., Rietkerk, M. and Loreau, M. 2008. Evolution of local facilitation in arid ecosystems. *The american Naturalist* 172(1): E1-E17.

Kenkel, N. C. 1988. Pattern of self-thinning in Jack Pine: testing the random mortality hypothesis. *Ecology* 69(4): 1017-1024.

Law, R., Illian, J., Burslem, D., Gratzer, G., Gunatilleke, C. and Gunatilleke, I. 2009. Ecological information from spatial patterns of plants: insights from point process theory. *Journal of Ecology* 97: 616-628.

Legendre, P. and Fortin, M-J. 1989. Spatial patterns and ecological analysis. *Vegetatio* 80: 107-138.

Legendre, P. and Legendre, L. 1998. *Numerical Ecology*. Second english edition. Elsevier science B.V., Amsterdam.

Liebhold, A. M. and Gurevitch, J. 2002. Integrating the statistical analysis of spatial data in ecology. *Ecography* 25: 523-557.

Maestre, F.T., Escudero, A., Martínez, I., Guerrero, C. and Rubio, A. 2005. Does spatial pattern matter to ecosystem functioning ? Insights from biological soil crusts. *Functional Ecology* 19: 566–573.

Maestre, F. and Escudero, A. 2009. "Introducción". En: Maestre, F.T., Escudero, A. and Bonet, A. (Eds.). *Introducción al análisis espacial de datos en ecología y ciencias ambientales: métodos y aplicaciones*. Universidad Rey Juan Carlos, Madrid. pp. 1–34.

McIntire, E.J.B. and Fajardo, A. 2009. Beyond description: the active and effective way to infer processes from spatial patterns. *Ecology* 90(1): 46-56.

Moore, P. G. 1954. Spacing in plant populations. *Ecology* 35, 222.

Perry, G. L. W., Enright, H. J., Miller, B. P. and Lamont, B. B. 2008. Spatial patterns in species-rich sclerophyll shrublands of southwestern Australia. *Journal of Vegetation Science* 19: 705-716.

Pielou, E. C. 1959. The Use of Point-to-Plant Distances in the Study of the Pattern of Plant Populations. *Journal of Ecology* 47(3): 607-613.

Rayburn, A.P., Schiffers, K. and Schupp, E.W. 2011. Use of precise spatial data for describing spatial patterns and plant interactions in a diverse Great Basin shrub community. *Plant Ecology* 212(4): 585–594.

Raventós, J., Wiegand, T., De Luis, M. 2010. Evidence for the spatial segregation hypothesis: a test with nine-year survivorship data in a Mediterranean shrubland. *Ecology* 91(7): 2110-2120.

Ripley, B. D. 1976. The second-order analysis of stationary point processes. *Journal of Applied Probability* 13: 255-266.

Ripley, B. D. 1977. Modelling spatial patterns (with discussion). *Journal of the Royal Statistics Society Series B* 39: 172-212.

Ripley, B. D. 1979. Tests of "Randomness" for spatial point patterns. *Journal of the Royal Statistical Society. Series B.* 41 (3): 368-374.

Ripley, B. D. 1981. *Spatial Statistics*, Wiley, New York.

Schenk, H. J., Holzapfel, C., Hamilton, J. G. and Mahall, B. E. 2003. Spatial ecology of a small desert shrub on adjacent geological substrates. *Journal of Ecology* 91: 383-395.

Seidler, T. and Plotkin, J. 2006. Seed Dispersal and Spatial Pattern in Tropical Trees. *PLoS Biology* 4(11): 2132-2137.

Stoyan, F. 2006. "Fundamentals of Point Processes statistics". En: Baddeley, A.; Gregori, P.; Mateu, J.; Stoica, R.; Stoyan, D. (Eds) *Case Studies in Spatial Point Process Modeling*. Springer Science+Buisness Media Inc. USA, Springer, pp. 3–21

Strauss, D.J. 1975. A Model for Clustering. *Biometrika* 62(2): 467-475.

Turnbull, L. A., Coomes, D. A., Purves, D. W. and Rees, M. 2007. How spatial structure alters population and community dynamics in a natural plant community. *Journal of Ecology* 95: 79-89.

Wiegand, T. and Moloney, K. 2004. Rings, circles and null-models for point pattern analysis in ecology. *Oikos* 104: 209-229.

Wiegand, T., Gunatilleke, S., Gunatilleke, N. and Okuda, T. 2007. Analyzing the Spatial Structure of a Sri Lankan tree Species with Multiple Scales of Clustering. *Ecology* 88(12): 3088 – 3102.

Wiegand, T. and Moloney, K. 2014. *Handbook of Spatial Point-Patterna Analysis in Ecology*. CRC Press. New York.

CAPÍTULO 1

Factors influencing the distribution and dispersal of *Arceuthobium oxycedri* in Central Spain: A new null model for marked point patterns

Abstract

The dwarf mistletoe *Arceuthobium oxycedri*, is a common parasite of *Juniperus oxycedrus*, in central Spain. This species can have negative effects on its host, including weakening and tree death. Understanding the mechanisms that control its distribution and dispersal is critical to assess its spreading potential. We studied, in two sampling plots, dwarf mistletoe distribution among host individuals. A new null model of parasitic dispersion was built using dispersal kernels which were employed to simulate the spread of the parasite and to compare the resulting spatial structures with the observed ones. Nine dispersal scenarios were constructed combining three different initial population of infected trees (Po= 5, 10 and 20 individuals) and three different kernel bandwiths (10, 20 and 30m) chosen to represent two alternative hypothesis: that dispersal of the mistletoe is mainly ballistic or that in adition to ballistic dispersal some additional vector contributes to larger dispersal. Spatial summary functions (Ripley's K, pair correlation function and nearest neighbor distance distribution) of the simulated scenarios were compared with those of the observed pattern, and significance was evaluated using the goodness of fit tests. Simulations models that considered long-distance dispersal were able to explain the observed spatial pattern in some scenarios suggesting that *A. oxycedry* uses other mechanisms in addition to ballistic seed shooting as secondary dispersion agents to spread at distances greater than 20 m. This implies that spreading across hosts may rely also on birds for seed transportation as the seed characteristics facilitate dispersal by adhesion.

Abbreviations.- AI: Sampling Area I, AII: Sampling Area II, IP: infection probability, SEM: Spatially explicit model.

Introduction

Most mistletoes are both mutualistic with their animal dispersers and parasitic of their host plants (Aukema 2003). However, the explosively dispersed dwarf mistletoes (*Arceuthobium spp.*) and wind dispersed Misodendraceae family do not have mutualistic animal dispersers. Mistletoe fruits have adhesive seeds that stick by viscous excretions to a host branch. In plants, dispersal vectors can act at different scales and generate different dispersal kernels for a particular species (Nathan 2007). Mistletoes dispersal is generally localized around the host plant (Maloney and Rizzo 2002). Overton's model (1994) assumes random dispersal. However, some studies suggest non-random distribution among host plants (Larson 1996, Wenny 2001). The response of birds facing seed transport to already infected hosts may increase seed rain within the patches already infected, resulting in a preferential dispersal (Aukema and Martinez del Rio 2002). Mistletoes dispersal form is a complex process that involves habitat factors as well as animal behavior, and is influenced by woodland fragmentation (Lavorel *et al.* 1999).

Arceuthobium oxycedri DC. M. Bieb, is the most widely distributed species of *Arceuthobium*, reported from 31 countries from Spain to western China (Ciesla *et al.* 2004). It parasitizes native and introduced species of *Juniperus* especially *Juniperus oxycedrus* (L.) and *Juniperus communis*, and some other introduced species in the family Cupressaceae (Rios Insua 1987, Ciesla *et al.* 2004). Fruiting and seed dispersal occurs between October and November, with a maturity period of 13 months (Catalan 1997). Dispersal is provided primarily by the ballistic mechanism of the plant itself (Catalan 1997), but birds may be indirect dispersal vectors if seeds adhere to the bird and are then transferred to other hosts (Zilka and Tinnin 1976, Ostry et al. 1983). Birds have been suggested as long-distance vectors of *A. oxycedri* in France and Pakistan, because songthrush ingests fruits of mistletoe, but quantitative data are lacking (Hawksworth and Geils 1996). *A. oxycedri* impacts its host through reduction of seed production and wood quality, and by making hosts more susceptible

to fungal attack (Rios Insua 1987), however, the mistletoes can provide habitat and a food source for some species of birds, insects and small mammals (Maloney and Rizzo 2002).

Hypothetically the mode of seed dispersal of *A. oxycedri* is autochory + epizoochory, i.e. is characterized by self-dispersal (physical and often explosive discharge of seeds from the fruit) also the secondary transport of seeds or directed dispersal when seed attached to the bird's body are transported (Watson and Rawsthorne 2013). *Juniperus oxycedrus,* the primary host, has fleshy fruit that attracts providing food for birds, this may facilitate long dispersal of misltetoes, however evidence is rarely reported (Watson 2011).

The purpose of this study is to generate dispersal patterns of mistletoe from spatially explicit null model to simulate different spreading scenarios and compare with the observed pattern. This study is a step in the construction of null models to test hypotheses of dispersal of parasitic plants. Specifically, using methods of spatial analysis, it is possible to describe variation in the spatial distribution and seed dispersal of some types of mistletoes and the scales at which these changes occur (Overton 1994, Aukema 2004). Overton (1996) and Lavorel et al. (1999) developed spatially structured models of mistletoe distributions. Some kinds of bird-dispersed mistletoes (*Amyema miquelii, Dicaeum hirundinaceum*) have been found to have a leptokurtic (short-distance seed dispersal from the parent plant) seed (Ward and Paton 2007). The analysis aims to answer the question: Is the observed pattern compatible with ballistic+bird seed dispersal? Therefore, we try to determine whether the dispersal of *A. oxycedri* is only ballistic, defined by a specific dispersion pattern, or if it is related to "epizoochory", observable in the spatial pattern of dispersal.

Material and methods

Study site and data collection

Data were collected from two sites in the protected area of the "Cuenca alta del Manzanares" located in the northwest of the Community of Madrid, Spain (Fig. 1-A). *A. oxycedri* was found parasitizing

Juniperus oxycedrus in this area (Zavala and Zavala 1993). The first site (hereafter "AI") was around 24.98 ha, near the center of the park, located at 1000 meters of altitude, with high capacity of local agricultural production and poor natural condition. *Juniperus oxycedrus* was strongly affected by the dwarf mistletoe in site AI. Here *J. oxycedrus* constitutes the third most dominant woody species after *Quercus ilex* and *Cistus ladanifer*. We mapped 126 *J. oxycedrus* trees in this area.

Fig. 1 Spatial distribution of *Arceuthobium oxycedri* parasitizing *Juniperus oxycedrus* in two sampling areas. (A) Study site in the Regional Park of Manzanares river upstream, Madrid-España (B) Sampling area I, and (C) Sampling area II.

Site "AII", called "área de producción agrícola", around 26.05 ha, was located to the northeast of the park with an average altitude of 1000 meters. *Juniperus oxycedrus* was less affected in site AII where this species is the most dominant tree. We mapped 234 trees in this area.

We mapped the boundaries of the two areas and the location of each individual of the host tree (Fig. 1-B, 1-C). In each site, we examined host trees and recorded whether they showed presence/absence of mistletoe infection. We found 65 and 233 infected trees for AI and AII respectively. These coordinates were obtained using of Differential Global Positioning System, then converted to the Universal Transverse Mercator (*UTM*) geographic coordinate system UTM - WGS84.

Spatial analysis

Univariate spatial point pattern analysis

We describe the spatial arrangement of individuals and tested hypotheses about spatial pattern, with Ripley's function K(*r*), pair correlation function g(*r*) and nearest-neighbor function G(*r*).

Ripley's K function (Ripley 1977) is a technique for assessing within-patterns point interactions at multiple scales through the analysis of a wide range of within-pattern point distances (Diggle 1983; Cressie 1991), and has been used in various forest spatial pattern analyses(Stoyan and Penttinen 2000; Dale and Powell 2001). K(r) function is the expected number of points in a circle of radius r centered on an arbitrary point, divided by the intensity of the pattern (Watson et al. 2007). Ripley (1976) proposed an estimator of the K-function:

$$\widehat{K}(r) = \frac{|A|}{n^2}\left[\sum\sum_{i \neq j} \frac{I_d(d_{i,j})}{w_{ij}}\right]$$

where r is the radius of a circle centered on a point in the pattern, n is the number of points in region A with area |A|, $d_{i,j}$ is the Euclidean distance between the i-th and j-th points, the weight w_{ij} corrects for edge effects, and I_d is a function that equals 1 if the distance $d_{i,j} \leq r$, otherwise $I_d=0$.

A problem with the K-function can be traced to the cumulative nature of the statistics, i.e., effects at short scales obscure the effects at broader scales (Getis and Franklin 1987l; Wiegand and Moloney 2004; Loosmore and Ford 2006; Wiegand and Moloney 2014). To overcome this limitation, the pair correlation function g(r), a noncumulative function that uses only points separated at r distance from each other, provides a complementary pattern description across scales, and identifies the precise scales where significant point-point interactions occur. The relationship between K-function and pair correlation function can be expressed as $dK(r)/dr=2\pi rg(r)$ (Ripley 1977; Stoyan and Stoyan 1996). Both K(r) and g(r) are based on the distribution of distances of all pairs of points, and use the information on all inter-point distances (Ripley 1976, 1977; Diggle 1983; Wiegand *et al.* 2007)..

Nearest-neighbor statistics provide a useful complement to the second-order statistics described above (Wiegand and Moloney 2014). The distribution function of nearest-neighbor distances, denoted by G(r) (Diggle 2003), represents the cumulative distribution of the distances r to the nearest neighbor, measured from a typical point of the pattern (Dixon 2006; Illian 2008). For a pattern with complete spatial randomness (CSR) is expectation is $G(r)= 1 – \exp(-\lambda\pi r^2)$, where λ is the intensity of points. G(r) provides information on the local neighborhood (Wiegand et al. 2013). In a first exploratory analysis, we used the K function to describe the spatial pattern of juniper trees in each site (i.e., we conducted a CSR test. Fig. 3 next section) and also to conduct a test of random labeling of infected trees (Watson et al. 2007). We subsequently employed all the functions (K, g and G) to describe the spatial pattern of infected trees in both study sites and to assess the efficiency of different models in describing the observed patterns.

Multivariate spatial point pattern analysis

Bivariate statistics are used to analyze the spatial association of two patterns. Here we consider the multivariate point pattern that arises from the original univariate pattern of trees marked by two host states, infected and uninfected. The spatial dependence between types (e.g., between infected and uninfected hosts) in a multivariate point process is related to second order properties of multivariate

point pattern, which are estimated by "cross-type" second-moment measures (Cressie 1991). One of the most frequently employed is the "cross-type" or multitype K function (Hanisch and Stoyan 1979; Diggle 2003). An extension of Ripley's estimator is given by (Dixon 2012):

$$\widehat{K}_{ij}(r) = (\hat{\lambda}_i \hat{\lambda}_j A)^{-1} \sum_k \sum_l w(i_k, j_l) I(d_{i_k, j_l} < r)$$

where λ_i, λ_j: are respectively the intensity of patterns *i* and *j*, w(i,j) is the fraction of the circumference of a circle centered at the k*th* location of process i with radius d that lies inside the study area. Here we consider the multivariate point pattern marked by infected hosts and we employed the multitype K to analyze the interaction between infected and uninfected trees.

Null Models and simulation

To make inferences about mistletoe dispersal, a spatially explicit model was defined, based on the following assumptions. 1) All individuals of the host species have the necessary qualities to be infected; 2) the probability of being both infected and uninfected plants depends on the local densities of plants. Plants live in a two-dimensional space larger enough for edge effects to be small. The landscape is assumed homogeneous, i.e. local host dispersal and interactions between individuals are the only influence on spatial structure of mistletoe.

We asume that the distribution of *A. oxycedri* is the consequence of its dispersal mechanism. To approach this dispersal, we use the dispersal kernel, defined as the probability density function of dispersal distances from individual plants (Ribbens et al. 1994). We considered two kernel functions, the bidimensional 2Dt (fat-tailed) and the Gaussian (thin-tailed), proposed by Clark et al. (1999). The Gaussian kernel is a reasonable model for a restricted set of conditions, being most sensitive to seeds dispersed over short distances, and less suitable to describe sporadic seed dispersed over long distances (Clark et al. 1999). The (reparametrized) formula for this function is:

$$k(r) = (\pi\sigma^2)^{-1} exp\left(-\frac{r^2}{\sigma^2}\right), \quad \sigma > 0$$

where σ is the standard deviation of the isotropic Gaussian smoothing kernel and *r* the distance.

On the other hand, the 2Dt-function allows one to fit short- and long-distance dispersal associated with different dispersal mechanisms. The (reparametrized) formula becomes (Clobert et al. 2012):

$$k(r) = \frac{b-1}{\pi a^2}\left(1+\frac{r^2}{a^2}\right)^{-\mathrm{b}}, \quad \mathrm{a} > 0, b > 1$$

where *a* is a scale parameter, *b* is a shape parameter and *r* is the r dispersal distance.

The parameters σ (in Gaussian kernel) and a (in 2Dt kernel) control the bandwidth or smoothing parameter. In the context of spatial analysis, it is not entirely clear how to choose an optimal value for the bandwidth in the general case (Bivand et al. 2013).

To simulate spatial patterns generated by dispersal limitation (dispersal described by Gaussian and 2Dt kernels), we started with a configuration of 5, 10 and 20 infected trees in each site. This configuration includes bandwidth values of 10, 20 and 30m for each initial population infected trees. In our study, the Gaussian and 2Dt models were evaluated at short distance (acting as ballistic dispersion) and large distance (acting as ballistic+bird dispersion). As ballistic seed dispersal of dwarf mistletoes reach a mean distance of 10 m (i.e., 30 to 40 ft.) (Turril 1920), to model ballistic dispersal we assigned a probability of dispersal = 0 for distances larger than 10 meters, forcing the null model to consider only a ballistic dispersal mechanism. Values for the parameters of models in the different scenarios are shown in Table 1.

Table 1 Parameter values of the simulation models

Kernel name	Parameter	Tail fatness
Gaussian	σ= 5, 10 y 15m	Thin-tailed
2Dt	a= 10, 20 y 30m; b=2	Fat-tailed

Once we had set the initial distribution of infected trees, we simulated successive dispersal steps. For each simulation we first built a map of dispersal probability, based on the coordinates of the infected trees and the dispersal kernels. From this map of dispersal probability we assigned to each healthy tree a probability of infection (p_i). Finally, we assigned the status infected/healthy to each individual as a Bernoulli trial with $p= p_i$.

We repeated the same process (construction of new dispersal probability maps and asignement of new infected status) while the number of infected trees in the simulated pattern was smaller than the infected trees in the observed pattern.

The scenarios with the value of h = 10 meters were considered as the average horizontal distance of ballistic dispersion of *A. oxycedri* (Turril 1920, Maloney and Rizzo 2002). A detailed description about Gaussian and 2Dt kernels is provided in Appendix 1.

For each kernel (Gaussian and 2Dt) we evaluated 9 scenarios, resulting from the combination of three different initial number of infected tress (5,10 and 20 individuals) and three different bandwidths (a=10, 20, and 30m) for the 2Dt and the equivalent for the Gaussian kernel (i.e., σ= 5, 10, and 15 m).

Evaluation of the simulated models

To assess differences between the spatial structure of the observed infected trees and the predictions from each model, we computed Ripley's K-function, pair correlation function *g(r)*, and nearest-neighbor distance distribution function G (r) on the pattern of infected trees in each study site, from distance r= 0m to r= 125m. We computed also simulation envelopes based on the simulated models..

For each scenario (i.e., combination of initial number of infected trees and kernel bandwith) and study site, we simulated 199 patterns and computed also the functions K, g and G. From the set of "simulated" functions we build for each function, the simulation envelopes wich included the highest and lowest simulated values. Significant departures from the simulated model were identified at r

distance, when the empirical function (K(r), G(r) or g(r)) was located outside of the simulation envelopes. Thus, if ballistic dispersal is prevalent, we would not expect significant differences at short scales *r* with Gaussian kernel and all values of scale parameter (sigma). In another way, if the mixture of ballistic and other forms of long-distance dispersal prevail, differences at medium and large scales r with 2Dt kernel, would not be expected.

We also computed the goodness-of-fit (GoF) test proposed by Loosmore and Ford (2006). Both the observed pattern and each of the patterns simulated by the null model are reduced to a single statistic (u_i), which represents the total squared deviation between the observed pattern and theoretical results over the range of r distances considered. It is important to remark that, for our objectives (i.e., evaluatingthe fitting of the models to the observed data) the relevant tets are those showing *non-significant* values for the *u* statistic (i.e., absence of significant deviations from the expected values under the null model).

All calculations were conducted using the program R (R Core Team 2013). Spatial analysis and model fitting were computed using the R packages "Spatstat" (Baddeley and Turner 2005) and "ecespa" (De la Cruz 2008).

Results

Spatial distribution of *Arceuthobium oxycedri*

We classified *Juniperus oxycedrus* in three categories: dead, affected and unaffected. Affected host plants occurred unequally in the two sampling areas, 45% in AI, and 17% in AII; unaffected hosts were 7% and 82% in AI and AII respectively (Table 2). We recorded a high mortality in AI (48%). The differences in the frequency of each type between sites were significant (χ^2 = 218.6, df = 2, p-value <0.00001), revealing a different distribution of marks between the two sampling areas (Table 2). Additionaly, the underlying pattern intensity of infected hosts is not the same between the two areas: in AI the average distance from one infected tree to the nearest neighbor infected tree was

22.2m, while in AII the closets distance tobetween two infected trees was 37.1m. In the case of uninfected hosts, these distances were 82.5m in AI and 14.6m in AII.

Table 2 Observed frequency host/parasite (*J. oxycedrus/A. oxycedri*)

Site	Affected (A)	Unaffected (N)	Dead (M)	Total (n)
Area I	57	8	61	126
Area II	40	193	1	234

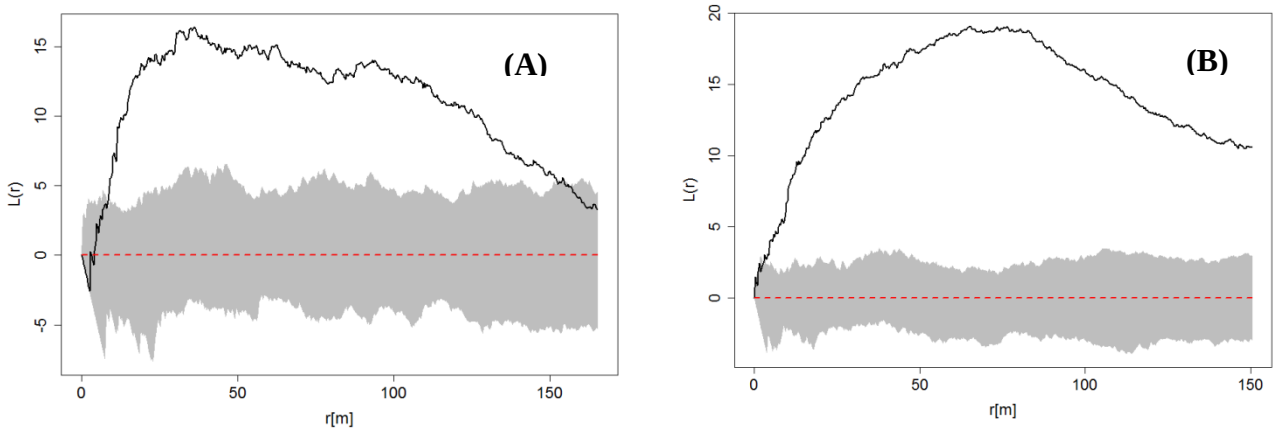

Fig. 2 Aggregation differences between host trees in both plots. The solid line represents the empirical values of L(r) and the dashed line represents homogeneous Poisson process. The gray region represents the 99% confidence envelops constructed with 99 Monte Carlo simulations K-functions of the A. *oxycedi* hosts point patterns assuming homogeneous Poisson process (red dashed line). (A) Sampling area AI, (B) Sampling area AII.

Univariate and multivariate spatial point pattern analysis

The host distribution showed strong aggregation in AI at scales from 20m to 130m and aggregation at all distances in AII, although slight clustering with random tendency at short distance (Fig. 2). The spatial pattern of infected trees was apparently random in both sampling sites (Fig. 3).

The pattern of infected and uninfected trees were independent (Fig. 4) although a moderate attraction between infected and uninfected trees from 0m to 80m, and repulsive tendency at large distance was evident in sampling area AI (Fig 4-A).

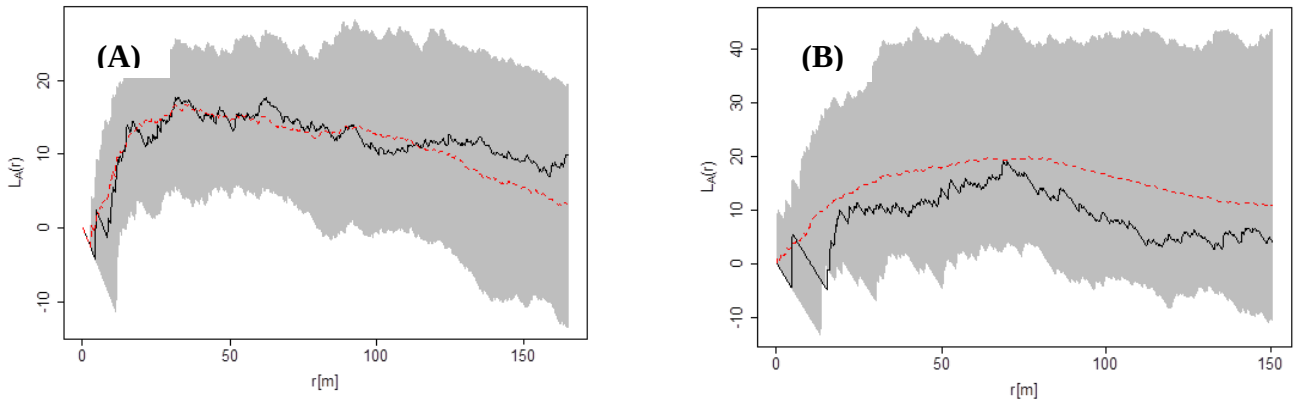

Fig. 3 Test of random labeling of the spatial pattern of infected host trees in sampling area AI (A) and sampling area AII (B). The solid lines represent the empirical values of L (r), dotted red line represents the average values of L (r), and the gray region represents 99% confidence envelopes constructed from 199 relabellings of the infected marks on the whole population of trees in each area.

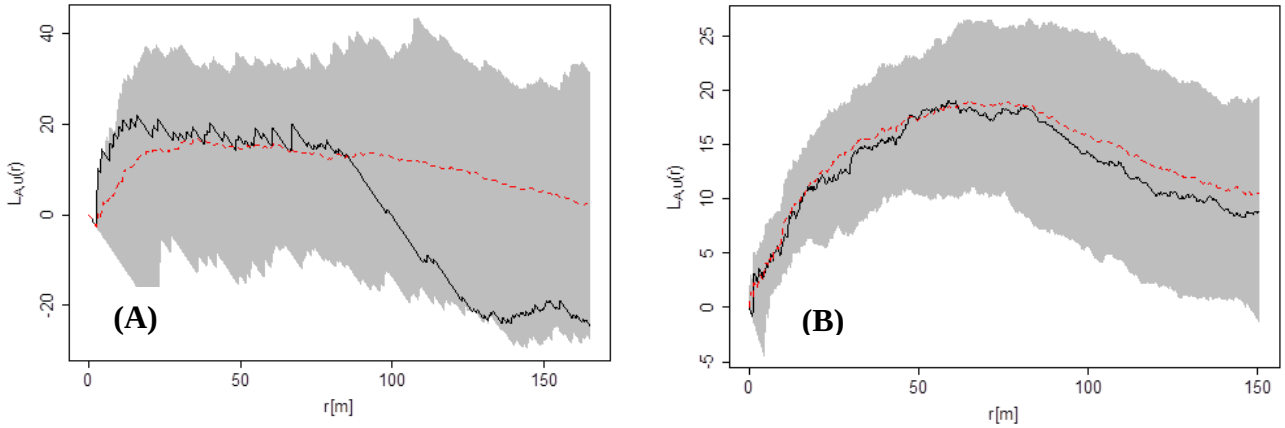

Fig. 4 Test of association between infected (A) and uninfected (U) *J. oxycedrus* trees with random labeling.. The solid lines represent the empirical values of $L_{A,U}(r)$, dotted red line represents the average of random labeling simulations and the gray region represents 99% confidence envelopes constructed from 199 relabellings of the infected marks on the whole population of trees in each area (A) Sampling area AI, (B) Sampling area AII.

Simulating dispersal scenarios

As the scenarios for σ= 5m did not converge (i.e., were unable to simulate the spread of the infection form the initial populations), only 6 scenarios could be analyzed for the Gausian kernel.

Among the 6 Gaussian models that converged in site AI, most showed significant differences with the observed patterns (see Fig. 5 and Table 3a). However, the models that included large bandwidths (σ= 15 m, i.e., h = 30 m) and medium and large original populations of infected individuals (i.e., P_0 = 10 and 20 individuals), were able to simulate the original patterns, i.e., there were no significant departures of the observed K, g and G functions from the simulation envelopes (see Table 3-a).

In the case of the 2Dt models, the results depended mostly on the summary function. For example, none of the models described appropriately the observed pair correlation function g(r) (see Table 4-a). However, the K function was within the envelopes for all models (i.e., all bandwidths) simulated with an original population of P_0 = 10, and the nearest neighbor distances distributions G(r) was correctly described for all values of P_0 (with some restrictions on the value of h in some cases) (see Table 4-a).

In the site AII, only the Gaussian model (with P_0 = 20) was able to describe the pattern of infected trees, and only for the K function (see Table 3b). On the contrary, none of the 9 combinations of parameters for the 2Dt models was able to describe any of the summary functions employed (Table 4-b).

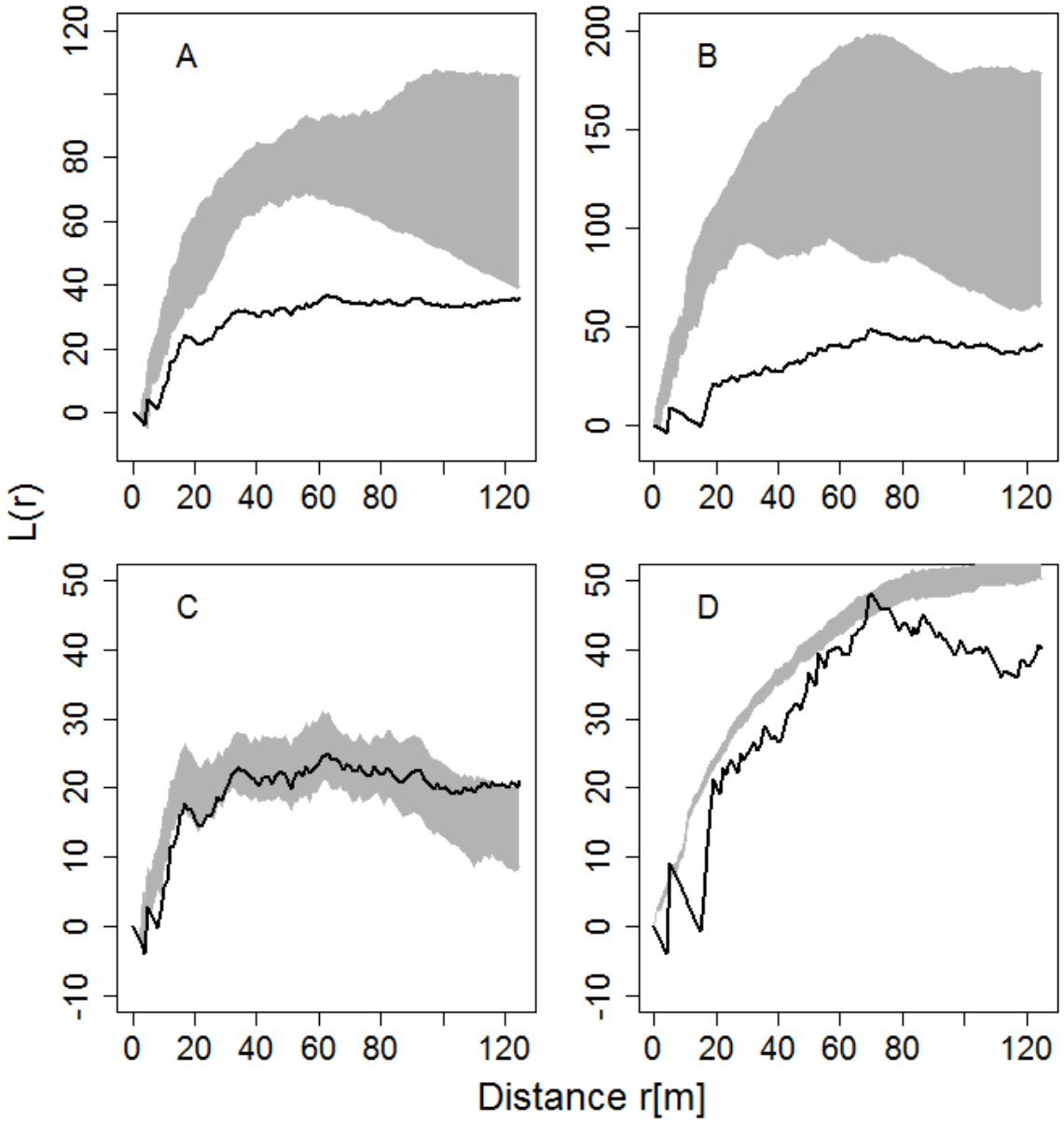

Fig. 5 Envelopes for the K-function from the simulation of different dispersal patterns of *A. oxycedri*. A-B null models with Gaussian kernel for AI and AII plots respectively. C-D null models with 2Dt kernel, with P_o=10 and σ=5m (Gaussian) and a=10m (2Dt), for AI and AII plots respectively. The solid lines are empirical values of K(r) and the gray region represents 99% confidence envelopes with from 199 simulations of the null model.

Table 3. GoF-test for the the Gaussian models of the dispersal pattern of *A. oxycedri*. Where K: Ripley's K function, G: nearest neighbor distances distribution, g: pair correlation function. (a) Area I, (b) Area II. Po: Initial infected population, h (=2σ): bandwidth. Symbols in the table indicate the significance of the deviations of the empirical function from the simulated model, * p <0.05, ** p <0.01, *** p <0.001, and ns: non-significant (p≥ 0.05), '-': no evaluated (non-convergence). Note that for our purposes, the relevant tests are those showing non-significant deviations (i.e., absence of significant deviations from the expected values under the null model).

(a)

		GOF test (p-valor)		
Po	**h**	**K**	**G**	**g**
5	10	-	-	-
	20	-	-	-
	30	-	-	-
10	10	***	***	***
	20	*	***	***
	30	ns	ns	ns
20	10	*	***	***
	20	*	***	*
	30	ns	ns	***

(b)

		GOF test (p-valor)		
Po	**h**	**K**	**G**	**g**
5	10	**	***	***
	20	*	***	*
	30	*	***	*
10	10	*	***	**
	20	*	***	**
	30	*	***	*
20	10	ns	***	**
	20	ns	***	*
	30	ns	***	*

Table 4. GoF test for the differences between the null 2Dt model simulation and the observed dispersal pattern of *A. oxycedri*. Where (a) Area I, (b) Area II. Po: Initial infected population, h: bandwidth. Symbols in the table indicate the significance of the deviations of the empirical function from the simulated model, * p <0.05, ** p <0.01, *** p <0.001, and ns: non-significant (p≥ 0.05). Note that for our purposes, the relevant tets are those showing non-significant deviations (i.e., absence of significant deviations from the expected values under the null model).

(a)

		GoF test (p-value)		
Po	**h**	**K**	**G**	**g**
5	10	*	*	***
	20	***	*	***
	30	*	ns	***
10	10	ns	ns	***
	20	ns	ns	***
	30	ns	ns	***
20	10	*	ns	***
	20	*	ns	***
	30	*	*	***

(b)

		GoF test (p-value)		
Po	**h**	**K**	**G**	**g**
5	10	***	***	***
	20	***	***	***
	30	***	***	***
10	10	***	***	***
	20	***	***	***
	30	***	***	***
20	10	***	***	***
	20	***	***	***
	30	***	***	***

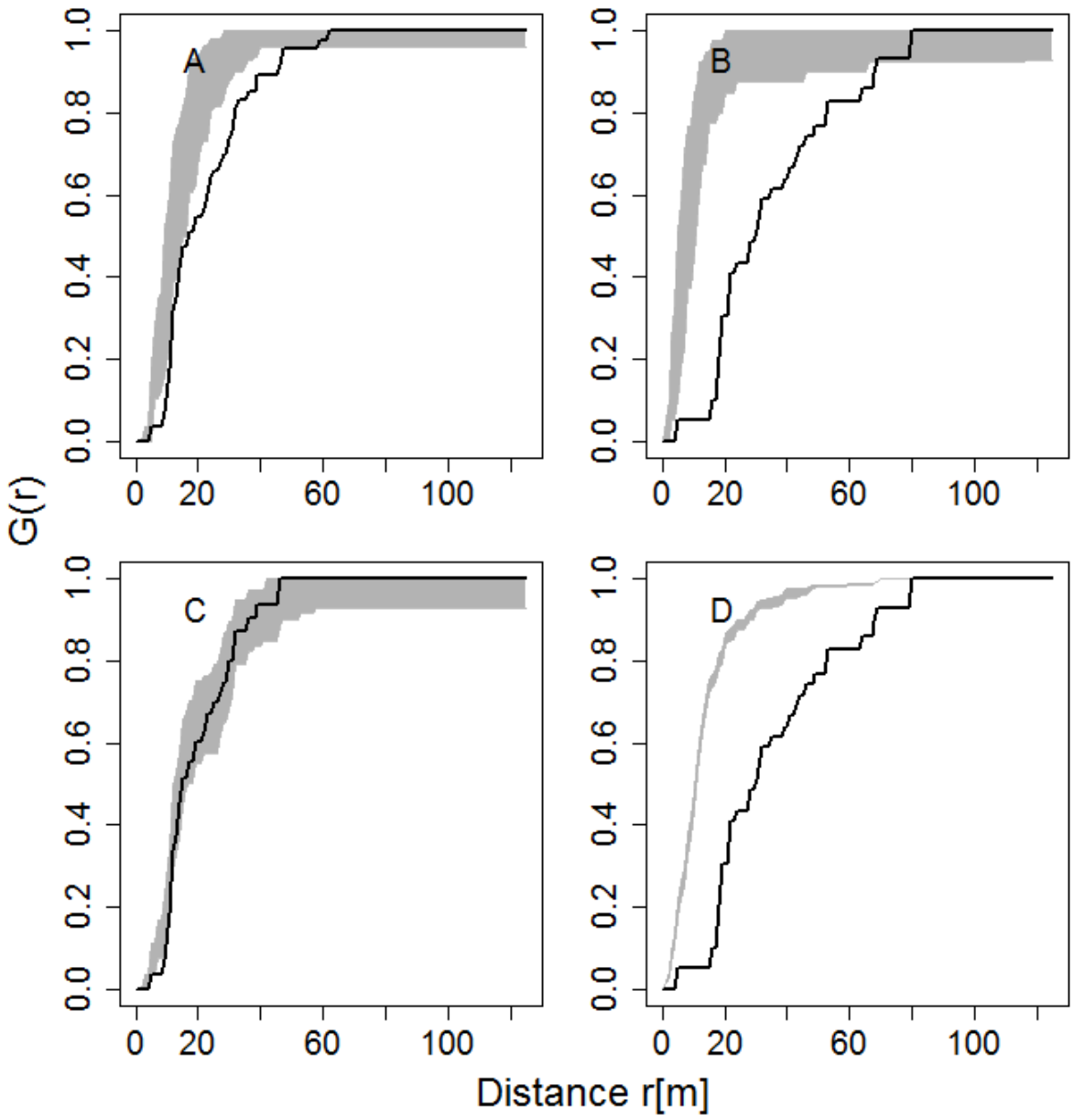

Fig. 6 Envelopes for the G-function from the simulation of different dispersal patterns of *A. oxycedri*. A-B null models with Gaussian kernel for AI and AII plots respectively. C-D null models with 2Dt kernel, with P_o=10 and σ=5m (Gaussian) and a=10m (2Dt), for AI and AII plots respectively. The solid lines are empirical values of K(r) and the gray region represents 99% confidence envelopes with from 199 simulations of the null model.

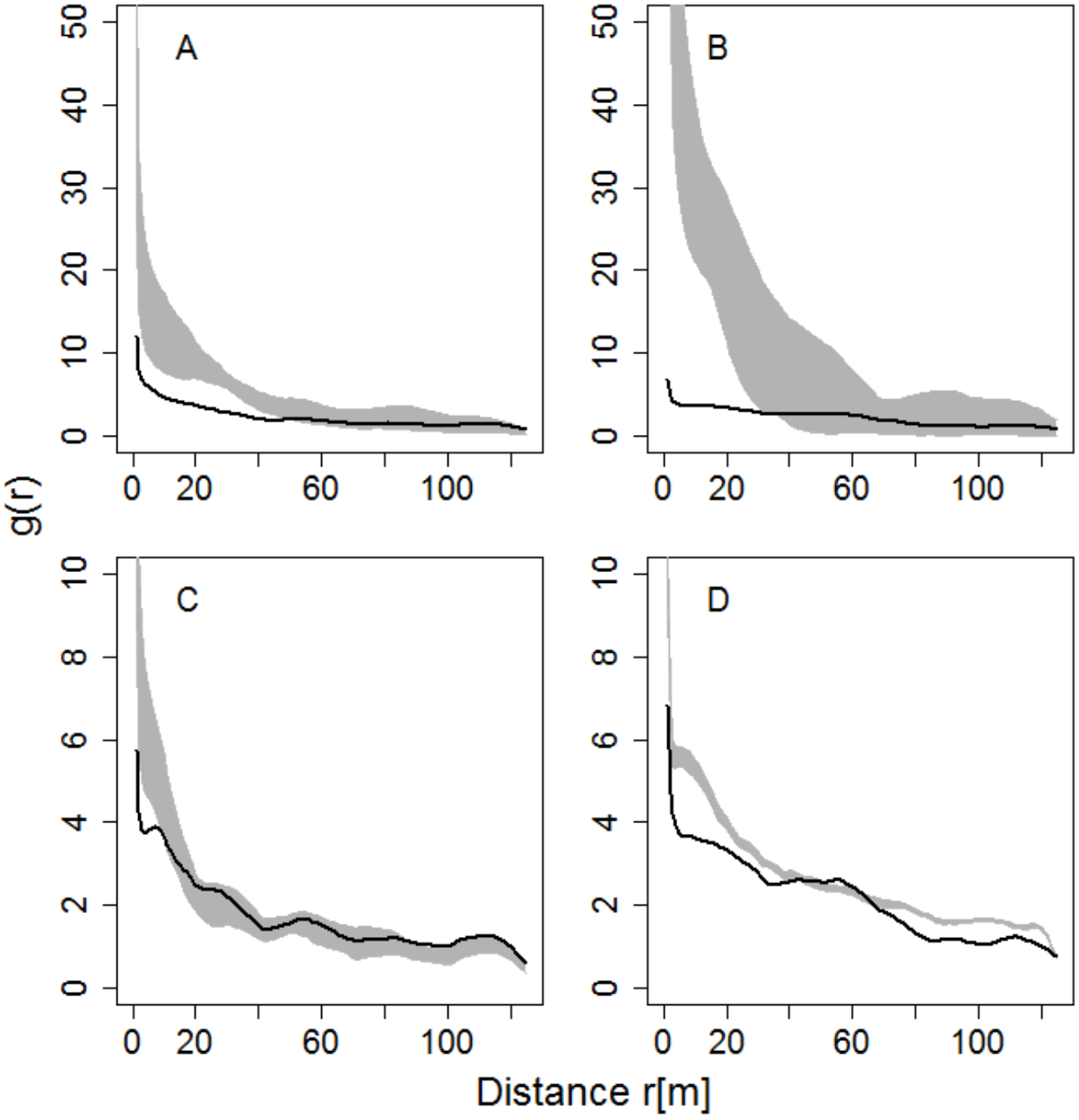

Fig. 7 Envelopes for the pair correlation function (g) from the simulation of different dispersal patterns of *A. oxycedri*. A-B null models with Gaussian kernel for AI and AII plots respectively. C-D null models with 2Dt kernel, with P_o=10 and σ=5m (Gaussian) and a=10m (2Dt), for AI and AII plots respectively. The solid lines are empirical values of K(r) and the gray region represents 99% confidence envelopes with from 199 simulations of the null model..

Discussion

Mistletoe distribution

Junipers (*Juniperus oxycedrus*) provide a suitable habitat for protection, nourishment and reproduction to its obligate parasitic *A. oxycedri* (Sarangzai et al. 2010). In our study site, the infection process varied across sites (and was more localized in plot AI). Prevalence infection rates were 45% and 17%, in AI and AII respectively Community composition can influence the establishment and prevalence of infection in the host (Holt *et al.* 2003), and different factors may influence mistletoe aggregation in opposing directions, sometimes acting to reduce the overall levels of aggregation (Rist *et al.* 2011). In fact, there is a difference in the floristic composition of both areas and, whereas in area AII *J. oxycedrus* the dominant shrub, in area AI the community is dominated by *Quercus ilex* and *Cistus ladanifer* (Zavala and Zavala 1993).

On the other hand, although the spatial pattern of hosts, play an important role of intensification events defining severity within the host tree (Shaw 2005) in our study, the average nearest neighbor distance for infected trees in AII (37.1m) was greater than in AI (22.2m), in contrast with the average nearest neighbor distance between trees (13.2m in AII, 17.6m in AI,). In other words, clustering of infected trees is not directly related to the aggregation of host trees, so infection intensity understood as the force of infection in the host (trees heavily infected in AI, see Zavala and Zavala 1993), could be a factor that explains infection prevalence, since a distinctive feature of dwarf mistletoes is the seed dispersal to short distances (Robinson and Geils 2006). This combined with the different level of disturbance that showed both plots, could explain in part the difference in spatial pattern of infected trees. Spatial heterogeneity in host tree susceptibility may also underlie mistletoe distribution (Ward and Paton 2007) (i.e. most infected and less vigorous hosts were observed in plot AI).

Simulation models

Mistletoe simulated patterns vs observed pattern

Although horizontal displacement by ballistic dispersal in this kind of mistletoes could reach up to 16m, an average horizontal average distance of 10m is more common (Hawksworth *et al.* 2002). In most scenarios, the observed spatial structure was different from the expected for the models that simulated exclusively ballistic dispersal (Gaussian kernel, bandwidth=5m). This discrepancy suggests that other agents may influence dispersion of *A. oxycedri*, for example a combination of ballistics and birds. The Gaussian model with 30 m bandwidth l explained the spatial pattern in plot A1, whereas 20 m and smaller bandwidths could not. In plot AII, only the Gaussian null model generated consistent simulations, for bandwidths from 10 to 30 m. This large bandwidths suggest the existence of other factors influencing mistletoe dispersal, besides the ballistic dispersion. On the other hand, although host -tree aggregation at smaller spatial scales was more evident in AII than in AI, the clustering of infected tress was not significantly different in both areas. This suggests that patterns in plot AII may result from a positive feedback in which high mistletoe prevalence leads to increased seed deposition in uninfected trees (Aukema 2004). Shaw et al. (2001) examined the spatial association between healthy and infected *Arceuthobium tsugense* trees, and they identified a negative association with infected trees aggregated and repulsive from uninfected trees. In our case, slight repulsive behavior was found in AI plot, occurring from 80m; however in AII plot, this association was neutral.

Watson (2009) suggested that variation in host quality influences the non-random dispersion of parasitic plants in many systems. The environmental differences between the two areas could be affecting differently the vigor of *J. oxycedrus* individuals and this could be reflected in a differential dispersal of *A. oxycedri* in each area. In AI-plot, affected trees have below-average vigor and are heavily infected, while in AII-plot, trees with average vigor are affected in a different way by the

dwarf mistletoe (Zavala and Zavala 1993). On the other hand, the difference in proportions of infected, uninfected and death individuals suggest that infection was present in plot AI before AII.

Despite of the ballistic dispersion form, the pattern of infected trees shows larger range of distances to the nearest neighbor than expected, i.e. infected trees are more scattered than would be expected by only ballistic dispersion and revealed by Gaussian null model, thereby revealing the presence of another vector, such as birds (Sarangzai *et al*. 2010).

Spatially explicit models can contribute to the decision making of forest managers. Management of dwarf mistletoes relies on scientific understanding of the ecology and epidemiology of these important pathogens in the context of on-the-ground forest conditions (Hawksworth and Weins 1996). Further observational and experimental studies are needed in order to clarify the mechanisms underlying this pattern. For example current infected patterns may reflect a legacy from previous demographic or human induced processes both in tree spatial distributions and within the tree. Also host vulnerability may be conditioned by predisposing factors such as soil heterogeneity or microclimate as well as genetic host variability that combine to result in observed patterns. Despite of this we suggest that spatial null models in combination with empirical studies are of great potential to understand the mechanisms underlying *A. oxycedri* spreading. .

REFERENCES

Akkol, E.K.; Orhan, I.; Kartal, M.; Yesilada, E., 2010: Bioactivity guided evaluation of anti-inflammatory and antinociceptive activities of *Arceuthobium oxycedri* (D.C.) M. Bieb. *Journal of Ethnopharmacology* 128, 79-84.

Aukema, J.E.; Martínez del Rio, C., 2002: Mistletoes as parasites and seed-dispersing birds as disease vectors: current understanding, challenges, and opportunities. In: D. J. Levey, W. R. Silva, and M. Galetti, (eds) *Seed Dispersal and Frugivory: Ecology, Evolution and Conservation.* Pages 99-110. CAB International Press. Oxfordshire, UK.

Aukema, J.E., 2004: Distribution and dispersal of desert mistletoe is scale-dependent, hierarchically nested. *Ecography* 27, 137-144.

Baddeley, A.; Turner, R., 2005: Spatstat: an R package for analyzing spatial point patterns. *Journal of Statistical Software* 12(6), 1-42.

Baddeley, A., 2008: Analyzing Spatial Point Patterns in R. Workshop notes, CSIRO Materials science and engineering. Australia. Available in http://www.csiro.au/resources/Spatial-Point-Patterns-in-R.html.

Bivand, R.; Pebesma, E., Gómez-Rubio, V. 2013: Applied Spatial Data Analysis with R. Second Edition. Springer, New York.

Brown, D.; Bolker, B., 2004: The Effects of Disease Dispersal and Host Clustering on the Epidemic Threshold in Plants. *Bulletin of Mathematical Biology* 66, 341-371.

Carlo, T.A.; Morales, J.M., 2008: Inequalities in fruit-removal and seed dispersal: consequences of bird behaviour, neighbourhood density and landscape aggregation. *Journal of Ecology* 96, 609-618.

Catalán, P., 1997: *Arceuthobium*. En: Castroviejo, S.; Aedo, C.; Benedí, C.; Laínz, M.; Muñoz Garmendia, F.; Nieto Feliner, G. & Paiva, J. (Eds.), *Flora Iberica. Plantas vasculares de la Península Ibérica e Islas Baleares* (Vol. VIII, Haloragaceae-Euphorbiaceae). Real Jardín Botánico, CSIC. Madrid 164-166.

Ciesla, W.M.; Geils, B.W.; Adams, R.P., 2004: Host and Geographic Distribution of *Arceuthobium oxycedri*. RMRS-RN-11WWW. Fort Collins, CO: U.S. Department of Agriculture, Forest Service, Rocky Mountain Research Station. Available in http://www.fs.fed.us/rm/pubs/rmrs_rn11/.

Clark, J.S.; Silman, M.; Kern, R.; Macklin, E.; HilleRisLambers, J., 1999: Seed Dispersal Near and Far: Patterns Across Temperate and Tropical Forests. *Ecology* 80(5), 1475-1494.

Cressie, N.A., 1991. *Statistics for Spatial Data*. Wiley, New York, USA.

Dale, M.R.T.; Powell, R.D., 2001: A new method for characterizing point patterns in plant ecology. *Journal of Vegetation Science* 12, 597-608.

De la Cruz, M., 2008: Métodos para analizar datos puntuales. In: Introducción al Análisis Espacial de Datos en Ecología y Ciencias Ambientales: Métodos y Aplicaciones (eds. Maestre, F. T., Escudero, A. y Bonet, A.), pp 76-127. Asociación Española de Ecología Terrestre, Universidad Rey Juan Carlos y Caja de Ahorros del Mediterráneo, Madrid. ISBN: 978-84-9849-308-5.

Diggle, P.J., 2003: *Statistical analysis of spatial point patterns*. Second edition. Arnold. London. UK.

Dixon, P.M., 2006: Nearest Neighbor Methods. *Encyclopedia of Environmetrics* 3.

Erran Seaman, D.; Powell, R.A., 1996: An Evaluation of the Accuracy of Kernel Density Estimators for Home Range Analysis. Ecological Society of America. *Ecology* 77(7), 2075-2085.

Getzin, S.; Wiegand, T.; Wiegand, K.; Fangliang, He., 2008: Heterogeneity influences spatial patterns and demographics in forest stands. *Journal of Ecology* 96, 807-820.

Hanisch, K.H.; Stoyan, D., 1979: Formulas for the second-order analysis of marked point processes. *Math. Operationsforschung Stat. Ser. Stat.* 10, 555-560.

Hawksworth, F.G.; Geils, B.W., 1996: "Biotic Associates". In: Hawksworth, Frank G.; Wiens, Delbert. (Eds.). Dwarf mistletoes: Biology, pathology, and systematics. Agricultural Handbook 709. Washington, D.C.: U.S. Dept. of Agriculture, Forest Service. 410 p.

Hawksworth, F.G.; Wiens, D.; Geils, B.W., 2002: Arceuthobium in North America. In: *Mistletoes of North American conifers*. Chapter 4. General Technical Report RMRS-GTR-98. United States, Department of Agriculture, Forest Service, Rocky Mountain Research Station, Ogden, UT.

Holt, R.D.; Dobson, A.P.; Begon, M.; Bowers, R.G.; SChauber, E.M., 2003: Parasite establishment in host communities. *Ecology Letters* 6, 837-842.

Illian, J.; Penttinen, A.; Stoyan, H.; Stoyan, D., 2008: *Statistical Analysis and Modeling of Spatial Point Patterns*. John Wiley & Sons Ltd. England.

Kelsall, J.; Diggle, P., 1998: Spatial Variation in Risk of Disease: A Nonparametric Binary Regression Approach. *Appl. Statist.* 47(4), 559 – 573.

Lavorel, S.; Stafford, M.; Reid, N., 1999: Spread of mistletoes (Amyema reissii) in fragmented Australian woodlands: a simulation study. *Landscape Ecology* 14, 147–160.

Liu, D.; Kelly, M.; Gong, P.; Guo, Q., 2007: Characterizing spatial-temporal tree mortality patterns associated with a new forest disease. *Forest Ecology and Management* 253, 220-231.

Lloyd, Ch., 2007: *Local Models for Spatial Analysis.* Queen's University Belfast. Edit. CSC Press.

Loosmore, N.B.; Ford, E.D., 2006: Statistical Inference using the G or K Point Pattern Spatial Statistics. *Ecology* 87 (8), 1925-1931.

Maloney, P.; Rizzo, D., 2002: Dwarf Mistletoe–Host Interactions in Mixed-Conifer Forests in the Sierra Nevada. *Phytopathology* 92, 597-602.

Marchette, D., 2009: *Filtered kernel density estimation.* John Wiley & Sons, Inc. WIREs Comp Stat 1, 106–10.

Martínez Beneito, M.A., 2005: *Métodos estadísticos en la detección de focos de riesgo en brotes epidémicos*. Disertación. Facultad de Matemáticas - Universidad de Valencia.

MØller, J.; Waagepetersen, R., 2004: *Statistical Inference and Simulation for Spatial Point Processes*. Edit. Chapman & Hall/CRC.

Nathan, R., 2007: Total dispersal kernels and the evaluation of diversity and similarity in complex dispersal systems. In: Dennis, A.J., Schupp, E.W., Green, R.J. & Westcott, D.W. (Eds.) *Seed Dispersal: Theory and its Application in a Changing World*. CAB International, Wallingford, UK, pp. 252–276.

Nickrent, D.L., 2002: Parasitic Plants of the World. In: J A López-Sáez, P Catalán and L Sáez (Eds.) *Parasitic Plants of the Iberian Peninsula and Balearic Islands*. Chapter 2. Mundi-Prensa, Madrid, pp. 7-27.

Ostry, M.E., Nicholls, T.H. and French, D.W. 1983: Animal Vectors of Eastern Dwarf Mistletoe of Black Spruce. U.S. Dept. of Agriculture. Forest Service. North Central Forest Experiment Station. Research paper NC-232.

Overton, J.M., 1994: Dispersal and infection in mistletoe metapopulations. *Journal of Ecology* 82, 711-723.

Overton, J.M., 1996: Spatial autocorrelation and dispersal in mistletoes: Field and simulation results. *Vegetation* 125, 83-98.

Ribbens, E.; Silander, J.A.; Pacala, S.W. 1994: Seedlings recruitment in forest: calibrating models to predict patterns of tree seedling dispersion. *Ecology* 75, 1794-1806.

Rios Insua, V., 1987: Contribución al estudio de la biología de *Arceuthobium oxicedri* (DC.) M. Bieb. (1819). *Bol. San. Veg. Plagas* 13, 53-62.

Ripley, B.D., 1977: The Second-Order Analysis of Stationary Point Processes. *Journal of Applied Probability* 13(2), 255-266.

Rist, L.; Shaanker, R.U.; Ghazoul, J., 2011: The spatial distribution of mistletoe in a Souther Indian tropical forest at multiple scales. *Biotropica* 43(1), 50-57.

Robinson, D.; Geils, B., 2006: Modelling dwarf mistletoe at three scales: life history, ballistics and contagion**.** *Ecological modelling* I99, 23–38.

Shaw, D.; Chen, J.; Freeman, E.; Braun, D., 2005: Spatial and population characteristics of dwarf mistletoe infected trees in an old-growth Douglas-fir - western hemlock forest. *Canadian Journal of Forest Research* 35, 990-1001.

Silverman, B.W., 1986: *Density Estimation for Statistics and Data Analysis*. CHAPMAN & HALL/CRC. New York.

Sorensen, A.E., 1986: Seed dispersal by adhesion. *Annual Review of Ecology and Systematics* 17, 443-463.

Stoyan, D.; Stoyan, H., 1996: Estimating Pair Correlation Functions of Planar Cluster Processes. *Biometrics Journal* 38(3), 259-271.

Stoyan, D; Penttinen, A., 2000: Recent applications of point process methods in forestry statistics. *Statistical Science* 15(1), 61-78.

Ward, M.; Paton, D.C., 2007: Predicting mistletoe seed shadow and patterns of seed rain from movements of the mistletoe bird. *Dicaeum hirundinaceum*. *Austral Ecology* 32, 113-121.

Watson, D.M.; Roshier, D.A.; Wiegand, T., 2007: Spatial ecology of a root parasite from pattern to process. *Austral Ecology* 32, 359-369.

Watson, D.M., 2009: Determinants of parasitic plant distribution: the role of host quality. *Botany* 87, 16-21.

Watson, D.M., 2011: *Mistletoes of southern Australia*. CSIRO Publishing, Collingwood.

Watson, D.M. and Rawsthorne, J., 2013: Mistletoe specialist frugivores: latterday 'Johnny Applesseds'of self-serving market gardeners? *Oecologia* 172, 925-932.

Wiegand, T.; Gunatilleke, S.; Gunatilleke, N., 2007: Species Associations in a Hetrogeneous Sri Lankan Dipterocarp Forest. *The American Naturalist* 170(4), E77 – E95.

Wiegand, T.; Moloney, K., 2004: Rings, circles and null-models for point pattern analysis in ecology. *Oikos* 104, 209-229.

Worton, B.J., 1989: Kernel Methods for Estimating the Utilization Distribution in Home-Range Studies. *Ecology* 70, 164 – 168.

Zavala, I.; Zavala, M., 1993: Global Positioning System as a tool for ecosystem studies at the landscape level: an application in the Spanish Mediterranean. *Landscape and Urban Planning* 24, 95 – 104.

Zilka, P.J.; Tinnin, R.O., 1976: Potential avian influence in the distribution of dwarf mistletoe. *Northwest Science* 50(1).

CAPÍTULO 2

Development and test of tools for analyzing replicated point patterns with a two-way analysis of variance model

Abstract

Most ecological studies involving point pattern analyses are based on a single plot. This prevents disentangling the effects of several processes which could be acting simultaneously and limits the conclusions that can be extracted from these studies. However, considering the spatial distribution of individuals in several plots as replicates of the same process could help to differentiate specific effects from those of other confounding processes.

We introduce a novel two-way ANOVA-like method to analyze replicated spatial point patterns. Having summarized the spatial patterns with K-functions, the method computes averaged K functions for each level of the two factors (i.e., predictors) and for each combination of levels, and estimates the sum of squared deviations from the overall mean K function. An inference on the strength of the relationship between the predictors, their interaction and the spatial structure, was the main goal. Non-parametric bootstrap procedure was used to cuantify the dependency among spatial scales.

We illustrate the approach analyzing the effects of altitude (with two levels; low, high) and topography (with two levels: flat, steep slope) on the spatial pattern of *Croton wagneri*, a dominant shrub in an Andean dry scrubland. Our method revealed significant effects of both topography and of their interaction with altitude, which could not have been detected with current point pattern analysis methodology.

The prevalence of single-plot analysis in ecological studies may be due to both the lack of familiarity with the methods, the complexity of these and the absence of appropriate software to deal with replicated point patterns. Our approach allows us to address a significant amount of ecological questions while maintaining a simple, understandable and easily reportable methodological framework.

Abbreviations.- ANOVA: analysis of variance, BTSS: between treatments sums of squares, PCP: Poisson cluster process.

Introduction

The spatial ecology paradigm (Tilman and Kareiva 1998) highlights the relevance of space in the functioning of ecosystems and recognises that the assembly and functioning of plant populations and communities are also ruled by spatial processes. From the pioneering work of Watt (1947) extensive evidence has accumulated showing that the spatial distribution of plant species is not random but instead individuals often show local aggregation and/or overdispersion within populations and communities (e.g., Watt 1947, Pielou 1977, Kenkel 1988, Barot *et al.* 1999, Condit *et al.* 2000). In this context, point pattern analysis has emerged as a powerful tool to integrate space in ecological theory and more specifically to connect the realized patterns with their generating processes (Wiegand and Moloney 2014). The basic assumption when analysing ecological point patterns is that the patterns conserve some signature from past processes and therefore constitute an "ecological archive" from which it is possible to recover information on the underlying processes (McIntire and Fajardo 2009; Wiegand and Moloney 2014). For example, aggregated spatial patterns can be related to limited dispersal (e.g., Seidler and Plotkin 2006), and overdispersed patterns to intraspecific competition (Kenkel 1988).

The link between processes and realized patterns is not always evident or direct, because it may be confounded by the interaction between several processes (Wiegand *et al.* 2009) or by the intrinsic spatial nature of the processes generating the pattern (e.g. environmental heterogeneity; Getzing *et al.* 2008, Chacón-Labella *et al.* 2014, Jara-Guerrero *et al.* 2015). In fact, a methodological limitation which contributes to the prevalence of these confounding effects is the fact that most ecological studies involving point pattern analysis are based in just one plot (or in several plots but analysed individually). However, the spatial distribution of plants in several plots can be considered replicates of the same process (Bagchi and Illian 2015) and could help to disentangle its effects from the effects of other confounding processes (e.g., the typical confounding between a clustering process and environmental heterogeneity; Law *et al.* 2009, Diggle 2014). In consequence, the use of replicated patterns in combination with an appropriate sampling design would help to generalize the insights gained from point pattern analysis, and could also be employed to test specific hypotheses about specific processes affecting the spatial structure of the studied populations or communities. For example one could test whether differences of aggregation exists between different groups of species in a community or between life-stages (i.e., adult vs. juvenile) in a population (LeMay *et al.* 2009) or if these differences arise because the populations grow on different soil substrates (Schenk *et al.* 2003).

Although methods for analysing replicated point patterns are available in the statistical literature, they have scarcely been used in ecological studies (but see Schenk *et al.* 2003, LeMay *et al*. 2009). Succinctly, they can be classified into parametric and non-parametric methods (Landau and Everall 2008). Parametric methods use maximum likelihood or pseudo-likelihood methods to fit the parameters of a point process model. They have been employed to fit certain homogeneous point processes such as pairwise interaction (Diggle *et al*. 2000, Mateu 2001) or Gibbs point processes (Bell and Grunwald 2004). Non-parametric methods evaluate differences in summary functions (mainly Ripley's K function) among experimental or observational groups. Within the non-parametric methods, two alternative approaches have been developed: the method of Diggle *et al.* (1991), analogous to the analysis of variance (ANOVA) for the one-way design, and the method of Landau and Everall (2008) for the repeated measurements (and other more complicated) designs. In general, the prevalent idea is that the performance of non-parametric methods is more efficient in comparison with the parametric ones and is less prone to model miss-specifications (Diggle *et al*. 2000, Bagchi and Illian 2015). This versatility suggests their use and application in ecological contexts. Precisely, in order to promote their use in ecological studies, Bagchi and Illian (2015) have recently summarized the non-parametric methods, mostly focusing on the repeated measures approach, which involves linear mixed modelling of parameters describing the differences of spatial aggregation among groups of treatments or the effect of covariates, considering random effects. Although this approach is extremely useful in some contexts (for example when there are many groups or levels --and replicates-- for each treatment), many important ecological questions can be more easily answered with even simpler methods (Murtaugh 2007). In fact, in contrast with linear mixed models, non-parametric ANOVA-like methods are less prone to mistakes and are straightforward to explain and understand (Murtaugh 2007).

Here, we propose an extension of Diggle *et al.* (1991) ANOVA-like method for replicated point patterns to the two-way case, where the interest is focused on the interactions of the two factors considered in the (experimental) sampling design.

This new method is applied in a case study of a dry scrubland dominated by *Croton* in Southern Ecuador. *Croton wagneri* Müll. Arg. is an endemic shrub than provides most of the biomass to the Ecuadorian Dry Mountain Scrub ecosystem, where he acts as a key ecosystem engineer providing refuge and shelter against hard environmental conditions to many other species (Valencia *et al*. 2000, Espinosa *et al.* 2014). Its spatial structure, therefore, rules the functioning of these communities. Observational evidence shows that *C. wagneri* populations have an aggregated spatial distribution

and suggest that the intensity of the spatial aggregation varies along an altitude gradient in response to changing environmental conditions.

In the case of *C. wagneri*, as for any other desert or semiarid shrub, aggregated patterns could be the result of limited dispersal (Ellner and Shmida 1981, Seidler and Plotkin 2006), facilitation (i.e., the nurse effect, Flores and Jurado 2003), the preference for favourable microsites where water and nutrients are more accessible (Schlesinger *et al*. 1996, Rietkerk *et al.* 2002) or a combination of all these mechanisms. In fact, it has been suggested that the characteristic biphasic bare-cover mosaic of drylands results from the interplay between local positive interactions and competition for water, which generates a scale-dependent feedback, locally positive and negative farther away (Rietkerk and Van de Koppel 2008; Maestre and Escudero 2009). It has been shown, both theoretically (Lefever *et al*. 2009, Siteur *et al*. 2014) and empirically (Deblauwe *et al*. 2011) that different environmental conditions, in particular referred to aridity and slope (Lefever et al. 2009, Deblauwe *et al*. 2011) can alter or modify this feedback, which results in different spatial configurations of standing biomass (Maestre and Escudero 2009).

In our case study, we want to test if these mechanisms rule the spatial distribution of the individuals of *C. wagneri*. This scrubland extends along an altitudinal gradient (from 1000 to 2500 m) where aridity decreases from lower to higher altitudes (Richter and Moreira-Muñoz 2005). We hypothesized that the effect of aridity on the spatial structure of *C. wagneri* will be modified by the slope, with populations on steeper slopes being similarly aggregated, irrespective of altitude because of the stressful conditions (thin soils and run-off), independent of rainfall, that are prevalent in steep slopes (in contrast to populations on mild slopes or flat ground, which will show a marked effect of aridity, i.e. altitude, on aggregation). Translated to the two-way ANOVA jargon, we expect the existence of an interaction between slope and altitude. We used our extension of Diggle *et al*. (1991) method for the two-way design to test the existence of this interaction. We compared the results of our test with those of a more traditional approach (e.g., Seidler and Plotkin 2006) which consist in a classical ANOVA on the parameters of a spatial point process model (a Poisson cluster model) fitted to each *C. wagneri* pattern.

Methods

Study site

The study was conducted in southern Ecuador, on the slopes of an Andean valley (Alamala, cantón Catamayo, 03 ° 58 '29' S, 01 ° 25 '22' W), covering an altitudinal gradient from 1400 to 1900 m.a.s.l.

Annual average temperature and rainfall vary from 33.8 °C and 423mm respectively in the lower zone to 27.4 ºC and 562mm in the upper zone. Rain is mostly distributed from January to April and almost inexistent for the rest of the year (Espinosa et al. 2014). Vegetation forms conspicuous perennial patches interspersed in bare soil areas (occupied by annual plants during the rainy season). *Croton wagneri* (Euphobiaceae) is the dominant patch-forming scrub that conform the vegetation patches, and other perennial species are represented by rare isolated individuals (Espinosa et al. 2014).

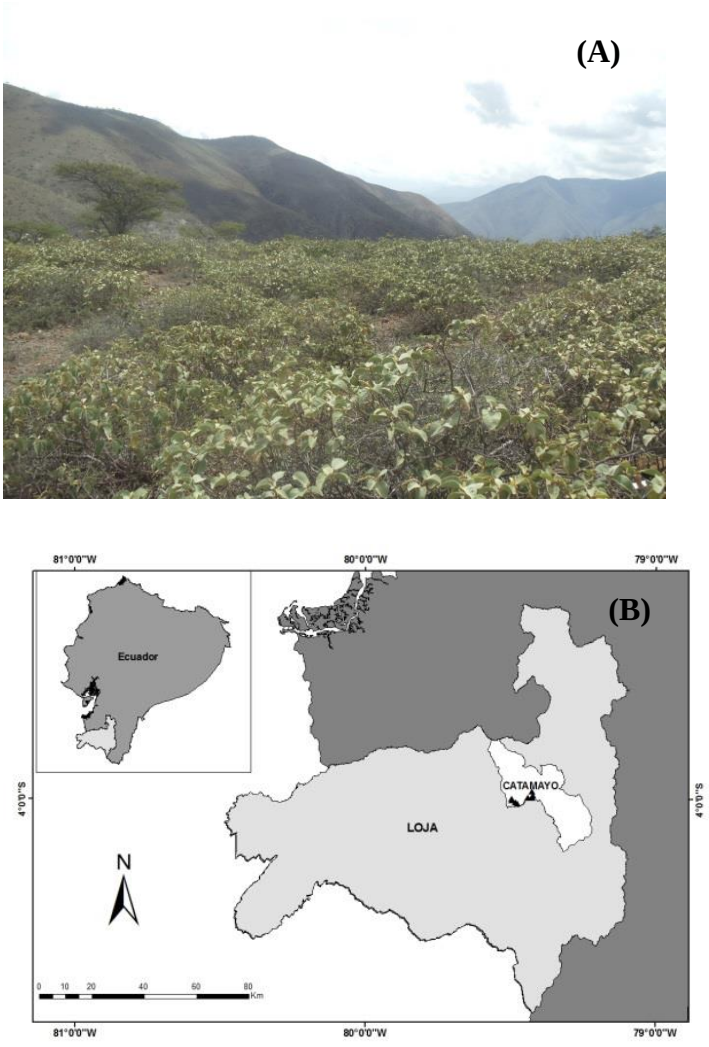

Figure 1 (A) Shrubland dominated by *Croton wagneri*. (B) Study site location

Data collection

A total of 16 (30x30m) plots were installed, on two altitude levels: "low altitude" (between 1400 and 1500 m.a.s.l.), and "high altitude" (between 1750 and 1900 m.a.s.l.). In each altitudinal level four plots were placed on flat ground and four on steep slopes (> 27º inclination). Plots at each altitude were located no less than 200 m apart from each other. In each plot, all *Croton wagneri* individuals were mapped using a compact Electronic Laser Hypsometer TruPulse 360º, which allowed us to calculate horizontal distance, inclination and azimuth (central angle), from a fixed common vertex to the rooting point of each individual with a precision of 1 cm.

Spatial pattern description

To summarize the spatial pattern of *C. wagneri* in each plot, we used Ripley's K function (Ripley 1977). λK(r), where λ is the intensity of the plot, is the expected number of points within in a circular area radius *r* around a typical point of the pattern. The expected value for a random pattern is $K(r) = \pi r^2$.

The K functions were calculated using a standard unbiased estimator (Ripley 1976) with isotropic edge correction

$$\widehat{K}(r) = n^{-2} A \sum_{g \neq h} e^{-1}(g,h) I[d(g,h) \leq r]$$

where $d(g,h)$ represents the Euclidean distance between individuals g and h, for each replicate in all level of altitude (A) and topography (B) factors. I[.] is the indicator function and $e^{-1}(g,h)$ is an edge correction defined as the proportion of the circumference of a circle centered on individual g with radio $d(g,h)$ and contained within the sampling area A.

To characterize the magnitude of aggregation in each plot, we additionally fitted a Poisson cluster process (PCP) model to each observed K function using the method of minimum contrast (Diggle 2003). A PCP describes the formation of the pattern as a two-step process. First, a Poisson pattern of "parent" points is generated with intensity ρ. Then, each parent point produces "offspring"; the number of offspring per parent follows a Poisson distribution, and their locations are independent and isotropically normally distributed around the parent points, with mean zero and standard deviation σ. The theoretical K function for a PCP is

$$K(r;\ \rho, \sigma) = \pi\, r^2 + \frac{1 - e^{(-r^2/4\sigma^2)}}{\rho},$$

Estimation of K function for replicated data and between-groups comparison in a two-factorial design.

A detailed description of the non-parametric ANOVA-like method for the one-way design proposed by Diggle *et al.* (1991) and modified by Diggle (2003) is presented in Appendix 2 in the Supplementary material. When we have an experimental design with two crossed factors, A, with levels i=1,…*a*, and B, with levels j = 1, …, *b*, it is straightforward extending Diggle *et al*. (1991) approach. The structure of the model used to describe the data would be:

$$K_{ijk}(r) = K_0(r) + A_i + B_j + A_iB_j + e_{ijk}(r)$$

where $K_{ijk}(r)$ is the K-function for the *k*th replicate in the *ij*th cell of the observational or experimental design, A_i, B_j and A_iB_j are respectively the effects of the corresponding levels of factors *A*, *B* and their interaction, $K_0(r)$ is the overall mean K-function and $e_{ijk}(r)$ is the residual error associated to the function $K_{ijk}(r)$.

In the case of a two-factorial design, the main interest resides in testing the existence of an interaction between the two factors. A statistic analogous to the sum of squares for the interaction term in a two-way ANOVA would be:

$$BTSS = \sum_{i=i}^{a}\sum_{j=1}^{b} n_{ij} \int_0^{r_0} w(r)\{\widehat{K}_{ij}(r) - \widehat{K}_i(r) - \widehat{K}_j(r) + \widehat{K}_0(r)\}^2 dr$$

where n_{ij} is the total number of points (summed up among the *k* replicates) in the *ij*th cell, r_0 is the largest scale (i.e., the maximum *r*) for which we are interested in spatial differences, $w(r)$ is a function to normalize large scale variation in the differences between K functions; $\widehat{K}_0(r)$ is the overall weighted averaged K-function, and $\widehat{K}_{ij}(r)$, $\widehat{K}_i(r)$ and $\widehat{K}_j(r)$ are the weighted average K-functions estimated for different levels and combinations of levels of the factors *A* and *B*. Specifically,

$$\widehat{K}_l(r) = \sum_{x=1}^{m_l} n_x \widehat{K}_x(r) \Big/ \sum_{x=1}^{m_l} n_x$$

where m_l is the number of replicates where level *i*, level *j* or combinations of level *i* and *j* of factors A and B applies, and n_x and $\widehat{K}_x(r)$ are respectively the number of points and the K-function in replicate *x*.

Following the approach of Diggle *et al*. (1991), we use sampling with replacement to estimate the sampling distribution of this BTSS. First, we compute the residual function as

$$\hat{R}_{ijk}(r) = n_{ijk}^{0.5}\left[\hat{K}_{ijk}(r) - \hat{K}_i(r) - \hat{K}_j(r) + \hat{K}_0(r)\right]$$

This function will estimate the $e_{ijk}(r)$ term in our model. Including (and subtracting) $\hat{K}_i(r)$,and $\hat{K}_j(r)$ allows the individual effects of *A* and *B* factors to be removed and guarantees that the residual functions are exchangeable under the null and alternative hypotheses (Anderson & Ter Braak 2003).

Analogously to the single-factor analysis in Diggle *et al.* (1991), by sampling with replacement from the set of residual functions $\hat{R}_{ijk}(r)$ we obtain resamples $R^*_{ijk}(r): k = 1, \dots, m_{ij};\ i = 1, \dots, a; j = 1, \dots, b$ and we use them to compute a set of resampled K-functions under the null hypothesis of no interaction as:

$$\hat{K}^*_{ijk} = \hat{K}_i(r) + \hat{K}_j(r) - \hat{K}_0 + n_{ijk}^{-0.5} R^*_{ijk}(r)$$

Again, each resample is a complete set of K-functions (i.e., as many functions as replicates in the study), and it is used to compute a resampled BTSS value.

Inference for the test is obtained comparing the observed BTSS value with the distribution of *s* resampled BTSS values. In case that the null hypothesis of no interaction is not rejected, one could proceed to test the effects of each of the individual factors. This could be made using the methodology of Diggle *et al.* (1991) for the one-factor case.

Analysis of validity and power of the test

To analyze the validity and power of the test proposed for detecting interactions, we have followed the same procedure of Diggle *et al.* (1991). The validity of the test in the context of our study (i.e., its ability to provide an acceptable probability of making type I error) was tested by applying a bootstrap procedure to generate 1000 sets of 16 replicated patterns (i.e., the same number of replicates than in our study), simulated to conform with the null hypothesis (i.e., absence of interaction). If the test is valid, we expect that the probability of rejecting the null hypothesis is near to its nominal (α) value.

We simulated replicates with abundance and spatial pattern similar to the observed ones. As most of them showed a clearly aggregated pattern, we first fitted a Poisson cluster process (PCP; Diggle 2003) to each of the 16 observed replicates. This allowed us to choose parameters for our

simulations. In order to simulate the null hypothesis of no interaction, we simulated 2 subsets (each 8 replicates), one highly aggregated (mean ρ = 0.05932577, i.e., 53.4 clusters/plot) and other less aggregated (mean ρ = 0.01784474, i.e., 16.1 clusters/plot). In both cases, dispersion was set to σ = 5m. These parameters were selected arbitrarily among the range of fitted parameters to the original patterns. The "highly aggregated" and "less aggregated" patterns were respectively assigned to the levels "flat" and "steep" of the factor slope, whereas the levels "low" and "high" of factor altitude were randomly assigned to each replicate. The number of points simulated in each replicate was similar to the ones recorded in the observed replicates.

In order to evaluate the power of the test and its dependence on differences of clustering between replicates, we implemented another 1000 simulations (16 replicates each) for each of a series of different scenarios of the alternative hypothesis (presence of interaction). For this, we assigned a fixed, low aggregated structure (PCP with ρ=0.39; i.e., around 350 clusters per plot) to the plots whit the combinations "low altitude -steep slope" and "high altitude -flat slope" and for all other groups (plots with the combinations "low altitude -flat slope" and "high altitude-steep slope") simulated more aggregated PCP processes (from ρ=0.350 to ρ=0.001, i.e., from 315 to just 1 cluster per plot).

Statistical analyses

We tested the existence of an interaction between the effects of altitude and slope on the spatial pattern of *C. wagneri* using the ANOVA-like procedure. We computed K(r) functions from r = 0 to 8 m, with 0.05 m intervals, with the isotropic edge correction. For the computation of the sum of squared differences (BTSS) we set $w(r) = r^{-2}$, following Diggle (2003). The significance of the computed statistic was evaluated with 1000 bootstrap resamples.

To compare our approach with other alternatives, we conducted also a rank-based ANOVA (Hetmansperger and McKean 2011) to analyze the variation, among the observational groups, of the parameter σ of the Poisson cluster processes fitted to each *C. wagneri* realized pattern. This parameter is usually employed as a measure of the degree of aggregation of spatial patterns and has been employed to assess differences among patterns generated by different processes (e.g., Seidler and Plotkin 2006, Jara-Guerrero *et al*. 2015).

All calculations were conducted in R (R Core Team 2013) using the packages "Rfit" (Kloke and Mckean, 2012), "spatstat" (Baddeley and Turner 2005) and "ecespa" (De la Cruz 2008). Functions to compute and test the ANOVA-like statistic both in the one- and two-way designs have been included in the R package "replicatedpp2w".

Results

In all plots, the observed K-functions revealed patterns compatible with Poisson cluster processes (Table 1, Fig. 2), with some plots showing also a small-scale inhibition (for r < 1 m) (Fig. 2). In general, plots in flat slopes at low altitude and plots in steep slopes at high altitude showed less clustering than the rest, although the group of flat slopes at low altitude was also the most aggregated at fine scales (r < 1 m; Fig. 2 and Fig. 3).

The analysis confirmed the existence of a significant interaction between slope and altitude on the spatial pattern of *Croton* (p = 0.009; Fig.4), and additionally a significant effect of topography (p = 0.039; Table 2).

Table 1. Summary of the plots attributes. Altitude: meters above sea level, Topography: landform. N: number of points (shrubs) per plot. Canopy: mean canopy area ±1se, estimated by the area of an ellipse from the canopy diameters. Parameters of the Poisson cluster process fixed to each plot. nclus: number of clusters (= ρ x 300 m x 300 m), mu: mean number of points per cluster, σ: dispersion parameter.

Plot	Altitude (m)	Topography	N	Canopy (m^2)	nclus	mu	σ (m)
1	1400	plane	859	0.2056±0.0120	36.2	23.7	2.45
2	1400	plane	239	0.1379±0.0137	79.8	3.0	1.14
3	1400	slope	285	0.2295±0.0194	1.8	162.0	8.78
4	1400	slope	395	0.2219±0.0207	20.0	19.8	2.93
5	1500	plane	815	0.1562±0.0069	38.1	21.4	3.00
6	1500	plane	724	0.0960±0.0067	165.0	4.4	1.24
7	1500	slope	296	0.2972±0.0260	33.2	9.0	2.86
8	1500	slope	665	0.1257±0.0079	18.3	36.4	3.90
9	1750	plane	650	0.1303±0.0111	30.5	21.3	2.15
10	1750	plane	679	0.3328±0.0190	19.2	35.4	3.30
11	1750	slope	1959	0.055±0.0022	81.0	24.2	2.05
12	1750	slope	541	0.313±0.0246	59.4	9.1	2.79
13	1900	plane	561	0.3397±0.0319	9.6	58.4	4.19
14	1900	plane	732	0.2865±0.0174	1.4	536.6	22.04
15	1900	slope	879	0.0513±0.0045	29.1	30.2	4.94
16	1900	slope	571	0.2430±0.0187	1.7	342.9	18.82

Table 2. Analysis of variance for replicated patterns. BTSS: sum of squared differences. p-value estimated after 1000 sampling with replacement (bootstrap) of residual functions. For the calculation of BTSS we have used K(r) functions estimated from r=0.05 to r=8 m, at intervals of 0.05 m.

Factor	BTSS	p-value
Slope	1373518.4	0.039
Altitude	259998.3	0.408
Slope : Altitude	2086014.1	0.009

Our validity analysis (Table S1) showed that, in general the test is somehow liberal and rejects the null hypothesis more frequently than expected by the nominal value. However, in the particular case of the test for the interaction, it is quite close to its nominal value. Given the small p value obtained in our study (0.009) we are confident that the null hypothesis of no interaction is rejected at least at the $\alpha = 0.05$ level.

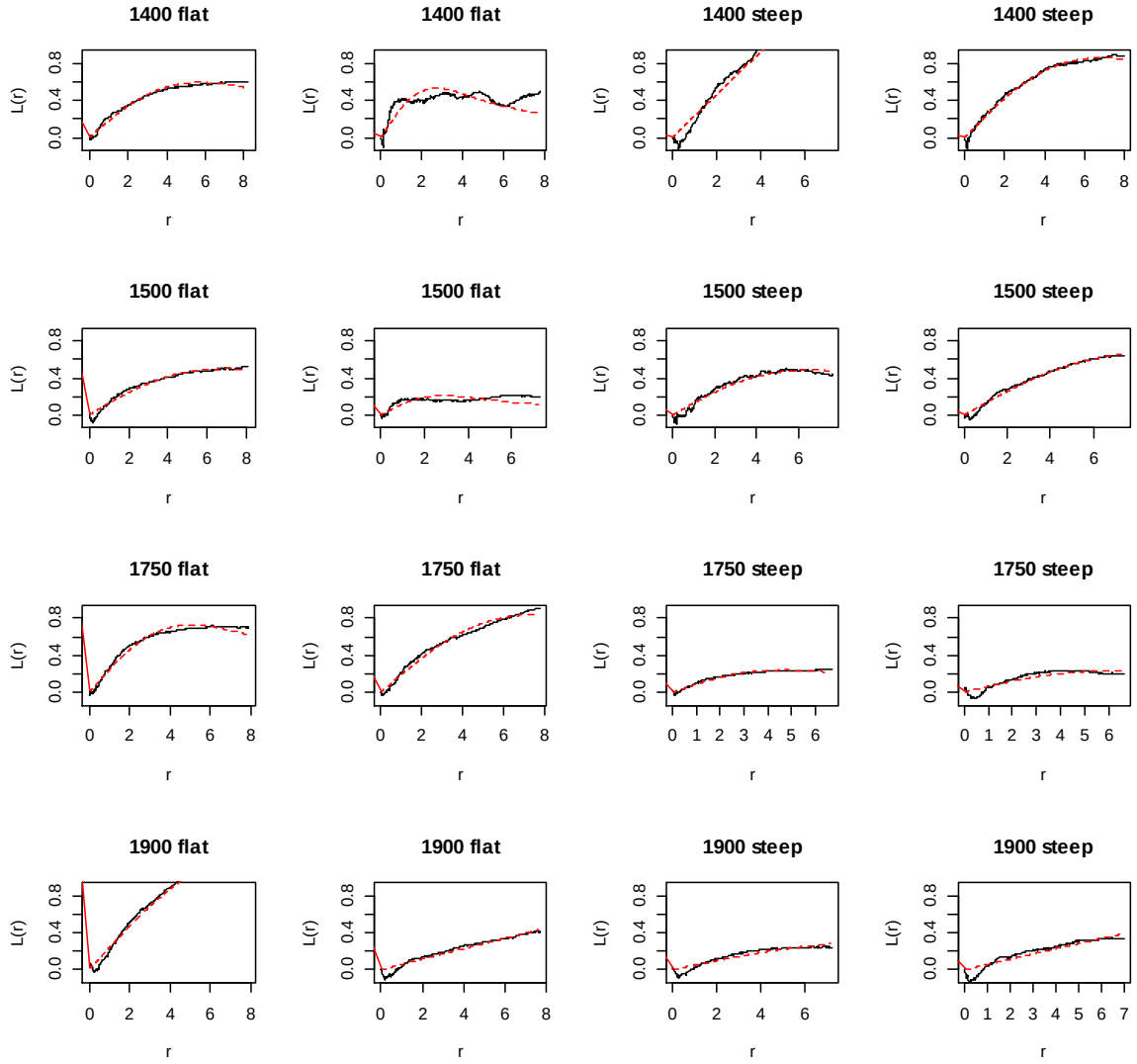

Figure 2 K-function of the *Croton sp.* point patterns at different altitude (number in meters) and topography. The continuous black lines represent the empirical values of L(r); the dashed red lines represent the fitted values of Poisson cluster process. For representation and interpretation purposes, we used the L(r) function, i.e., a standardized version of K(r) (Besag 1977) $L(r) = \sqrt{K(r)/\pi} - r$, which for a random pattern has an expected value of 0 at all distances r (Dixon 2001).

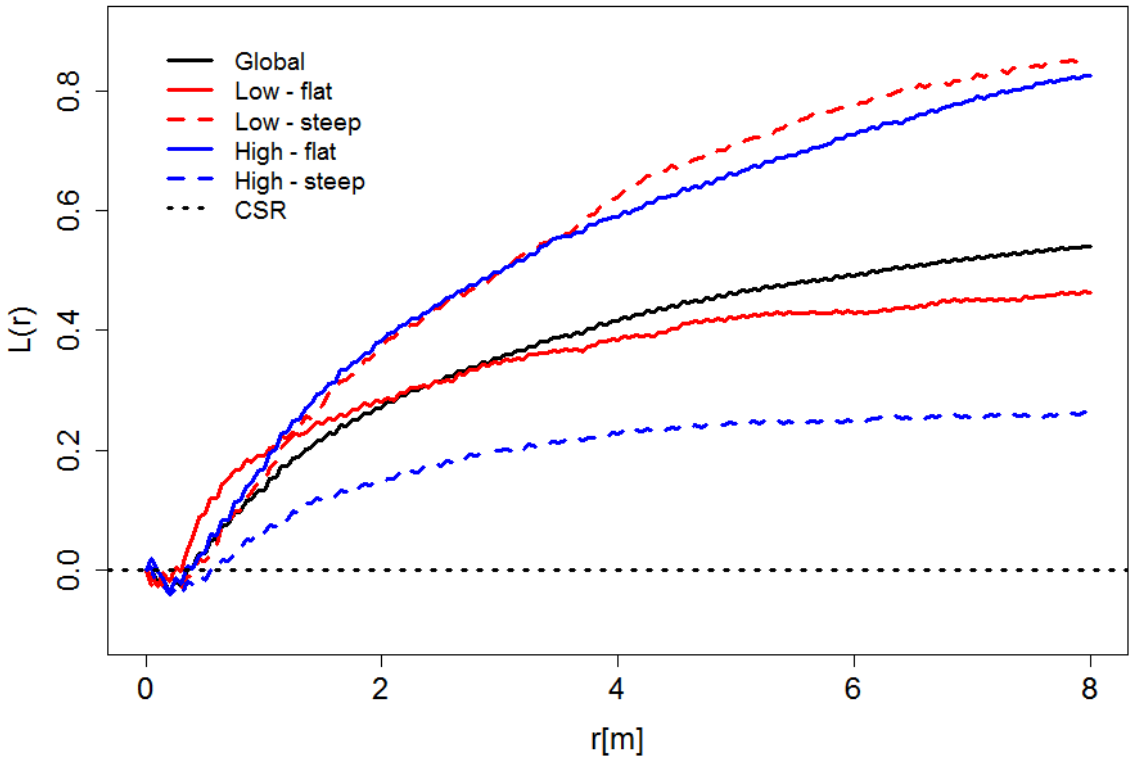

Figure 3 Averaged K(r) functions for each combination of treatments, (transformed as $L(r) = \sqrt{K(r)/\pi} - r$) to facilitate interpretation. CSR: expected value for a plot with Complete Spatial Randomness. Global: Overall average K(r) function.

On the other hand and quite logically, the power of the test increases as the differences in the number of clusters between combinations of factor levels increases (Table S2). In contrast, the rank-based ANOVA analysis could not confirm the existence of a difference of fitted σ values among altitude and slope groups nor an interaction (Table 3).

Table 3. Rank-based ANOVA results for the variation among groups of the σ parameter of the Poisson cluster process fitted to each point pattern. Df: degrees of freedom.

	Df	F value	p-value
Altitude	1	0.625	0.444
Slope	1	0.534	0.479
Altitude:Slope	1	0.663	0.431
Residuals	12		

Discussion

Our ANOVA-like method for analysing replicated patterns works and detects interactions between experimental factors. In our case study, the spatial pattern of all populations was aggregated. If we had followed the usual approach of using just one plot or simply had obtained a weighted average of the replicated plots (e.g. Raventós *et al*. 2010) to analyse the spatial pattern of *Croton wagneri*, we could only have arrived to the conclusion that the shrub showed aggregation, which is not quite surprising given that it is a dispersal-limited species (Jara-Guerrero *et al.* 2011). Using the approach of Diggle *et al*. (1991) to analyze the effects of slope or altitude individually, we would have concluded that altitude was irrelevant to the spatial organization of *C. wagneri*. However, using our new non-parameric two-way ANOVA-like approach, we were able to detect that the spatial pattern of *C. wagneri* seems to be driven by the interaction of altitude and slope (Fig. 4). By the way, this result could have not been found by using the more traditional approach (e.g. Seidler and Plotkin 2006) of comparing the parameters of fitted individual Poisson cluster processes (Table 3).

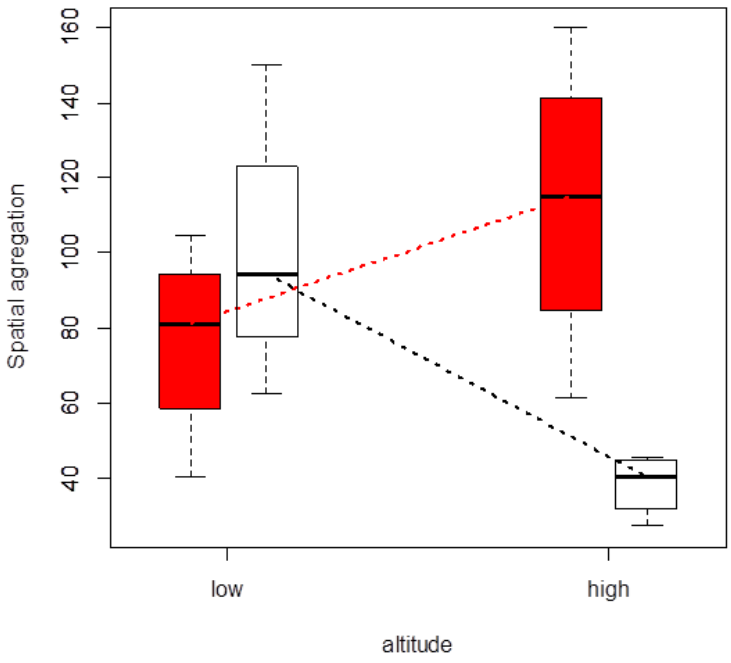

Figure 4 Differences of spatial aggregation between plots. Red boxes: plots in flat slopes; white boxes: plots in steep slopes. Here, "spatial aggregation" is measured for each plot as the sum of values of the L(r) function [$L(r) = \sqrt{K(r)/\pi} - r$]; for all plots K(r) was computed for r=0 to r=8 with 0.05 m intervals. The expected value of the empirical L-function respect to complete random process is L(r)=0, whereas positive values indicate aggregation.

We had hypothesized that the differences of aridity would generate differences of aggregation between the low- and high-altitude *Croton* populations growing on flat ground and that topography would exacerbate the effect of aridity in populations growing in steep slopes, which would promote the greatest aggregation, irrespective of altitude. We expected that this would show up as a significant interaction effect in our two-way analysis. In fact, a significant interaction was detected, but occasioned by a different mechanism. On the one hand, aggregation on steep slopes was not equally uniform, but differed between low and high altitudes, with plots on steep slopes in high altitude showing, on average, the lowest aggregation. On the other hand, and contrarily to our initial hypothesis, the largest aggregation, on average, occurred in the populations growing on flat ground at high altitude. This is surprising since this combination does not seem the most stressful. Although nurse effects, and consequently more aggregated patterns, are expected to be more important at the places with the most severe environmental conditions (e.g., in the dryer areas at low altitude; Flores and Jurado 2003; Maestre *et al.* 2009), other mechanisms could be responsible of the different aggregation of *C. wagneri* between different sites. On the one hand, as a barochorous species, it is intrinsically dispersal-limited (Jara-Guerrero *et al.* 2011) which could affect the expected spatial structures resulting from the scale-dependent feedbacks between plants and soil water availability (Pueyo *et al*. 2008). On the other hand, *Croton* seeds have the potential for secondary dispersal by ants (Jara-Guerrero *et al*. 2011), which could be acting differently along altitude (Smith *et al*. 1989) and interfering with the formation of the spatial structures of *C. wagneri* by other mechanisms (Kalisz *et al*. 1999, Zhou *et al*. 2007).

Alternatively, the "unexpected" results for the populations growing on flat grounds at low and high altitude are a consequence of a shift in the structure of the vegetation in response to the decrease of aridity with altitude. Deblawe *et al*. (2011) showed that a decrease of aridity conditions causes the transition from isolated "spots" to larger, connected masses ("labyrinths") of standing biomass. In fact, the average σ parameter of the fitted Poisson clusters for the populations on flat ground at high altitude is the largest (σ = 7.92 m, corresponding to an average cluster size of 22.40 m) and the mean density of clusters (estimated from the fitted ρ parameter) is the smallest (only 15.2 clusters in the 30 x 30 m plot). In contrast, in the populations on flat ground at low altitude these parameters are respectively the smallest (σ =1.96 m, corresponding to an average cluster size of 5.54 m) and largest (79.7 clusters). This could help to explain why the average K function of this group is the largest at small scales (Fig. 3). In other words, there is a transition from small abundant spots at low altitude (i.e., more severe condition) to a few large patches at high altitude. This suggests that, irrespective of

(or in addition to) nurse effects and limited dispersal, the spatial organization of *C. wagneri* is mainly driven by a eco-hydrologic feedback processes (Pueyo *et al*. 2008).

The effect of slope sharply varied between altitudes. Contrary to our initial hypothesis, the smallest spatial aggregation appeared in the steep slope plots at high altitude. Average size of the patches in these plots is not quite different from that in the high altitude plots in flat ground (σ = 7.15 m) but they present the largest spatial inhibition at fine scales (Supplementary information; Fig. S1). Since we are using the K function to measure spatial aggregation, which has "memory" (Wiegand and Moloney 2014), the low densities at small scales are influencing (i.e., decreasing) the values of the function at larger scales, with the final result of these "less aggregated" findings. In any case, the spatial inhibition reaches up to 0.8 m, which discards the existence of nurse effects at this location.

On the other hand, the increase of spatial aggregation with respect to flat ground populations at low altitude is caused by an increase in the average size of patches (σ = 4.62 m; average size = 13.01 m) and a parallel decrease in their number (average number of cluster per plot= 18.2). Applying the same reasoning employed previously, this would suggest a better hydrological environment on the slopes than in the flat ground, which seems odd. An alternative or complementary hypothesis could be related to the fact that *Croton* is reaching its uppermost local limit which suggest that climate conditions are far from its optimum at these sites. Under such milder conditions, *Croton* physiological performance would be limited and the species would be seriously stressed. This paradox, the worst performing on flat ground, would be compatible with the patterns arisen in steep, high altitude scenarios simply because those more xeric conditions are more physiologically favourable to the species.

In conclusion, our new two-way ANOVA-like method, in combination with replicated point patterns obtained from an appropriate sampling or experimental design, can shed light on processes and mechanisms unaffordable with other spatial techniques. Our method is easy to use and their results are straightforwardly interpretable in ecological terms. In addition its reliability and its power can be easily assessed in any specific context. We think that all this would stimulate the use of replicated spatial point pattern analyses by ecologists in the future.

REFERENCES

Anderson, M. J. and Ter Braak, C. J. F. 2003. Permutation tests for Multi-factorial Analysis of Variance. - J. Statist. Comput. Simul. 73(2): 85-113.

Baddeley, A. and Turner, R. 2005. Spatstat: an R package for analyzing spatial point patterns. - J. Stat. Softw. 12(6): 1-42.

Bagchi, R. and Illian, J. B. 2015. A method for analyzing replicated point patterns in ecology. - Methods Ecol. Evol. doi: 10.1111/2041-210X.12335.

Barot, S. et al. 1999. Demography of a savanna palm tree: Predictions from comprehensive spatial pattern analyses. - Ecology 80(6): 1987-2005.

Bell, M. L. and Grunwald, G. K. 2004. Mixed models for the analysis of replicated spatial point patterns. - Biostatistics 5(4): 633-648.

Chacon-Labella, J. et al. 2014. Negative density dependence and environmental heterogeneity effects on tree fernus across succession in a tropical montane forest. Perspect. - Plant Ecol. Evol. 16(2): 52-63.

Condit, R. et al. 2000. Spatial patterns in the distribution of tropical tree species. - Science, 288: 1414-1418.

De la Cruz, M. 2008. Métodos para analizar datos puntuales. - In: Maestre, F. T., Escudero, A. y Bonet, A. (eds.) Introducción al Análisis Espacial de Datos en Ecología y Ciencias Ambientales: Métodos y Aplicaciones. AEET, Universidad Rey Juan Carlos y Caja de Ahorros del Mediterráneo, Madrid. pp. 76-127.

Deblawe, V. et al. 2011. Environmental modulation of self-organized periodic vegetation patterns in Sudan. - Ecography 34: 990-1001.

Diggle, P. J. et al. 1991. Analysis of Variance for Replicated Spatial Point Patterns in Clinical Neuroanatomy. - *J. Am. Stat. Assoc.* 86(415): 618-625.

Diggle, P. J. et al. 2000. A Comparison between Parametric and Non-Parametric Approaches to the Analysis of Replicated Spatial Point Patterns. - Adv. Appl. Probab. 32(2): 331-343.

Diggle, P. J. 2003. *Statistical analysis of spatial point patterns*. Second edition. - Arnold, London.

Diggle, P. J. 2014. *Statistical Analysis of Spatial and Spatio-Temporal Point Patterns*. Third edition. - CRC Press, Boca Raton, Florida, USA.

Ellner, S. and Shmida, A. 1981. Why are adaptations for long-range seed dispersal rare in desert plants?. - Oecologia 51: 133-144.

Espinosa, C.I. et al. 2014. Climate and grazing control nurse effects in an Ecuadorian dry shrubby community. - J. Trop. Ecol. 30(1): 23-32.

Flores, J., and Jurado, E. 2003: Are nurse-protégé interactions more common among plants from arid environments?. - J. Veg. Sci. 14: 911-916.

Getzin, S. et al. 2008. Heterogeneity influences spatial patterns and demographics in forest stands. - J. Ecol. 96: 807-820.

Hettmansperger, T. P. and McKean J. W. 2011. Robust Nonparametric Statistical Methods. 2nd Ed. - Chapman Hall, New York.

Jara-Guerrero, A. et al. 2011. Seed dispersal spectrum of Woody species in South Ecuadorian dry forests: Environmental correlates and the effect of considering species abundance. - Biotropica 43: 722-730.

Jara-Guerrero, A. et al. 2015. Does spatial heterogeneity blur the signature of dispersal syndromes on spatial patterns of woody species? A test in a tropical dry forest. - Oikos. doi: 10.1111/oik.02098.

Kalisz, S. et al. 1999. Ant-mediated seed dispersal alters pattern of relatedness in a population of *Trillium grandiflorum*. - Ecology 80(8): 2620-26-30.

Kenkel, N. C. 1988. Pattern of self-thinning in Jack pine: Testing the random mortality hypothesis. - Ecology 69(4): 1017-1024.

Kloke, J. D. and Mckean, J. W. 2012. Rfit: Rank-based estimation for linear models. - The R Journal 4: 57-64.

Landau, S. and Everall, I.P. 2008. Nonparametric bootstrap for K-functions arising from mixed-effects models with applications in neuropathology. Stat. Sinica 18: 1375-1393.

Law, R. et al. 2009. Ecological information of spatial patterns of plants insights from point process theory. - J. Ecol. 97: 616-628.

Lefever, R. R. et al. 2009. Deeply gapped vegetation patterns: On Crown/root allometry, criticality and desertification. - J. Theor. Biol. 261(2): 194.

LeMay, V. et al. 2009. Spatio-temporal structure of multi-storied, multi-aged interior Douglas fir (Pseudotsuga menziesii var. glauca) stands. - J. Ecol. 97: 1062-1074.

Maestre, F. T. and Escudero, A. 2009. Is the patch size distribution of vegetation a suitable indicator of desertification processes? - Ecology 90(7): 1729-1735.

Maestre, F. T. et al. 2009. Refining the stress-gradient hypothesis for competition and facilitation in plant communities. - J. Ecol. 97: 199-205.

Mateu, J. 2001. Parametric procedures in the analysis of replicated pairwise interactions point patterns. - Biom. J. 43(3): 375-394.

McIntire, E. J. B. and Fajardo, A. 2009. Beyond description: the active and effective way to infer processes from spatial patterns. - Ecology 90(1): 46-56.

Murtaugh, P. A. 2007. Simplicity and complexity in ecological data analysis. - Ecology 88(1): 56-62.

Pielou, E. C. 1977. Mathematical Ecology. - Wiley, New York.

Pueyo, Y. et al. 2008. Dispersal strategies and spatial organization of vegetation in arid ecosystems. - Oikos 117: 1522-1532.

R Core Team 2013. R: A language and environment for statistical computing. R Foundation for Statistical Computing, Vienna, Austria.

Raventós, J. et al. 2010. Evidence for the spatial segregation hypothesis: a test with nine-year survivor data in a Mediterranean shrubland. - Ecology 91(7): 2110-2120.

Richter, M. and Moreira-Muñoz, A. 2005. Heterogeneidad climática y diversidad de la vegetación en el sur del Ecuador: un método de fitoindicación. - Rev. Per. Biol. 12(2): 217-238.

Rietkerk, M. et al. 2002: Self-organization of vegetation in arid ecosystems. - Am. Nat. 160(4): 524-530.

Rietkerk, M. and van de Koppel, J. 2008. Regular pattern formation in real ecosystems. - Trends Ecol. Evol. 23(3): 169-175.

Ripley, B. D. 1976. The second-order analysis of stationary point processes. - J. Appl. Probab. 13: 255-266.

Ripley, B. D. 1977. Modelling spatial patterns (with discussion). – J. R. Stat. Soc. Series B 39: 172-212.

Schenk, H. J. et al. 2003. Spatial ecology of a small desert shrub on adjacent geological substrates. - J. Ecol. 91: 383-395.

Schlesinger, W. H. et al. 1996. On the spatial pattern of soil nutrients in desert ecosystems. - Ecology 77(2): 364-374.

Seidler, T. G. and Plotkin, J. B. 2006. Seed dispersal and spatial pattern in tropical trees. - PLoS Biol. 4(11): 2132-2137.

Siteur, K. et al. 2014. Beyond Turing: The response of patterned ecosystems to environmental change. - Ecol. Complex. 20: 81-96.

Smith, B. H. et al. 1989. Spatial patterns of seed dispersal and predation of two myrmecochorous forest herbs. - Ecology 70(6): 1649-1656.

Tilman, D. and Kareiva, P. 1998. The role of space in population dynamics and interspecific interactions. - Monographs in Population Biology 30. Princeton. New Jersey. USA.

Valencia, R. et al. 2000. Libro Rojo de las Plantas Endémicas del Ecuador. - Herbario QCA, Pontificia Universidad Católica del Ecuador, Quito.

Watt, A.S. 1947. Pattern and processes in the plant community. - J. Ecol. 35(1): 1-22.

Wiegand, T. et al. 2009. Recruitment in tropical tree species: revealing complex spatial patterns. – Am. Nat. 174(4): E106-E140.

Wiegand, T. and Moloney, K. A. 2014. Handbook of Spatial Point Pattern Analysis in Ecology. - Chapman & Hall/CRC. Iowa, USA.

Zhou, H. et al. 2007. Ant-mediated seed dispersal contributes to the local spatial pattern and genetic structure of *Globba lancangensis* (Zingiberaceae). - J. Hered. 98(4): 317-324.

CAPÍTULO 3

Nuevas herramientas para describir la relación entre el síndrome de dispersión y el patrón de distribución espacial: desentrañando los efectos de la dispersión limitada y de la heterogeneidad ambiental.

Resumen

Estudiar la relación entre la dispersión y el patrón espacial de las especies vegetales, es crucial para entender los mecanismos que estructuran una comunidad. En este trabajo evaluamos la importancia relativa de la limitación de la dispersión y la heterogeneidad ambiental en la formación de patrones de puntos de los árboles en la parcela subtropical permanente de la isla de Barro Colorado (BCI), Panamá. Hemos considerado 229 especies cuyo patrón espacial fue modelizado utilizando cuatro procesos: Poisson homogéneo (HPP), Poisson inhomogéneo (IPP), Poisson agregado homogéneo (HPCP) y Poisson agregado inhomogéneo (IPCP). Se ha identificado el efecto de la dispersión limitada, de la heterogeneidad del hábitat y el efecto conjunto, a partir de la diferencia entre el patrón espacial formado por los árboles de cada especie y el proceso de puntos teórico. Para estimar la heterogeneidad se utilizaron 56 valores de intensidad, en total se evaluaron 114 modelos diferentes para cada especie; luego en base al mejor modelo para cada especie se analizó la relación con cada uno de los cinco síndromes de dispersión considerados en este estudio. El mayor porcentaje de las especies revelaron efecto conjunto de dispersión limitada y heterogeneidad, mientras que un número menor mostró efectos individuales de dispersión limitada o heterogeneidad. También se determinó alto grado de agregación a corta distancia, mayor para las especies con auto-dispersión y menor para las especies dispersadas por animales.

Abreviaturas.- BCI: Isla de Barro Colorado, HPP: proceso de Poisson homogéneo, IPP: proceso de Poisson heterogéneo, HPCP: proceso de Poisson cluster homogéneno, IPCP: proceso de Poisson cluster heterogéneo, AIC: criterio de información de Akaike.

Introducción

Una de las formas más intuitiva para conocer el funcionamiento de poblaciones y comunidades de plantas es mediante el estudio de su organización espacial (Watt 1947) y, a partir de los patrones observados, inferir los procesos ecológicos subyacentes (Dale 1999, McIntire y Fajardo 2009). El patrón inicial originado a partir de la dispersión establece el marco sobre el cual actúan otros procesos ecológicos subsiguientes, generando el patrón final de las plántulas y los adultos (Schupp y Fuentes 1995, Nathan y Muller-Landau 2000, Jansen et al. 2008). El patrón de árboles establecidos es un subconjunto del patrón original de propágulos que llegaron al suelo y fueron filtrados por un

conjunto de importantes procesos e interacciones biológicas como depredación y/o parasitismo de semillas (Nathan y Muller-landau 2000), herbivoría y/o parasitismo de plántulas (Jansen 1970, Coley y Barone 1996, Wright 2002, Novotny y Basset 2005), competencia intra- e interespecífica entre plántulas, o entre juveniles (Holmgren et al. 1997, Silvertown 2004, Massey et al. 2006, Comita et al. 2010). Así mismo pueden ser determinantes factores ambientales como la fertilidad, humedad del suelo y la iluminación local (Cornwell et al. 2006, Canhan et al. 1990, Denslow 1987, Harms et al. 2000, Sheil et al. 2006).

A pesar de la relación más o menos directa entre patrones espaciales y procesos ecológicos, cuando varios de estos procesos actúan simultáneamente, sus efectos aditivos y/o antagonistas pueden resultar en patrones espaciales complejos y difíciles de explicar (Barot et al. 1999). Además, procesos distintos pueden generar exactamente el mismo patrón (Baddeley y Silverman 1984), lo que imprime cierta incertidumbre en la identificación del proceso responsable. Otros procesos tales como la heterogeneidad ambiental (Harms, 2001, Phillips et al. 2003, John et al. 2007, Getzin et al. 2008), la dispersión limitada alrededor de los padres (Hubbell 1979, Condit et al. 2000, Nathan y Muller-Landau 2000, Hardesty y Parker 2002, Seidler y Plotkin 2006, Wiegand et al. 2009), la facilitación (Escudero et al. 2005, de la Cruz et al. 2008b) o la existencia de interacciones de facilitación en las etapas tempranas de vida de la planta (Callaway y Walker 1997), podría distorsionar el patrón de dispersión inicial originando patrones agregados (Levine y Murrell 2003, Lin et al. 2010) e interfiriendo con el desarrollo succesional de la comunidad (Jacquemyn et al. 2001).

Numerosos estudios han abordado la interrogante de cómo los procesos de dispersión de semillas afectan los patrones espaciales de las plantas (Hubbell 1979, Schupp y Fuentes 1995, Condit et al. 2000, Nathan y Muller-Landau 2000, Seidler y Plotkin 2006), y han determinado que los síndromes de dispersión son importantes atributos en la formación del patrón espacial (Hubbell 1979, Condit et al. 2000, Seidler y Plotkin 2006). Hubbell (1979) inició los estudios orientados a demostrar una relación entre los síndromes de dispersión y el patrón espacial de las especies de árboles adultos en los bosques tropicales , Más tarde, Seidler y Plotkin (2006) también encontraron una fuerte correlación entre los síndromes de dispersión de las semillas y los patrones espaciales de árboles en dos bosques tropicales. Aunque estos estudios se basan en el consenso general de que la dispersión es un factor clave para explicar la distribución espacial de los adultos (Hubbell 1979, Condit et al. 2000, Seidler y Plotkin 2006, Wiegand et al. 2009), como se ha comentado anteriormente, una serie de mecanismos podrían empañar esas relaciones (Schupp y Fuentes 1995, Seidler y Plotkin 2006).

Conjuntamente con los efectos de la dispersión limitada, la heterogeneidad ambiental podría llevar a una falta de correspondencia entre los patrones espaciales de semillas dispersadas y la ubicación de las plántulas o adultos (Comita et al. 2007, Wiegand et al. 2007b, Cousens et al. 2008, Pinto and MacDougall 2010), facilitando la supervivencia y generando densidades mayores en micrositios ambientalmente favorables y aumentando la mortalidad y disminuyendo la densidad en los menos favorables (Purves and Law 2002, Wright 2002, Getzin et al. 2008, Murrell 2009). Este efecto se refleja en la generación de patrones aparentemente agregados a todas las escalas espaciales y se conoce como "agregación virtual" donde la heterogeneidad a gran escala impone una firma a todas las escalas espaciales (Wiegand y Moloney 2004, Schiffers et al. 2008, Wiegand y Moloney 2014) que se pueden confundir con los efectos debidos a la dispersión limitada.

Por lo tanto, a la hora de examinar las relaciones entre atributos biológicos (como los síndromes de dispersión) y los patrones espaciales de las especies es necesario considerar conjuntamente los efectos de dispersión limitada y heterogeneidad ambiental, evaluando la importancia relativa de cada proceso (Pinto and MacDougall 2010, Shen et al. 2013). Aunque complicado, es abordable con las técnicas modernas de análisis de patrones de puntos (Waagepetersen and Guan 2009, Shen et al. 2009, Shen et al. 2013).

En este estudio intentamos avanzar en este aspecto, reanalizando los datos de distribución espacial de árboles adultos y sus síndromes de dispersión en el bosque de Barro Colorado analizados por Seidler y Plotkin (2006) y examinando en qué medida los patrones detectados se explicarían como un efecto de la limitación a la dispersión, de la heterogeneidad ambiental o de ambas. Nuestra hipótesis de trabajo es que los patrones espaciales observados para cada especie son el resultado de la acción secuencial del síndrome de dispersión (Hubbell 1979, Seidler y Plotkin 2006) que determina una distribución inicial sobre la que actúan posteriormente procesos ligados a la heterogeneidad ambiental (Webb y Peart 2000), difuminando el patrón inical y determinando la distribución final de árboles adultos. Al considerar como un elemento adicional la heterogeneidad ambiental, esperamos que las fuertes relaciones entre el patrón espacial de árboles y los síndromes de dispersión encontrados por Seidler y Plotkin (2006) sean menos evidentes.

Nuestra hipótesis de trabajo es que el patrón espacial es el resultado de un proceso de dos etapas donde el síndrome de dispersión primero configura la distribución espacial inicial (Hubbell 1979, Seidler y Plotkin 2006) y luego el proceso ecológico enlazado a la heterogeneidad ambiental (Webb y Peart 2000) difumina el patrón original de dispersión de las semillas y determina el patrón de árboles adultos.

Para discernir el papel de los procesos responsables de la estructura espacial de las distintas especies de árboles usamos herramientas de análisis de patrones de puntos espaciales en conjunción con un y un conjunto de hipótesis previas (McIntire y Fajardo 2009). En concreto, para cada especie ajustamos cuatro tipos de modelos espaciales, que pueden interpretarse fácilmente desde un punto de vista del efecto de procesos biológicos y/o condiciones ambientales (Shen et al. 2009, Lin et al. 2011). Los modelos ajustados consideran procesos puramente aleatorios (proceso Poisson homogéneo), procesos aleatorios en hábitats heterogéneos (proceso Poisson inhomogéneo), dispersión limitada (proceso Poisson agregado) y el efecto conjunto de la dispersión limitada y la heterogeneidad ambiental (Proceso Poisson agregado inhomogéneo). De este modo, si la distribución final de los árboles establecidos es consecuencia exclusiva de los procesos dispersivos, 1) esperamos encontrar que las especies zoócoras tengan patrones compatibles con procesos Poisson homogéneos, ya que las semillas serían transportadas por organismos muy móviles que podrían llegar a cualquier punto del territorio, es decir patrones no limitados a distancias específicas. Del mismo modo, 2) esperamos encontrar que las plantas autócoras sean descritas por un patrón Poisson agregado homogéneo, ya que los adultos servirían de fuente para el reclutamiento de nuevos individuos en su vecindad, en un proceso temporalmente anidado (Coussens et al. 2008)- Finalmente esperamos que 3) las especies anemócoras, dependiendo de su eficiencia de dispersión (arquitectura, propiedades aerodinámicas de las diásporas, Muller-Landau et al. 2008) muestren patrones compatibles con procesos Poisson homogéneos (en el caso de las muy eficientes) o con procesos Poisson agrupado hommogéneo (en las menos eficientes, pero en todo caso, con menor agregación que las especies autócoras). Por el contrario, si la heterogeneidad tiene un papel importante sobre el establecimiento de las plantas, esperaríamos que los patrones de las especies sean descritos por procesos inhomogéneos (Poisson inhomogéneo o Poisson agregado inhomogéneo, dependiendo de la mayor o menor limitación a la dispersión).

Métodos

Sitio de estudio

El conjunto de datos utilizado en este estudio fue compilado de una parcela permanente de 50 Ha de bosque tropical húmedo semideciduo situada en la isla de Barro Colorado (BCI), Panamá (9º 10’ N, 79º 51’ W, Fig. 1) (Condit 1998, Hubbell et al. 1999). La parcela, con una extensión de 1000 x 500 m presenta un rango altitudinal de 120 a 160 m, con pendientes que varían entre 7º y 20º. La temperatura media diaria máxima y mínima es de 30.8ºC y 23.4ºC respectivamente; la precipitación

media anual es de 2600 mm, concentrada principalmente a lo largo de 8 meses, y reducida (solo el 10% del total anual) durante una estación seca de 4 meses de duración.

Datos

La parcela de BCI fue censada por primera vez entre 1981 y 1982 (Condit, 1998), todos los árboles con diámetro a la altura del pecho (dap) ≥ 1cm fueron medidos, identificados y mapeados. Un segundo censo fue efectuado en 1985 y censos posteriores se han realizado cada 5 años. Para el presente estudio hemos empleado los mismos datos utilizados por Seidler y Plotkin (2006), correspondientes al cuarto censo (1995). En este censo se registraron un total de 317 354 árboles, repartidos en 310 especies distintas. La abundancia de las diferentes especies oscila desde 1 (mínima abundancia) hasta 55 399 (máxima abundancia). Para nuestro análisis (similar a Seidler y Plotkin 2006) incluimos las especies representadas con 20 ó más individuos en la parcela, es decir, un total de 229 especies.

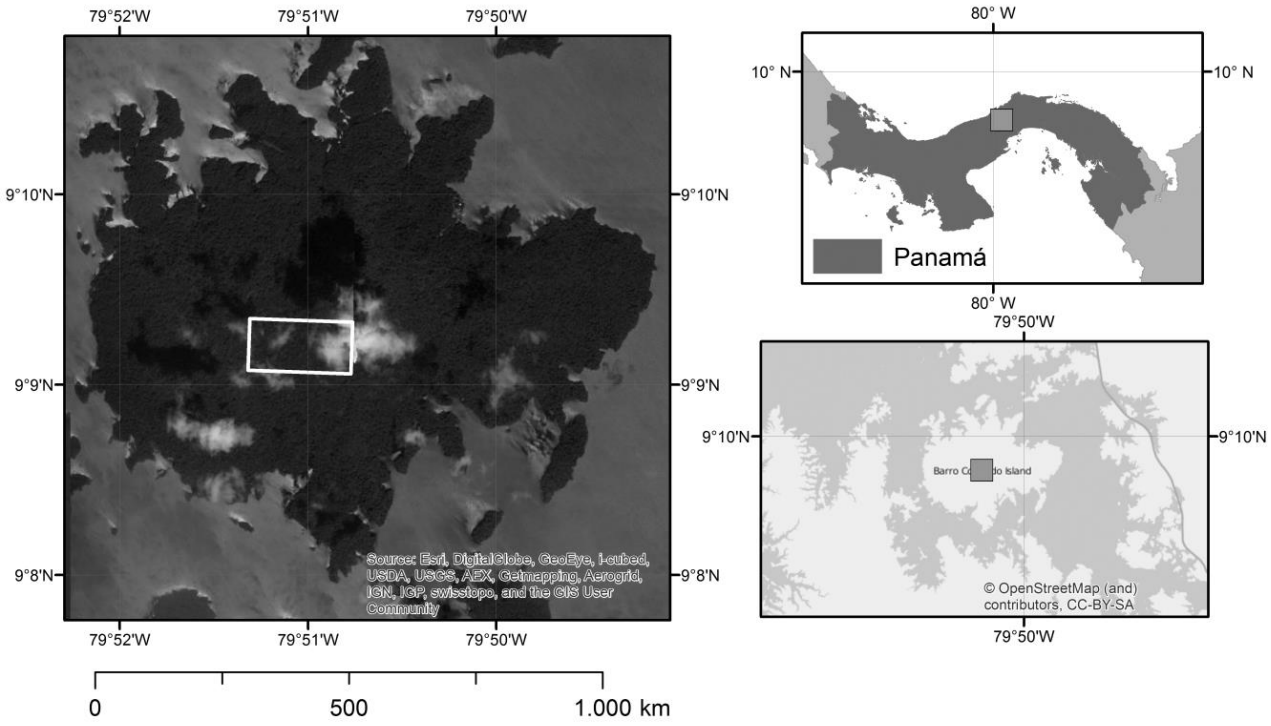

Fig. 1. Ubicación de la parcela permanente de 50 Ha en Barro Colorado Island (BCI), Panamá.

Basándonos en los trabajos de Muller-Landau y Hardest (2005) y Wright et al. (2007), se han distinguido cinco síndromes de dispersión: dispersión balística, anemócora, y dispersión zoócora con tres categorías en función del tamaño del fruto (Tabla 1). Estas categorías se corresponden con las mismas empleadas por Seidler y Plotkin (2006) con la excepción de la dispersión zoócora, en la que nosotros hemos distinguido las tres categorías mientras que Seidler y Plotkin sintetizaron en aves/murciélagos y mamíferos en una sola.

Tabla 1. Categorías de dispersión animal en la parcela de BCI. N.sp: número de especies. N.gen: número de géneros. N.fam: número de familias. N.arb.sp: número medio de árboles por especie ± error estándar.

Nombre	Diámetro del fruto	Dispersor	N.sp	N.gen	N.fam	N.arb.sp
Animal 1	<2cm	Aves, mamíferos	115	79	41	1309±351
Animal 2	2 – 5cm	Aves grandes, mamíferos	57	45	23	1117±237
Animal 3	> 5cm	Murciélagos, otros mamíferos	28	15	12	672±209

Análisis estadístico

Para caracterizar y ajustar los modelos de procesos de puntos, utilizamos la función K de Ripley (Ripley 1977, Stoyan y Stoyan 1994). Para un patrón de puntos homogéneo con intensidad λ, $\lambda K(r)$ es el número esperado de puntos dentro de un círculo de radio r alrededor de un punto cualquiera del patrón.

Ajuste y selección de modelos

En el estudio comparamos el patrón espacial de cada especie (caracterizado por la función K) con el patrón esperado para cada uno de los cuatro procesos de punto espaciales considerados (Shen et al. 2009, Lin et al. 2011). 1) un proceso Poisson homogéneo (HPP), que asume que la posición espacial de cada punto (es decir, de cada árbol) es independiente de los demás y su intensidad es constante a lo largo y ancho de todo el área. Este es el proceso más sencillo y considera que el patrón observado resulta exclusivamente de procesos aleatorios (Shen et al. 2009; Lin et al. 2011). 2) un proceso de Poisson inhomogéneo (IPP), que asume independencia entre los puntos pero reconoce la existencia de variaciones de intensidad a lo largo del área de estudio; normalmente se asume que estas

variaciones en la intensidad están relacionadas con la heterogeneidad ambiental (Wiegand et al. 2007b). 3) Un proceso de Poisson agrupado homogéneo (HPCP), que asume intensidad constante y considera la agregación de los puntos como un resultado de la dispersión limitada (Shen et al. 2009); el HPCP asume que el patrón agregado se genera en dos pasos: en primer lugar se genera un HPP de puntos "padres" con intensidad ρ, y posteriormente, cada punto padre produce un número de "hijos" que sigue una distribución de Poisson y que se dispersan a su alrededor siguiendo una distribución gausiana bivariada con media 0 y desviación estándar σ. (Seidler y Plotkin 2006, Shen et al. 2009, Lin et al. 2011). 4) un proceso de Poisson agrupado inhomogéneo (IPCP) que asume que el patrón espacial se crea por dispersión limitada (como un HPCP) pero con una intensidad que varía en respuesta a la heterogeneidad ambiental (Wiegand y Moloney 2014). Una descripción detallada de los cuatro modelos de procesos considerados en este estudio, se encuentra en el Apéndice 3.

Para seleccionar el modelo que mejor se ajustó al patrón observado empleamos el criterio de información de Akaike (AIC), calculado a partir de la suma de desviaciones entre la función K observada y la función K de los modelos ajustados, así como del número de parámetros ajustados en cada modelo (Webster y McBratney 1989, Shen et al. 2009). La descripción matemática de los modelos ajustados y la justificación de los métodos de selección aparecen descritas en el Apéndice 1.

Relación síndrome - patrón espacial

Una vez seleccionado el modelo que mejor describe el patrón de cada especie, contrastamos la hipótesis de independencia entre el tipo de modelo y los síndromes de dispersión, es decir contrastamos diferencias en la frecuencia del tipo de patrón espacial (HPP, IPP, HPCP o IPCP) entre los diferentes síndromes, mediante una prueba exacta de Fisher para tablas mayores que 2x2. Utilizamos la función fisher.test() del paquete stats de R. El valor p asociado a esta prueba se obtuvo mediante simulaciones de Monte Carlo basado en 10000 réplicas.

Para aquellas especies en las que el modelo seleccionado incluía limitaciones a la dispersión (HPCP o IPCP), contrastamos la existencia de diferencias entre síndromes para el parámetro σ. Este parámetro está relacionado con el tamaño promedio del tamaño de los agregados (Seidler y Plotkin 2006). Dado que la distribución del parámetro σ no resultó normal ni homocedástica, para contrastar su relación con los síndromes de dispersión empleamos una prueba de Kruskall-Wallis. Posterior a este análisis global de la varianza, realizamos también pruebas de rangos con signo de Wilcoxon para comparar la variación del parámetro σ entre pares de síndromes y entre grupos de síndromes.

Adicionalmente, contrastamos la existencia de diferencias en la estructura espacial entre síndromes, empleando un análisis tipo ANOVA de una vía siguiendo la metodología de Diggle et al. (1991), que como mostramos en el capítulo 2, puede llegar a detectar diferencias no detectables con el análisis de los parámetros de agregación σ.

Todos los cálculos se efectuaron utilizando el programa R (R Core Team 2013) y los paquetes "spatstat" (Baddeley y Turner 2005) y "ecespa" (de la Cruz 2008a).

Resultados

Relación entre el proceso espacial y el síndrome de dispersión

El proceso de Poisson agrupado inhomomgéneo produjo el mejor ajuste para el 63% de las especies (144 especies). El proceso de Poisson agrupado homogéneo se ajustó mejor para el 20% de las especies (45 especies), mientras que el 17% (40 especies) se explicó mejor mediante el modelo de Poisson inhomogéneo. Ninguna especie se explicó por un proceso Poisson homogéneo (Tabla 2). En resumen, la inclusión de la heterogeneidad mediante procesos inhomogéneos, ajustó mejor al 80 % de las especies del bosque.

El test de Fisher descartó la independencia entre síndrome y patrón espacial (p = 0.04116, para una tabla de 5 x 3). La desviación de independencia se debe principalmente a la alta prevalencia del patrón Poisson agrupado entre las especies anemócoras (mientras que en la dispersión animal y balística es poco frecuente (Fig. 2).

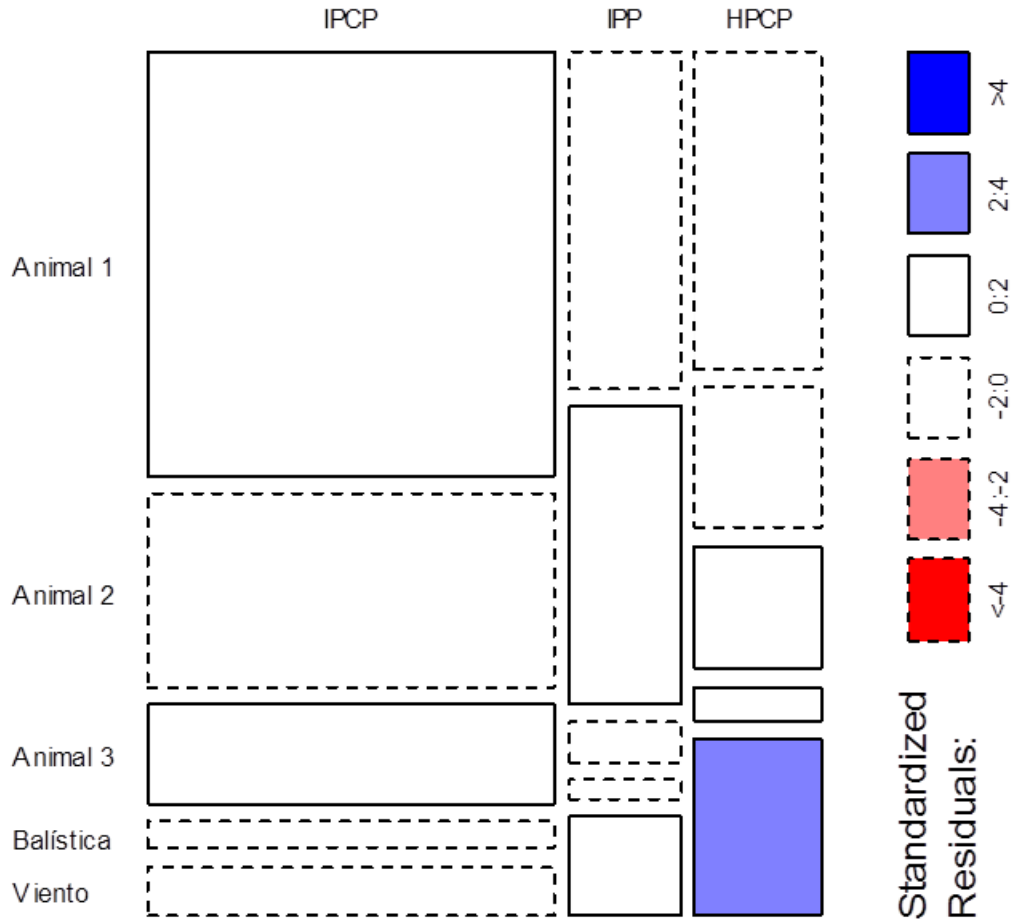

Figure 2. Mosaico de la frecuencia de especies en cada síndrome explicadas por cada tipo de modelo. El área de cada tesela es proporcional a la frecuencia en cada celda de la Tabla 2. Los bordes contínuos y discontinuos indican respectivamente desviaciones positivas y negativas de las fecuencias esperadas asumiendo independencia entre síndrome y patrón espacial. El color de las celdas indica el valor de los residuos estandarizados. Residuos entre 2-4 indican una desviación del valor esperado con un =0.05.IPCP: proceso de Poisson agrupado inhomogéneo. IPP: proceso de Poisson inhomogéneo.HPCP: proceso de Poisson agrupado homogéneo.

Diferenciación del patrón espacial de los diferentes síndromes de dispersión.

Las funciones K(r) mostraron que el patrón general para los cinco síndromes está fuertemente agregado para cortas y medianas distancias (hasta aproximadamente 100 m). La mayor agregación la presentaron las especies con dispersión balística y las anemócoras, con la mínima diferencia entre estos dos síndromes, mucho más agregadas que las especies con dispersión por animales (Fig. 3). Entre las especies dispersadas por animales, las especies con frutos pequeños se presentaron algo más agregadas que el resto, pero las diferencias entre los diferentes grupos de especies dispersadas por animales fueron despreciables. El contraste de tipo ANOVA (Diggle et al. 1991) no detectó

diferencias significativas entre las funciones K de los diferentes síndromes (btss = 285755462873 *p* = 0.589).

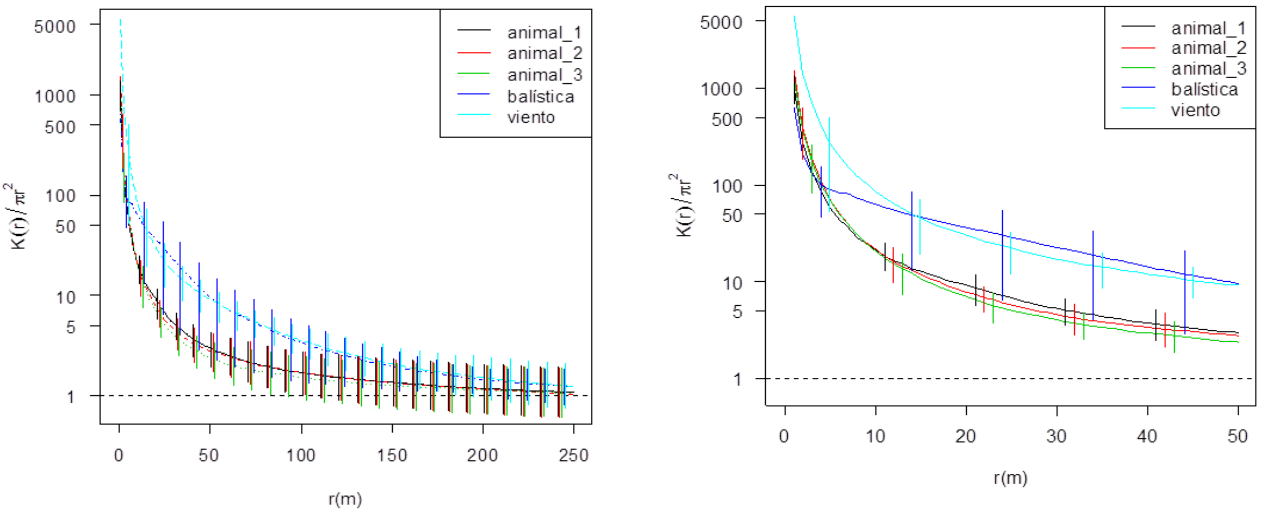

Figura 3. Estadístico de agregación espacial $K(r)/\pi r^2$ ±1 error estándar (evaluado cada 10m de distancia). La línea punteada indica la función $K(r)/\pi r^2$ para una distribución espacial aleatoria de Poisson. El gráfico de la derecha es una ampliación para mostrar el detalle de lo que ocurre a escala pequeña.

No se observó relación significativa entre los síndromes de dispersión y el parámetro de dispersión (σ) (Kruskal-Wallis, χ^2 = 4.9317, df = 4, *p* = 0.2944). De forma similar no se observó diferencia significativa en la dispersión (estimada mediante σ) entre las especies dispersadas por animales y aquellas de dispersión mecánica (balística y viento) (suma de rangos de Wilcoxon, W= 1733.5, *p* = 0.1368) ni entre los diferentes tipos de fruto con dispersión animal (Kruskal-Wallis, χ^2 = 1.588, df = 2, *p* = 0.452) . La distribución de valores del parámetro de dispersión σ entre las 189 especies para las que la selección de modelos eligió un proceso de Poisson agrupado (homogéneo o inhomogéneo) fue significativamente menor que el que se obtendría ajustando un proceso Poisson agrupado homogéneo de manera indiscriminada, como hicieron Seidler y Plotkin (2006) (Fig. 4; suma de rangos de Wilcoxon, W = 11035, *p* < 0.00001). Los valores correspondientes al modelo de mejor ajuste presentaron una tendencia muy constante, sin embargo la tendencia fue muy congruente para los dos métodos de estimación (Fig. 4). En ambos casos la agregación de las especies con auto-dispersión resultó ser menor en comparación al resto de síndromes de dispersión.

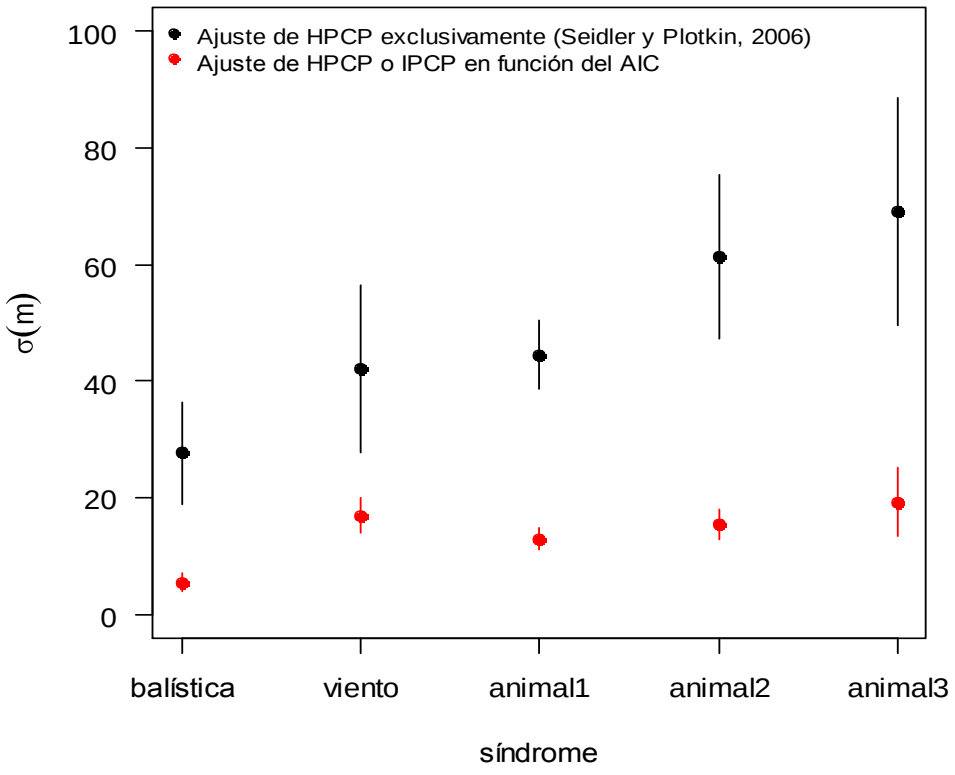

Figura 4. Comparación de la distribución entre los síndromes de los valores del parámetro de dispersión (σ) de los modelos Poisson agregado ajustados siguiendo el criterio de Seidler y Plotkin (2006), es decir, sólo homogéneos (HPCP; en negro, 229 especies) y eligiendo entre procesos homogéneos e inhomogéneos de acuerdo con el AIC (HPCP e IPCP; en rojo, 189 especies). Se representa el valor medio de σ ± 1error estándar

Respecto al ancho de banda ajustado para los procesos inhomogéneos, no se observó relación con el síndrome de dispersión (Kruskal-Wallis, χ^2 = 2.317, df = 4, p = 0.6777). Tampoco se encontró diferencia en el tamaño del ancho de banda entre las especies dispersadas pos animales y las no dispersadas por animales (suma de rangos de Wilcoxon W= 1497, p = 0.5255). Sí que se observó una diferencia neta entre los anchos de banda seleccionados para especies descritas por un modelo Poisson inhomogéneo y las descritas por un proceso de Poisson agrupado inhomogéneo (Fig. 5, Tabla 2).

Tabla 2. Número de especies en cada síndrome de dispersión por cada uno de los procesos de patrones de puntos. IPP: proceso de Poisson inhomogéneo, HPCP: proceso de Poisson agregado homogéneo, IPCP: proceso de Poisson agregado inhomogéneo, Síndrome: forma de dispersión de las especies (Animal 1, Animal 2 y Animal 3: especies zoócoras con fruto de diámetro < 2 cm, diámetro entre 2 y 5 cm, y diámetro > 5 cm respectivamente), N: número de especies, Ancho de banda: valor medio ± 1 error estándar del parámetro σ del kernel gausiano empleado para estimar la intensidad de los procesos inhomogéneos, σ: valor medio ± 1 error estándar del parámetro de dispersión ("agregación") para los procesos de Poisson agregados.

	IPP		HPCP		IPCP		
Síndrome	N	Ancho de banda (m)	N	σ (m)	N	Ancho de banda (m)	σ (m)
Animal 1	17	59.9 ± 10.3	18	33.6 ± 6.3	77	198.4 ± 4.5	7.7 ± 1.2
Animal 2	15	79.3 ± 17.8	8	29.3 ± 6.7	35	207.0 ± 7.4	11.0 ± 1.7
Animal 3	2	71.0 ± 40.0	7	51.0 ± 18.1	18	181.1 ± 8.0	9.3 ± 2.7
Balística	1	51.0	2	11.0 ± 1.34	5	223.8 ± 15.1	8.1 ± 4.5
Viento	5	70.2 ± 17.5	10	21.2 ± 4.9	9	218.6 ± 13.4	11.2 ± 2.8

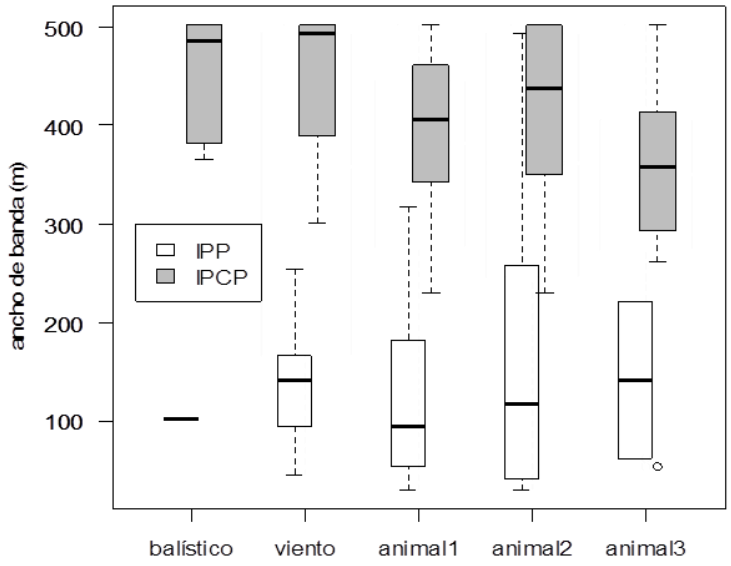

Figura 5. Variación entre síndromes del ancho de banda (= 2*σ) seleccionado para describir la heterogeneidad de cada modelo mediante un *kernel* gausiano. IPP: Proceso de Poisson inhomogéneo. IPCP: Proceso de Poisson agrupado inhomogéneo.

Discusión

Los efectos de la heterogeneidad ambiental son prevalentes entre las especies de BCI

Determinar la importancia relativa de los procesos bióticos y abióticos en la configuración de los patrones y estructuras de poblaciones y comunidades ha sido un tema principal en ecología (Hubbell 2001). Nuestros resultados, obtenidos con una nueva metodología que permite discernir ente patrones con agregación "pura" y "virtual" señalan el importante papel de la heterogeneidad ambiental en la configuración de los patrones de las especies de BCI (el 80 % de las especies presentaron patrones inhomogéneos). Este efecto fue prevalente independientemente del síndrome de dispersión, e incluso *Hura crepitans*, una especie con dispersión explosiva que debería mostrar un patrón con agrupación pura fue descrita mejor por un IPP.

Un buen número de estudios en bosques lluviosos tropicales han sugerido que los patrones agregados observados a pequeña escala (a escala de parcela cuando se usan patrones de puntos) para la mayoría de las especies son generados fundamentalmente por limitaciones a la dispersión (Plotkin et al. 2002, Seidler y Plotkin 2006), mientras que los efectos de la heterogeneidad ambiental (en forma de gradientes ambientales) afectarían sólo al patrón a grandes escalas (Beaudrot et al. 2013). Sin embargo, los efectos conjuntos a "escala de parcela" de la heterogeneidad ambiental y de la limitación a la dispersión se han puesto de manifiesto también en otros bosques tropicales (Comita et al. 2007, Shen et al. 2009, Jara-Guerrero et al. 2015) y subtropicales (Shen et al. 2009, Lin et al. 2011), lo que sugiere que ambos factores son fundamentales para la estructuración de este tipo de comunidades megadiversas. Shen et al. (2009) y Lin et al. (2011) propusieron que estos dos factores actuarían secuencialmente. En un primer momento, la dispersión generaría un patrón inicial de plántulas. Posteriormente, la heterogeneidad ambiental generaría el patrón final, a través de sus efectos variables sobre las tasas de crecimiento y supervivencia de las plántulas. Diversos estudios han puesto de manifiesto la marcada heterogeneidad ambiental de la parcela de BCI (Harms et al. 2001, John et al. 2007, Schreeg et al. 2010). Nuestros resultados muestran que los efectos de la heterogeneidad pueden modificar el patrón de dispersión original en direcciones opuestas: bien diluyendo el patrón agregado de especies autócoras (como en el caso de *Hura crepitans*) para generar agregación virtual o restringiendo (teóricamente) la mayor dispersión de especies zoócoras y anemócoras.

Relación entre el modelo de estructura espacial y el síndrome de dispersión

Hemos encontrado una gran variación en el modelo que describe la estructura del patrón espacial de las especies, incluso entre aquellas que presentan el mismo síndrome de dispersión. Exceptuando el patrón Poisson homogéneo, todos los procesos considerados se han ajustado a alguna de las especies en todos los síndromes (Tabla 2). Aunque el test de Fisher descartó la independencia entre síndromes y procesos, tan sólo encontramos desviaciones significativas (en exceso) de la frecuencia esperada para el proceso Poisson agregado homogéneo (HPCP) en las especies anemócoras (Figura 2). Aunque la prevalencia de procesos agregados en especies anemócoras entra dentro de nuestras expectativas, el hecho de que sean homogéneos, cuando la tendencia general en el resto de síndromes indica una dominancia de procesos inhomogéneos, es digno de mención.

En el caso de las especies zoócoras tan sólo un 17 % (34 especies) mostraron patrones compatibles con dispersión no limitada (es decir fueron explicadas por un IPP), mientras que el resto (83%) mostraron patrones compatibles con dispersión limitada (HCP o IPCP). Este efecto es máximo en las especies con frutos grandes ("animal 3"), de las que tan sólo un 7% (2 especies) muestran dispersión no limitada. Estos patrones podrían haberse generado por otros procesos no considerados explícitamente ene este trabajo, como los "efectos percha" causados por desplazamientos no aleatorios de los animales dispersores (Herrera et al. 1994, Schupp y Fuentes 1995, Jara-Guerrero et al. 2015). Estudios previos han sugerido el papel del efecto percha como causa del patrón espacial agregado de algunas especies zoócoras (Godoy and Jordano 2001, Muller-Landau et al. 2008). Además, en ocasiones los movimientos de los dispersores tienen lugar a cortas distancias en los alrededores de las plantas fructíferas (Godoy y Jordano 2001, Muller-Landau et al. 2008). En el sentido contrario, ya se ha comentado el caso de *Hura crepitans*, (autócora) que en vez de presentar el esperado patrón agregado es descrita mejor por un proceso Poisson inhomogéneo. Aunque en otros casos se ha explicado el patrón inhomogéneo de especies autócoras como una consecuencia de procesos de dispersión secundaria por herbívoros (Jara-Guerrero et al. 2015), en el caso de *H. crepitans* esta explicación no parece adecuada.

Señal de los síndromes de dispersión en los patrones de agregación espacial.

Todas las especies mostraron agregación espacial, con un incremento de esta señal a cortas distancias independientemente del síndrome de dispersión (Fig. 3). En general, las especies autócoras mostraron la mayor agregación, lo que es consistente con estudios previos (Condit et al. 2000, Seidler y Plotkin 2006, Jara-Guerrero et al. 2015). Sin embargo, sorprendentemente las especies

zoócoras presentaron una agregación similar o incluso superior a la de las autócoras a pequeña escala (0-5 m). Esto podría estar motivado por el efecto percha (Godoy y Jordano 2001) comentado anteriormente. En todo caso, la mayor agregación a escalas pequeñas (0-10 m) es para las especies anemócoras, lo que contrasta con los resultados encontrados en otros bosques (Pasoh, Indonesia: Seidler y Plotkin 2006; Arenillas, Ecuador: Jara-Guerrero et al. 2015), o incluso con los resultados reportados para BCI por Seidler y Plotkin (2006). Por otro lado, el parámetro de dispersión ajustado para las especies anemócoras es de los más grandes (sólo por detrás del de dispersión animal de tipo 3). En conjunto, esto podría estar indicando que las especies anemócoras experimentan dos tipos de dispersión: una más restringida y otra más extendida. Varios estudios han mostrado que la distancia de dispersión en especies anemócoras depende de la interacción entre la morfología del propágulo (que afecta a sus propiedades aerodinámicas) y la estructura del bosque (que afecta a la circulación del viento) (Shupp y Fuentes 1995, Muller-Landau et al. 2008). De esta forma, algunas especies (o algunos individuos de algunas especies) podrían dispersar sus semillas lejos de la planta madre mientras que otras dispersarían a escasos metros. Se ha sugerido también que la dispersión anemócora está afectada por las condiciones meteorológicas que tienen lugar cuando ocurre la dispersión, con ambientes húmedos y lluviosos dificultando el vuelo de los propágulos y ambientes secos facilitándolos (Muller-Landau et al. 2008). Una alternancia de condiciones húmedas y secas a lo largo del periodo de dispersión podría generar este tipo de señal. Recientemente, Teller et al. (2015) han señalado que la variación de la fuerza del viento requerida para provocar la abscisión de los propágulos, entre individuos de la misma especie o incluso dentro del mismo individuo, tiene efectos remarcables en las características de la dispersión, lo que podría explicar también esta variación en la señal de las especies anemócoras.

Por otro lado, aunque se aprecia una tendencia entre las especies zoócoras a que la dispersión aumente con el tamaño de fruto (Fig. 4), las diferentes categorías de dispersión animal apenas difieren en su patrón espacial, en contraste con lo señalado por Seidler y Plotkin (2006). Probablemente, buena parte de las diferencias de agregación entre las diferentes categorías distinguidas para la dispersión animal detectadas por Seidler y Plotkin (2006) son debidas a diferencias en agregación virtual. Dado que, en general, los animales generan una dispersión más focalizada, ligada en muchas ocasiones a hábitats concretos (Russo y Augspurger 2004, Li et al. 2009, García et al. 2011), el patrón de árboles resultante podría estar condicionado por la distribución de los hábitats preferidos por cada animal dispersor. Es decir, en el caso de la dispersión animal, el efecto de la heterogeneidad ambiental podría actuar en dos momentos (y por lo tanto a dos escalas distintas): en un primer momento condicionando la potencialidad de sitios en los que las semillas

podrían ser depositadas (que estaría operando además a la misma escala a la que se produce la dispersión) y un segundo momento en el que las condiciones particulares de cada localidad afectarían a las tasas de crecimiento y supervivencia de las plántulas (que podría operar a la misma escala que la anterior o a una escala diferente dependiendo de la especie). Los animales que dispersan frutos pequeños probablemente perciben el paisaje de manera distinta a los que dispersan frutos más grandes, lo que repercute en un diferente grado de agregación virtual entre ambos. Una vez que el efecto de la agregación virtual es descontado mediante un modelo inhomogéneo, las diferencias entre síndromes no son tan grandes (Fig. 4). Es notable además cómo nuestra aproximación de selección de modelos redunda en una disminución de la variabilidad de los parámetros de agregación dentro de cada síndrome (Fig. 4).

En conclusión, las predicciones sobre los patrones espaciales de especies forestales y de su relación con el síndrome de dispersión pueden mejorarse seleccionando el mejor modelo para cada especie de entre un conjunto de modelos que consideren diferentes mecanismos causales, en vez de forzar el ajuste de un único tipo de modelos para todas las especies. Nuestro estudio contribuye a aclarar el debate sobre la importancia de los diferentes mecanismos que intervienen en el ensamblaje de las comunidades de bosque tropical (Hubbell 1979, Leibold 1995, López-Martínez et al. 2013). Por un lado, nuestro estudio apoya la hipótesis de que los patrones locales no son independientes de los atributos biológicos de las especies (Seidler y Plotkin 2006, Shen et al. 2009, Lin et al. 2011). Por otro lado, el hecho de que el 80 % de las especies sean explicadas por un modelo que incluye el efecto de la heterogeneidad pone de manifiesto la necesidad de considerarla como un factor tan importante como la dispersión limitada para el ensamblaje de la comunidad.

BIBLIOGRAFÍA

Baddeley, A. y Silverman, B.W. 1984. A cautionary example on the use of second-order methods for analyzing point patterns. *Biometrics* 40(4): 1089-1093.

Baddeley, A. y Turner, R. 2005. Spatstat: an R package for analyzing spatial point patterns. *Journal of Statistical Software* 12(6): 1-42. Disponible en: www.jstatsoft.org.

Barot, S., Gignoux, J. y Menaut, J-C. 1999. Demography of a savanna palm tree: predictions from comprehensive spatial pattern analyses. *Ecology* 80(6): 1987-2005.

Beaudrot, L., Rejmánek, M. y Marshall, A. J. 2013. Dispersal modes affect tropical forest assembly across trophic levels. *Ecography* 36: 984 – 993.

Canham, Ch.D., Denslow, J.S., Platt, W.J., Runkle, J.R., Spies, T.A. y White, P.S. 1990. Light regimes beneath closed canopies and tree-fall gaps in temperate and tropical forest. *Canadian Journal of Forest Research* 20(5): 620-631.

Callaway, R.M. y Walker, L.R. 1997. Competition and Failitation: A synthetic approach to interactions in plant communities. *Ecology* 78(7): 1958-1965.

Coley, P.D. y Barone, J.A. 1996. Herbivory and plant defenses in tropical forest. *Annual Review of Ecological Systematics* 27: 305-335.

Comita, L.S., Condit, R. y Hubbell, S.P. 2007. Developmental changes in hábitat associations of tropical trees. *Journal of Ecology* 95: 482-492.

Comita, L.S., Muller-Landau, H.C. Aguilar, S. y Hubbell, S.P. 2010. Asymmetric density dependence shapes species abundances in a tropical tree community. *Science* 329: 330-332.

Condit, R. 1998. *Tropical Forest Census Plots.* Springer-Verlag and R. G. Landes Company, Berlin, Germany, and Georgetown, Texas.

Condit, R., Ashton, P.S., Baker, P., Bunyavejchewin, S., Gunatilleke, S., Gunatilleke, N., Hubbel, S.P., Foster, R.B., Itoh, A., LaFrankie, J.V., Lee, H.S., Losos, E., Manokaran, N., Sukumar, R. y Yakamura, T. 2000. Spatial patterns in the distributions of tropical tree species. *Science Reports* 88: 1414 – 1418.

Cornwell, W.K., Schwilk, D.W. y Ackerly, D.D. 2006. A trait-based test for habitat filtering: convex hull volume. *Ecology* 87(6): 1465-1471.

Cousens, R., Dytham, C. y Law, R. 2008. *Dispersal in Plants. A population perspective*. Oxford University Press. New York.

Dale, M.R.T. 1999. *Spatial Pattern Analysis in Plant Ecology.* Cambridge University Press. Madrid, Spain.

De la Cruz, M. 2008a. Métodos para analizar datos puntuales. En: Maestre, F.T., Escudero, A. y Bonet, A. (eds). *Introducción al Análisis Espacial de Datos en Ecología y Ciencias Ambientales: Metodos y Aplicaciones.* pp 76-127. Asociación Española de Ecología Terrestre, Universidad Rey Juan Carlos y Caja de Ahorros del Mediterráneo, Madrid.

De la Cruz, M., Romao, R.L., Escudero, A. y Maestre, F.T. 2008b. Where do seedlings go? A spatio-temporal analysis of seedlings mortality in a semi-arid gypsophyte. Ecography 31: 720-730.

Denslow, J.S. 1987. Tropical rainforest gaps and tree species diversity. *Annual Review of Ecology and Systematics* 18: 431-451.

Diggle, P.J., Lange, N. y Benes, F.M. 1991. Analysis of variance for replicated spatial point patterns in Clinical Neuroanatomy. Journal of the American Statistical Association 86(415): 618-625.

Escudero, A., Romao, R.L., de la Cruz, M. y Maestre, F.T. 2005. Spatial pattern and neighbour effects on *Helianthemum squamatum* seedlings in a Mediterranean gypsum community. *Journal of Vegetation Science* 16: 383-390.

García, D., Zamora, R. Amico, G. C. 2011. The spatial scale of plant-animal interactions: effects of resource availability and habitat structure. *Ecological Monographs* 81(1): 103-121.

Getzin, S., Wiegand, T., Wiegand, K. y He, F. 2008 Heterogeneity influences spatial patterns and demographics in forest stands. *Journal of Ecology* 96: 807-820.

Godoy, J. y Jordano, P. 2001. Seed dispersal by animals: exact identification of source trees with endocarp DNA microsatellites. *Molecular Ecology* 10: 2275 – 2283.

Hardesty, B.D. y Parker, V.T. 2002. Community seed rain patterns and a comparison to adult community structure in a West African tropical forest. *Plant Ecology* 164: 49-64.

Harms, K.E., Wright, S.J., Calderón, O., Hernández, A. y Herre, E.A. 2000. Pervasive density-dependent recruitment enhances seedling diversity in a tropical forest. *Nature* 404: 493-495.

Harms, K.E., Condit, R., Hubbell, S.P. y Foster, R.B. 2001. Habitat associations of trees and shrubs in a 50-ha Neotropical forest plot. *Journal of Ecology* 89: 947-959.

Herrera, C. M., Jordano, P., Lopez-Soria, L. y Amat, J.A. 1994. Recruitment of a mast-fruiting, bird-dispersed tree – bridging frugivore activity and seedling establishment. *Ecological Monographs* 64: 315 – 344.

Holmgren, M., Scheffer, M. y Huston, M.A. 1997. The interplay of facilitation and competition in plant communities. *Ecology* 78(7): 1966-1975.

Hubbell, S.P. 1979. Tree dispersion, abundance, and diversity in a tropical dry forest. *Science* 203: 1299–1309.

Hubbell, S.P., Foster, R.B., O'Brien, S.T., Harms, K.E., Condit, R., Wechsler, B., Wright, S.J. y Loo de Lao, S. 1999. Light gap disturbances, recruitment limitation, and tree diversity in a neotropical forest. *Science* 283: 554-557.

Hubbell, S.P. 2001. *The Unified Neutral Theory of Biodiversity and Biogeography*. Monographs in Population Biology. Princenton University Press. Princenton and Oxford. New Jersey.

Jacquemyn, H., Butaye, J. y Hermy, M. 2001. Forest plant species richness in small, fragmented mixed deciduous forest patches: the role of area, time and dispersal limitation. *Journal of Biogeography* 28: 801-812.

Jansen, P.A., Bongers, F, y van der Meer, P.J. 2008. Is farther seed dispersal better? Spatial patterns of offspring mortality in three rainforest tree species with different dispersal abilities. Ecography 31: 43-52.

Janzen, D.H. 1970. Herbivores and the number of tree species in tropical forest. *The American Naturalist* 104(940): 501-528.

Jara-Guerrero, A., De la Cruz, M., Espinosa, C. I., Méndez, M. y Escudero, A. 2015. Does spatial heterogeneity blur the signature of dispersal syndromes on spatial patterns of woody species? A test in a tropical dry forest. *Oikos*. doi: 10.1111/oik.02098.

John, R., Dalling, J.W., Harms, K.E., Yavitt, J.B., Stallard, R.F., Mirabello, M., Hubbell, S.P., Valencia, R., Navarrete, H., Vallejo, M. y Foster, R.B. 2007. Soil nutrients influence spatial distributions of tropical tree species. *Proceedings of the National Academy of Science* USA 104: 864–869.

Leibold, M. A. 1995. The niche concept revisited: mechanistic models and community context. *Ecology* 76: 1371 – 1382.

Levine, J.M. y Murrell, D. J. 2003. The community-level consequences of seed dispersal patterns. *Annual Review of Ecology, Evolution and Systematics* 34:549 –574.

Li, L., Huang, Z., Ye, W., Cao, H., Wei, S., Wang, Z., Lian, J., Sun, I.-F., Ma, K. y He, F. 2009. Spatial distributions of tree species in a subtropical forest of China. Oikos, 118: 495–502.

Lin, Y-C., Chang, L-W., Yang, K-Ch., Wang, H-H. y Sun, I-F. 2010. Point patterns of tree distribution determined by habitat heterogeneity and dispersal limitation. *Oecologia* 165: 175-184.

López-Martínez, J. O. et al. 2013. β -Diversity of functional groups of woody plants in a tropical dry forest in Yucatan. *PLoS ONE* 8(9): e73660.

Massey, F.P., Massey, K., Press, M.C. y Hartley, S.E. 2006. Neighbourhood composition determines growth, architecture and herbivory in tropical rain forest tree seedlings. *Journal of Ecology* 94: 646-655.

McIntire, E.J.B. y Fajardo, A. 2009. Beyond description: the active and effective way to infer processes from spatial patterns. *Ecology* 90(1): 46-56.

Muller-Landau, H.C. y Hardesty, B.D. 2005. Seed dispersal of woody plants in tropical forest: concepts, examples and future directions. En: Burslem, D.F.R.P.; Pinard, M.A.; Hartley, S.E. (eds) *Biotic Interactions in the Tropics: Their Role in the Maintenance of Species Diversity*. Cambridge University Press.

Muller-Landau, H.C., Wright, S.J., Calderón, O., Condit, R., y Hubbell, S.P. 2008. Interspecific variation in primary seed dispersal in a tropical forest. *Journal of Ecology* 96: 653-667.

Murrell, D.J. 2009. On the emergent spatial structure of size-structured populations: when does self-thinning lead to a reduction in clustering? *Journal of Ecology* 97: 256-266.

Nathan, R. y Muller-Landau, H.C. 2000. Spatial patterns of seed dispersal, their determinants and consequences for recruitment. *Tree* 15(7): 278-285.

Novotny, V. y Basset, Y. 2005. Host specificity of insect herbivores in tropical forest. *Proceedings of the Royal Society* 272: 1083-1090.

Phillips, O.L., Núñez-Vargas, P., Monteagudo, A.L., Peña-Cruz, A., Chuspe-Zans, M.E., Galiano-Sánchez, W., Yli-Halla, M. y Rose, S. 2003. Habitat association among Amazonian tree species: a landscape-scale approach. *Journal of Ecology* 91: 757-775.

Pinto,S.M. y MacDougall, A.S. 2010. Dispersal limitation and environmental structure interact to restrict the occupation of optimal habitat. *The American Naturalist* 175(6): 675-686.

Plotkin, J.B., Chave, J. y Ashton, P.S. 2002. Cluster analysis of spatial patterns in Malaysian tree species. The American Naturalist 160(5): 629-644.

Purves, D.W. y Law, R. 2002. Fine-scale spatial structure in a grassland community: quantifying the plant's-eye view. *Journal of Ecology* 90: 121-129.

R Core Team 2013. R: A language and environment for statistical computing. R Foundation for Statistical Computing, Vienna, Austria. Disponible en: http://www.r-project.org/.

Ripley, B.D. 1977. Modeling spatial patterns. *Journal of the Royal Statistical Society. Series B (Methodological)* 39(2): 172-212.

Russo, S. E. y Augspurger, C. K. 2004. Aggregated seed dispersal by spider monkeys limits recruitment to clumped patterns in *Virola calophylla*. Ecology Letters 7: 1058–1067.

Schiffers, K., Schurr, F.M., Tielborger, K., Urbach, C., Moloney, K. y Jeltsch, F. 2008. Dealing with virtual aggregation - a new index for analysing heterogeneous point patterns. *Ecography* 31: 545-555.

Schreeg, L.A., Kress, W.J., Erickson, D.L. y Swenson, N.G. 2010. Phylogenetic analysis of local-scale tree soil association in a lowland moist tropical forest. *PLoS ONE*, **5**, e13685.

Scupp, E.W. y Fuentes, M. 1995. Spatial patterns of seed dispersal and the unification of a plant population ecology. *EcoScience* 2: 267-275.

Seidler, T. y Plotkin, J. 2006. Seed Dispersal and Spatial Pattern in Tropical Trees. *PLoS Biology* 4(11): 2132-2137.

Sheil, D., Salim, A., Chave, J., Vanclay, J. y Hawthorne, W.D. 2006. Illumination-size relationship of 109 coexisting tropical forest tree species. *Journal of Ecology* 94: 494-507.

Shen, G., Yu, M., Hu, X-S., Mi, X., Ren, H., Sun, I-F., y Ma, K. 2009. Species-area relationship explained by the joint effects of dispersal limitation and hábitat heterogeneity. *Ecology* 90(11): 3033-3041.

Shen, G., He, F., Waagepetersen, R., Sun, I-F., Hao, Z-S.Ch., Chen, Z-S. y Yu, M. 2013. Quantifying effects of habitat heterogeneity and other clustering processes on spatial distributions of tree species. *Ecology*. 94:2436–2443.

Silvertown, J. 2004. Plant coexistence and the niche. *Trends in Ecology and Evolution* 19(11): 605-611.

Stoyan, D. y Stoyan, H. 1994. *Fractals, Random Shapes and Point Fields. Methods of Geometrical Statistics*. John Wiley & Sons. New York.

Teller, B. J., Marden, J. H. y Shea, K. 2015. Covariation in abscission force and terminal velocity of windborne sibling seeds alters long-distance dispersal projections. *Methods in Ecology and Evolution* 6: 593–599.

Waagepetersen, R. y Guan, Y. 2009. Two-step estimation for inhomogeneous spatial point processes. *Journal of the Royal Statistical Society: Series B (Statistical Methodology)*, 71: 685–702.

Watt, A.S. 1947. Pattern and Process in the Plant Community. *Journal of Ecology* 35(1): 1-22.

Webster, R. y Mcbratney, A.B. 1989. On the Akaike information criterion for choosing models for variograms of soil properties. *Journal of Soil Science* 40: 493–496.

Weeb, C.O. y Peart, D.R. 2000. Habitat associations of trees and seedlings in a Bornean rain forest. *Journal of Ecology* 88: 464-478.

Wiegand, T. y Moloney, K. 2004. Rings, circles and null-models for point pattern analysis in ecology. *Oikos* 104: 209-229.

Wiegand, T., Gunatilleke, S. y Gunatilleke, N. 2007. Species associations in a heterogeneous Sri Lankan Dipterocarp forest. *The American Naturalist* 170: E77–E95.

Wiegand, T., Martínez, I., y Huth, A. 2009. Recruitment in Tropical Tree Species: Revealing Complex Spatial Patterns. *The American Naturalist* 174(4): E106-E140.

Wiegand, T, y Moloney, K.A. 2014. *Handbook of Spatial Point-Pattern Analysis in Ecology*. Chapman & Hall/CRC. Iowa, USA.

Wright, S.J. 2002. Plant diversity in tropical forests: a review of mechanisms of species coexistence. *Oecologia* 130: 1-14.

Wright, S.J., Hernández, A. y Condit, R. 2007. The Bushmeat Harvest Alters Seedling Banks by Favoring Lianas, Large Seeds, and Seeds Dispersed by Bats, Birds, and Wind. *Biotropica* 39(3): 363-371.

CAPÍTULO 4

Placing species back into communitiesy: Individual Functional Diversity-Area Relationships reveal prevalence of limiting similarity processes (and niche partitioning) in a tropical forest.

Abstract

In the last years an increasing effort has been made to study community assembly from a functional perspective. However, even when most theories remark the importance of species interactions and inter-specific fitness differences on community assembly, very few studies have addressed the role that individual species play in this process and none, up to date, has examined how this is related to their functional attributes.

We propose the Individual Functional Diversity-Area Relationship (IFDAR) to measure scale-dependent, local functional diversity structures around individual species. IFDAR is based in spatial point pattern analysis techniques and measures the expected functional diversity in circular neighbourhoods with variable radius around an arbitrary individual of a target species. We use IFDAR to investigate if and at which spatial scales individual species in BCI (Panama) inhabit local assemblages with higher, lower or expected functional diversity

Controlling for coarse-scale habitat filtering, most species (55%) accumulated around them more functional diversity and were surrounded by species more functionally different than expected, which is compatible with niche partitioning and a limiting similarity process. A small proportion of species (24 %) was surrounded by less functional diversity than expected, suggesting the existence of an additional process of fine-scale habitat filtering.

Additional tests showed that species classified as accumulators by IFDAR were in fact more functionally different among them than expected by chance, which confirm the ability of IFDAR to disentangle community responses to niche partitioning. IFDAR also showed that both limiting similarity and habitat filtering processes leave spatial signals in the same fine-spatial scales, which goes against the expectations of both neutral and niche theories employed to explain community assembly. The ability to provide this kind of insights makes IFDAR a useful tool for community ecologists.

Abbreviations: IFDAR: individual functional diversity-area relationship, ISAR: individual species-area relationship, FDAR: functional diversity area relationship, BCI: Barro Colorado Island, FD:

functional diversity, GoF: Goodness of Fit, GD: Gower's distance, HP: heterogeneous Poisson process, FDis: functional dispersion.

Introduction

Over the last few years, plant ecology has enlarged the understanding on how physiological and functional processes shape the assembly of ecological communities (Weiher & Keddy 1995; McGill *et al.* 2006; Westoby & Wright 2006). Functional traits summarize essential aspects of species' performance and life-history strategies (Wright *et al.* 2004; Baraloto *et al.* 2010), providing a mechanistic relationship between ecological processes and community assembly (McGill *et al.* 2006; Westoby & Wright 2006). For example, some studies have shown the existence of correlations between environmental gradients and averaged community trait values (Kraft *et al.* 2008; Cornwell & Ackerly 2009), which has been presented as evidence for environmental filtering. Furthermore, the over-dispersion of some trait values within communities (*e.g.*, Kraft *et al.* 2008; Cornwell & Ackerly 2009; Paine *et al.* 2011) has been interpreted as the niche differentiation that results from inter-species competition. On the other hand, species' functional traits are the basis for measuring functional diversity (FD), one of the three axis of community diversity (together with taxonomic and phylogenetic diversity; Swenson 2011). It is generally assumed that a bidirectional link exists between FD and ecosystem functioning, with FD influencing ecosystem processes and services (Diaz *et al.* 2007; Petchey & Gaston 2006; Cadotte *et al.* 2011), and ecosystem processes affecting FD (Mayfield *et al.* 2010; Biswas & Mallik 2010; Lohbeck *et al.* 2012).

One of the rationales of the FD framework is that trait-based approaches have the potential to reveal general rules that species-specific responses have failed to identify (Adler *et al.* 2013). This has favoured the shift from species-based to trait-based community ecology (McGill *et al.*2006; Cadotte *et al.* 2011); in fact, in the recent literature about functional community ecology, species are considered mere "trait containers" whose presence or absence in a community simply adds to or subtracts from community's FD (Mouillot *et al.* 2008; Schemera *et al.* 2009). However, species interactions and inter-specific fitness differences are at the core of most hypotheses and theories about community assembly (Chesson 2000; HilleRisLamber *et al.* 2012), so it is natural to ask about the role that each individual species plays in the assembly of communities (Wiegand *et al.* 2007), *e.g.*, Are there any key species controlling the structure of a community's FD?

On the other hand, focusing on individual species could help scrutinize with more detail the effects of ecological processes on community assembly and might allow to address new questions, for example, whether all species respond similarly to the effects of limiting similarity and environmental filtering, or if these responses are consistent throughout space and time (*e.g.*, throughout ontogeny).

Recently, Chase (2014) recalled the necessity for prospecting simultaneously different spatial scales in order to solve discrepancies about the relative importance of the different processes involved in community assembly. Answering these questions and overcoming these difficulties requires both designing new analytic tools and reformulating the expectations of niche and for extension coexistence theory in terms of individual species responses to functional diversity.

Here, we propose computing Individual Functional Diversity-Area Relationships (IFDAR), an individual version of the functional diversity-area relationship function (Smith *et al.* 2013). IFDAR is based on spatial point pattern analysis techniques and allows functional diversity around individual species to be estimated and evaluated against the expectations of some assumed ecological process (McIntire & Fajardo2009). For example, if competitive effects are ruling the structure of a community, we would expect an increase (*i.e.*, accumulation) of FD around individual species. On the contrary, if only habitat filtering is affecting the assembly process, we should find that most species have small values of FD in their surroundings. Even more, if several processes were simultaneously ruling community assembly, IFDAR could detect their differential effects, at least when these are occurring at contrasting spatial scales.

To illustrate the kind of insights this approach can provide, we calculate IFDAR functions for the most abundant species in the Barro Colorado Island forest (hereafter BCI). Previous studies have demonstrated the existence of large-scale environmental heterogeneity and its influence on species distribution in the BCI plot (*e.g.*, Harms *et al.* 2001; John *et al.* 2007; Schreeg *et al.* 2010), although a perennial controversy remains about the role of this and other processes on community organization (Chase 2014).We will use IFDAR to disentangle the role of limiting similarity and habitat filtering mechanisms in determining the spatial pattern of functional diversity around individual species in BCI. For this, we partial out the effects of large-scale environmental filtering on each species with heterogeneous Poisson null models, and test for the existence of limiting similarity. In this context, if competitive effects are ruling the structure of the BCI community, we will find a significant accumulation of functional diversity around individual species at the spatial scales where these competitive effects would be taking place. On the contrary, if only habitat filtering is affecting the assembly process, we should find that most species have average (i.e. "normal") functional diversity in their neighbourhoods. If additional habitat filtering is occurring at finer spatial scales than those considered in the heterogeneous models, we expect to find a repulsion of functional diversity at the spatial scales where this filter is ruling community assembly.

As a way to check the results provided by IFDAR, we will test the degree of niche differentiation (measured as the Gower's distance in the space of traits) among the different species types emerging

from the IFDAR analyses, i.e. accumulators and repellers of functional diversity. If accumulation of functional diversity is driven by competitive processes and these promote niche partitioning, we expect that Gower's distances would be larger than expected among accumulator species and non-significantly different among repeller or "normal" species. Thereby definig a structured community as one in which species-specific differences affect the populations dynamic and consequently the community (Purves & Pacala 2005).

Methods

Individual functional diversity-area relationship

We defined the Individual Functional Diversity-Area Relationship *IFDAR(a)* as the expected functional diversity within circular areas $a=\pi r^2$ around a typical individual of a focal species, with r being the radius of a. It is estimated as:

$$IFDAR\ (a) = \frac{\sum_{i=1}^{n} FDis(a)_i}{n}$$

where n is the total number of individuals of the focal species and $FDis(a)_i$ is the functional dispersion (Laliberté & Legendre 2010) of the "local" community delimited by the circle within the area $a=\pi r^2$ around individual i of the focal species. For a community, *FDis* is computed as:

$$FDis = \frac{\sum_{j=1}^{S} x_j z_j}{\sum_{j=1}^{S} x_j}$$

where S is the total number of species, x_j is the abundance of species j in the community and z_j is the distance (usually Gower's distance) in the multivariate space of traits from species j to the centroid of the community (Laliberté & Legendre 2010).

Although several other indices have been proposed to estimate functional diversity (see references in Petchey & Gaston 2006 and Laliberté & Legendre 2012), we chose FDis because it is not affected by species richness (Laliberté & Legendre 2010). This makes it an ideal tool for estimating functional diversity at different spatial scales (i.e. at different community richnesses). An additional advantage of using Gower's distance to compute FDis is that it successfully deals with missing values, a common feature of most plant trait databases. Some recent studies (Pakeman 2013) have pointed out the sensitivity of functional indices to the completeness of species' trait data. However, when species with missing trait data are rare (as in our study) IFDAR values will not be severely biased as their effect will be diluted away when averaging the n individual FDis measurements to compute IFDAR.

Study area and plant functional traits

To illustrate the use of IFDAR, we employed mapped tree data from the 50-ha rectangular permanent plot on Barro Colorado Island, Panama (9º10'N, 79º51'W), a seasonally moist tropical forest. This plot was established in 1980 and all stems of trees and shrubs >1-cm diameter at breast height (dbh) have been mapped and identified on several occasions (Condit 1998; Hubbell *et al.* 1999; Hubbell *et. al.* 2005). Although the location of the plot was selected for its uniform relief and physical conditions (Condit *et al.* 2000), several studies have shown that species distribution is related to topographical (Harms *et al.* 2001) and edaphic (John *et al.* 2007; Schreeg *et al.* 2010) variation. Forest dynamics is mainly related to the creation of canopy gaps by tree falls (Hubbell & Foster 1986; Brokaw 1985).

For this study, we selected all trees with a dbh > 10 cm from the 1995 census. The final sample included 22,685 trees from 227 species. To characterize functional diversity, we used the four most common traits in plant ecology studies: wood density (WD), seed mass (SM), specific leaf area (SLA) and maximum height (H_{max}). All of them have well known connections with ecological strategies (Wright *et al.* 2010). We obtained values for all four traits from Wright *et al.* (2010) BCI trait-database for 119 species. We completed WD data for 62 additional species from the Global Wood Density Database (Chave *et al.* 2009) and SM for 64 species from the Royal Botanic Gardens Kew Seed Information Database (Royal Botanic Gardens Kew 2008). For the remaining species (mostly species with few individuals), we assigned mean genus- (or family-) WD and SM values.

IFDAR estimation and testing in BCI

We estimated IFDAR for the 64 most abundant species (i.e., with more than 60 individuals).To simplify interpretation and graphical representation, instead of IFDAR(a) we use IFDAR(r), were r is the radius of the circular area a. In order to span the range of spatial scales at which most population processes occur in BCI (e.g. plant-plant interactions, dispersal limitation, gap colonization) (Hubbell 1979; Plotkin *et al.* 2000; Condit *et al.* 2000), we computed IFDAR(r) at 1 m intervals around individual trees up to a scale of r=50 m. To avoid edge effects, we established a buffer area of 50 m in the periphery of the plot.

To test whether a species significantly accumulates or repels functional diversity, we made Monte Carlo simulations from null models of species distributions. For this, we employed heterogeneous Poisson models which account for first order effects (i.e. differences in intensity throughout the plot, Wiegand & Moloney 2004) and factor out spatial signals caused by habitat association. To simulate the heterogeneous Poisson model, we first estimated the intensity function $\lambda(x,y)$ for each species with a Gaussian kernel with parameter σ = 25 m. This removes all potential spatial structure in the pattern of the target species at scales <50 m but maintains spatial structure at scales of 50 m and

higher (Wiegand *et al.* 2007). The simulation of the heterogeneous point pattern first generates a homogeneous Poisson process of intensity λ_{max} , where λ_{max} is the maximum $\lambda(x,y)$ value, and then independently retains each point with retention probability $p(x,y) = \lambda(x,y)/ \lambda_{max}$ (Baddeley & Turner 2005).

Following the usual point pattern analysis methodology, we built simulation envelopes for each species from 99 simulations of their null models. If the observed IFDAR(r) curve for a focal species at a given *r* was greater than the second largest IFDAR(r) of all 99 simulations of the null model, we considered the species to be a functional diversity accumulator at scale *r*, with an approximate α level of 0.05. Likewise, we considered the species to be a functional diversity repeller at scale *r* when its empirical IFDAR(r) value was smaller than the second smallest simulated value at scale *r*. If the IFDAR curve was within the range of the null model, the species was considered "normal" at scale *r*. To avoid the problems associated with simultaneous inference (i.e. one test for each *r* scale), we also computed a goodness-of fit (GoF) test (Loosmore & Ford 2006).

Species whose observed IFDAR function was larger or smaller than the simulation envelopes for more than 10 *r* intervals (i.e. for more than 20 % of the total surveyed radii) were respectively considered as “accumulator” and “repeller” of functional diversity. Species whose observed function was inside the simulation envelopes at 40 or more *r* distances were considered "normal" species.

We also estimated the community Functional Diversity Area Relationship (FDAR), i.e., a curve analogous to the typical SAR curve. For this, we placed a grid of 3600 points over the BCI map (i.e., one point at every 10 m on the *x* and *y* axes, leaving a buffer of 50 m from the border) and computed FDis in circles centred around each point with radii ranging from 1 to 50 m. FDAR(r) represents the average FDis value of each *r* radius. Additionally, we averaged the IFDAR values of all species for each *r* scale and obtained the "average IFDAR" curve. Finally, to compare the accumulation and repulsion of functional diversity with the accumulation of *taxonomic* diversity around individual species we computed Individual Species-Area Relationships (ISAR; Wiegand *et al.* 2007). Functions to compute, test and summarize IFDAR and ISAR functions have been included in the R-package "idar".

Evaluation and testing of niche partitioning among the accumulator, repeller and normal species.

To check the results provided by IFDAR, we tested the degree of niche differentiation among species assigned to different groups. We first evaluated the functional distinctiveness of species in the accumulator, neutral and repeller groups by computing the average Gower's distance (GD) in the

multi-trait functional space from each of the 64 studied species to the other 227 species. We then computed the average GD distance for the accumulator, repeller and normal species groups and compared these averages to the "global" average GD (i.e. the averaged distance for all 227 species). We also examined the differences in traits among species groups. For this, we computed the average GD distance from all species in one group to all species in the other two groups (Table 2). Inference for the averaged distances was obtained by reshuffling the species names in the GD matrix 999 times, computing the average GD for the reshuffled groups each time and assessing the number of times that the observed mean GD of each group was larger than the mean of the reshuffled GDs.

Results

When comparing empirical IFDARs against the simulations of the heterogeneous null models, some species were clearly accumulators or repellers of functional diversity (Fig. 1). Of the 64 analyzed species, only 5 species were normal (i.e. their IFDAR values were not different from null model expectations) at all spatial scales, and another 6 species were normal for at least 45 of the 50 1-m *r* intervals considered. Most species were generally accumulators of functional diversity (e.g. 30 species had higher IFDAR values than predicted by their null model for at least 25 radii), and another group were clearly repellers of functional diversity (e.g. 13 species had lower IFDAR values than expected for at least 25 radii). Only 8 species had IFDAR values which were both higher and lower than expected. In these cases, one of the patterns (repeller or accumulator) was consistently manifested at most scales, while the other was only manifested occasionally (at only 1 to 3 *r* scales).

Although most species were normal (i.e. had IFDAR values neither larger nor smaller than expected) at small *r* scales, the proportion of accumulator species increased with radius (Fig. 2a). The proportion of accumulator species became greater than the proportion of normal species at *r*= 18 m and continued to increase until *r* =26 m where it reached a constant 55 %. No repeller species were found at *r*= 1-6 m, but from *r*= 7-20 m the proportion of repeller species increased up to 24% and remained more or less constant (Fig. 2a). These results were confirmed by the GoF tests which found that most species had normal IFDAR functions (*i.e.*, values were not significantly different from those expected from the heterogeneous null model) at small scales (*r*= 1-10 m) and significant deviations from the null models at larger scales (*r*= 11-50 m) (Table S1 in Supporting Information). IFDAR was similar for all studied species at short scales ($r < 10$ m), with values which increased from around 0.01 for $r = 1$ m to 0.13 for $r = 10$ m and then remained around this value up to $r = 50$ m.

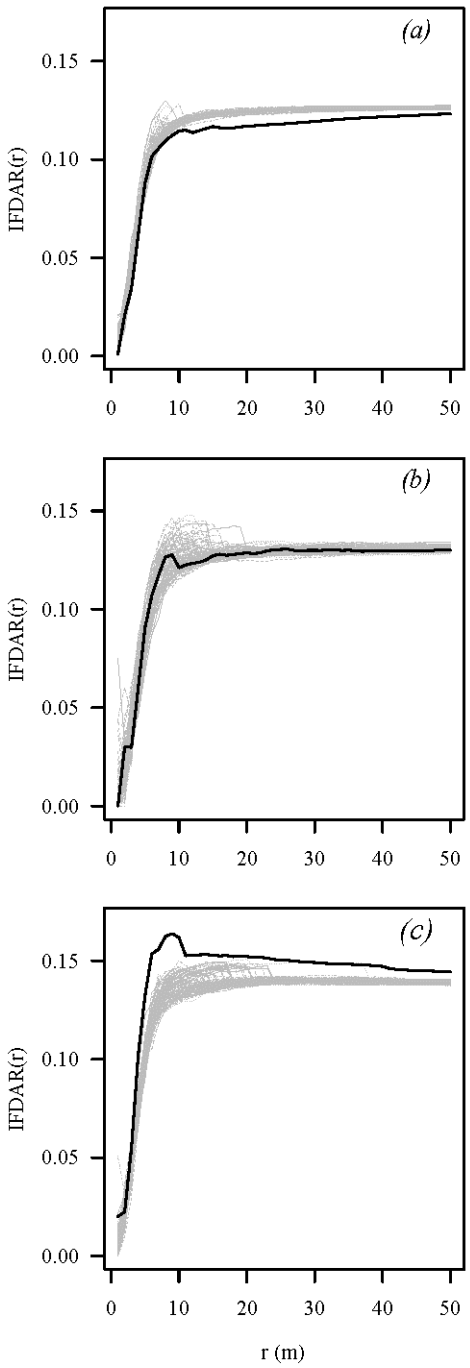

Figure 1. Individual Functional Diversity-Area Relationships (IFDAR) for some species representative of the three possible behaviors with respect to the heterogeneous Poisson null model: *Gustavia superba* (repeler) a); *Alchornea costaricensis* (normal) b); *Socratea exorrhiza* (accumulator) c). Black lines show the empirical IFDAR curve. Grey lines are IFDAR functions for the 99 simulated heterogeneous Poisson populations of each species.

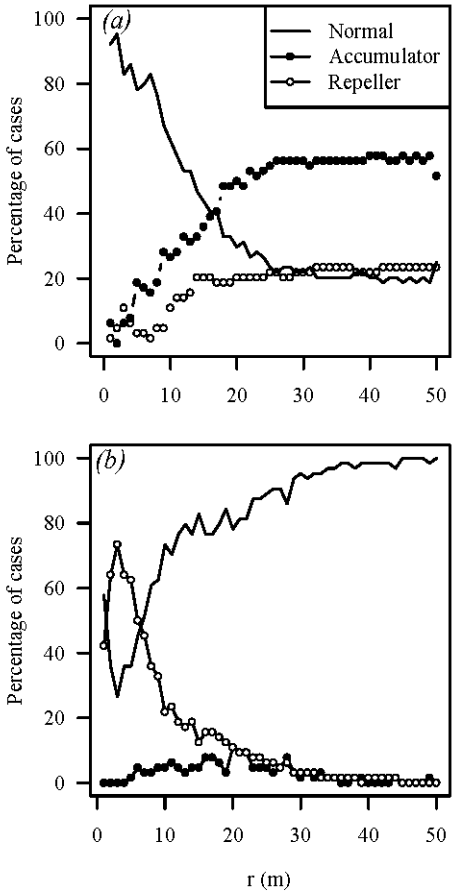

Figure 2. Proportion of significant accumulator, normal and repeller species for IFDAR a) and Individual Species-Area Relationships (ISAR) b) in BCI.

This behaviour was similar to the plot functional diversity-area (FDAR) curve, although average IFDAR was higher than whole-plot FDAR for *r* = 5-10 m (Fig. 3).

Mean Gower's distance between all 227 BCI species in the multivariate space of traits (GD_{all}) was 0.160. Mean Gower's distance from accumulators to all species was significantly greater than GD_{all} (mean distance = 0.193, p =0.001). However, mean Gower's distances from both normal and repeller species to all other species did not differ significantly from GD_{all}. Mean Gower distance's from accumulators to other accumulator, repeller or normal species were significantly greater than expected. On the contrary, mean Gower's distances between normal species, between repeller species or from repeller to normal species were not significantly different from expected values (Table 1).

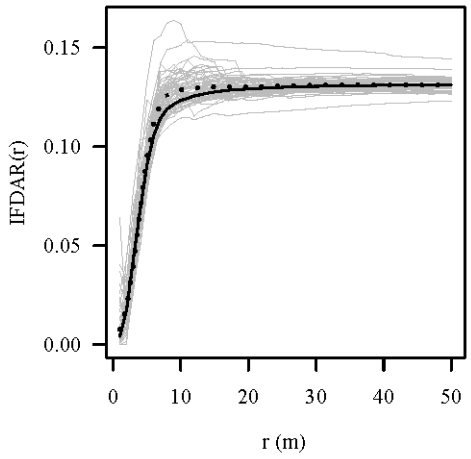

Figure 3. Individual Functional Diversity-Area Relationship (IFDAR) for the 64 most abundant species in BCI (grey lines). The solid black line represents the functional diversity-area curve (FDAR) of the whole community. The dotted black line represents the average IFDAR curve. The two conspicuously large and small IFDAR curves correspond respectively to *Socratea exorrhiza* and *Gustavia superba*.

Discussion

The new proposed IFDAR function is related to the classical species-area curve, and more specifically to Wiegand's *et al.* (2007) Individual Species-Area Relationship (ISAR), which describes the accumulation of *taxonomic* diversity around individual species. IFDAR is able to detect both positive and negative deviations of functional diversity from the expectations of a heterogeneous null model.

Since several types of coarse-scale habitat filtering may be occurring in BCI we have analyzed IFDAR functions in a framework of environmental filtering. Previous studies have shown that differences in slope and elevation allow several habitat types to be distinguished in BCI (Harms *et al.* 2001) and that community structure and composition respond to these abiotic variations (Kembell & Hubell 2006). Similarly, variation in soil chemistry has been shown to influence community composition in BCI (John *et al.* 2007), and Schreeg *et al.* (2010) demonstrated that this response is phylogenetically structured. Spatial autocorrelation for most soil nutrients reaches large distances (80-150 m, John *et al.* 2007), and the main habitat types in BCI are larger than 1 ha (Kembell & Hubell 2006).

Table 1. Mean Gower's distance, based on the 4 studied traits, among different species types. *(+):* distance larger than expected*; n.s.:* distance no significantly different from expected. P -values (*italics*) obtained from 999 mean distances computed on Gower's distance matrices with reshuffled species labels. Significant distances are presented in bold.

Species type	Accumulator	Normal	Repeller
Accumulator	(+) **0.219** *<0.001*	(+) **0.194** *0.041*	n.s. 0.188 *0.060*
Normal		n.s. 0.165 *0.572*	n.s. 0.161 *0.526*
Repeller			n.s. 0.156 *0.469*

The heterogeneous Poisson (HP) null models used to test IFDAR curves maintain the spatial association of the focal species with this coarse scale environmental variation whereas the spatial locations of the rest of the species remain fixed (Wiegand *et al.* 2007). So, if environmental filtering caused by coarse scale habitat or soil heterogeneity was the mechanism ruling community assembly, we should have found "normal" IFDAR curves for most species. However, only a small proportion of the studied species (12) can be considered normal in this sense, i.e. responding to habitat filtering. On the contrary, most species have greater IFDAR values than expected for the null model (i.e. they behave as accumulators). Furthermore, most analyzed species have greater IFDAR values than the plot FDAR, especially at short scales (Fig. 3), and average IFDAR is greater than plot FDAR. This suggests that a mechanism of limiting similarity is controlling community assembly at fine scales. If this were the case, inter-specific competition would make species avoid functionally similar species in their close proximity. This would generate neighbourhoods (i.e., local assemblages) with high FDis values, and, consequently, IFDAR values would be higher than average FDAR values of the forest. This also concurs with our findings that accumulator species were functionally different from the rest of species in BCI (i.e. had significantly greater Gower's distances to all other species than expected by chance). This suggests that accumulators are effectively partitioning the niche defined by the four studied traits.

An apparent contradiction to our conclusion about the relevance of limiting similarity is that many species showed a "normal" behaviour (i.e. compatible with habitat filtering) at small scales (r< 20 m). The main source of small-scale environmental variation in BCI is gap formation. Brokaw (1985) found that mean gap size in BCI was 86 m^2, and the largest gap was 360 m^2. However, these areas are considerably smaller than those for which we still detect this apparent abiotic filtering (a radius of 20 m implies areas of around 1257 m^2). Furthermore, Hubbell *et al.* (1999) pointed out that colonization and succession in BCI gaps is mainly ruled by random processes, and thus it would be independent of the functional adaptations of colonizing plants. Consequently, local assemblages generated within gaps should be functionally similar to the vegetation surrounding the gaps, and different functional signals should not be detected at short or medium scales around them. Thus, we believe this fine scale signal cannot be explained by the existence of gaps or other small environmental variations. On one hand, average IFDAR is larger than community FDAR even at these short spatial scales (Fig. 3). On the other hand, the absence of significant deviations from the null model for scales < 20 m could be easily explained as a mere structural effect: the number of trees in circular areas with radius < 20 m would not allow as many species to be accumulated as needed to obtain larger functional dispersion values than expected by the null model. In fact, 20 m is the upper limit for significant ISAR deviations in BCI; for circular areas with r < 20 m, a high proportion of species are "repellers" of *taxonomic* diversity (Wiegand *et al.* 2007; Fig. 2 b). This means that the number of different species at these scales is too small to obtain enough functional diversity, i.e. too small to detect significant deviations from the null model.

The explanation for the existence of some repeller species within a context of limiting similarity is not so straightforward. It could be related to the spatial distribution of each species. Highly-aggregated species would not leave enough room around their individuals for other species, which in turn would decrease (functional) diversity at the local scale (Wiegand *et al.* 2007). However, the spatial structure of repeller species was not significantly different from that of accumulators. In fact, both *Socratea exorrhiza* (the greatest accumulator species) and *Gustavia superba* (the greatest repeller) had the most clustered spatial distribution (Fig. 4, Table S2).

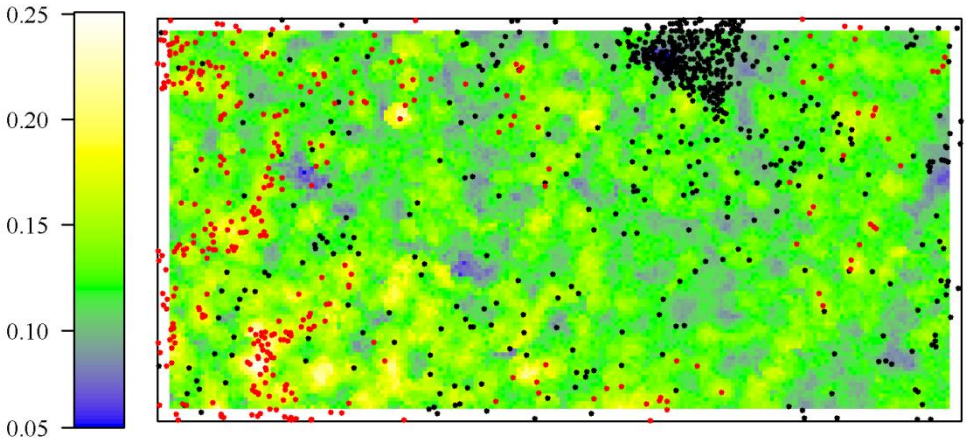

Figure 4. Spatial distribution of the most accumulator species (*Socratea exorrhiza*, red dots) and the most repeller species (*Gustavia superba*, black dots) in the BCI plot. Background colors (see ribbon) show the value of functional dispersion (FDisp) estimated in circular areas of radius = 15 m around 3600 points in a 10 x 10 m grid (i.e., one point at every 10 m on the *x* and *y* axes). The white area around the plot represents the buffer area of 50 m width where no estimations have been made.

Additionally, unexpected low functional diversity around repellers is not always caused by low taxonomic diversity, e.g. some IFDAR repellers are surrounded by more taxonomic diversity than other normal or even accumulator species (see Fig. S3).

Another explanation to these patterns would be related to species abundance. Even if they are not spatially aggregated, abundant species would have many conspecifics as neighbours, decreasing functional diversity in their neighbourhoods. However, repeller species abundance was not significantly different from accumulator abundance (Kruskal-Wallis rank sum test, p-value = 0.130). One plausible explanation is that repellers are habitat specialists which perceive a finer environmental grain than the other species. As our heterogeneous Poisson null models disrupt all spatial structure associated to grains < 50 m, any species responding to finer structured habitat heterogeneity would have higher functional diversity in the simulations and would appear as repeller. This behaviour would be more exacerbated (or more easily detectable) as the species becomes more abundant.

Conclusion

Recently, Cadotte *et al.* (2013) complained about the insufficient information available linking traits to community processes and exposed how this is limiting our ability to explain community assembly.

Even more, trait dispersion tests have shown low power to detect niche partitioning (Kraft & Ackerly 2010; Adler *et al.* 2013). However, with only four simple traits and the IFDAR function, we have been able to explain the assembly of a significant proportion of species in the rich community of BCI. Although this emblematic forest inspired the Neutral Theory of Biodiversity (Hubbell 2001; Condit *et al.* 2012), we found that community assembly seems governed by limiting similarity and habitat filtering at different spatial scales. This species-specific variation in biological traits observed has direct relevance for the functioning of the community (Purves and Pacala 2005). The importance of each mechanism depends on the implicated species and scale. This is especially remarkable in the case of repeller species, where the spatial scale at which habitat filtering is operating is similar to the small spatial scale where species interactions would occur. Contrarily to recent interpretations which assign different spatial extent to habitat- *vs.* competition-based processes (Chase 2014), IFDAR functions show that both processes can leave spatial signals in the same range of scales. The ability to provide this kind of insights makes IFDAR a useful tool for community ecologists.

References

Adler, P.B., Fajardo, A., Kleinhesselink, A.R. & Kraft, N.J.B. (2013) Trait-based tests of coexistence mechanisms. *Ecology Letters*, **16**, 1294-1306.

Baddeley, A. & Turner, R. (2005) Spatstat: an R package for analyzing spatial point patterns. *Journal of Statistical Software*, **12**(6), 1-42.

Baraloto, C., Paine, C.E.T., Poorter, L., Beauchêne, J., Bonal, D., Domenach, A.-M. *et al.* (2010) Decoupled leaf and stem economics in rain forest trees. *Ecology Letters*, **13**, 1338-1347.

Biswas, S.R. & Mallik, A.U. (2010) Disturbance effects on species diversity and functional diversity in riparian and upland plant communities. *Ecology*, **91**, 28-35.

Brokaw, N.V.L. (1985) Treefalls, regrowth, and community structure in tropical forests. *The Ecology of Natural Disturbance and Patch Dynamics* (eds. S.T. Pickett & P.S. White), pp. 53-69. Elsevier, New York.

Cadotte, M. W., Carscadden, K. & Mirotchnick, N. (2011) Beyond species: functional diversity and the maintenance of ecological processes and services. *Journal of Applied Ecology*, **48**, 1079-1087.

Cadotte, M., Albert, C.H. & Walker, S.C. (2013) The ecology of differences: assessing community assembly with trait and evolutionary distances. *Ecology Letters*, **16**, 1234-1244.

Chase, J.M. (2014) Spatial scale resolves the niche versus neutral theory debate. *Journal of Vegetation Science*, **25**, 319-322.

Chave. J., Coomes, D.A., Jansen, S., Lewis, S.L., Swenson, N.G. & Zanne, A.E. (2009) Towards a worldwide wood economics spectrum. *Ecology Letters*, **12**, 351-366.

Chesson, P. (2000) Mechanisms of maintenance of species diversity. *Annual Review of Ecology and Systematics*, **31**, 343-366.

Condit R., Chisholm, R.A. & Hubbell, S.P. (2012) Thirty years of forest census at Barro Colorado and the importance of immigration in maintaining diversity. *PLoS ONE*, **7**, e49826.

Condit, R. (1998) *Tropical Forest Census Plots*. Springer-Verlag and R. G. Landes Company, Berlin, and Georgetown, TX.

Condit, R., Ashton, P.S., Baker, P., Bunyavejchewin, S., Gunatilleke, S., Gunatilleke, N. *et al.* (2000) Spatial patterns in the distributions of tropical tree species. *Science*, **288**, 1414-1418.

Cornwell, W.K. & Ackerly, D.D. (2009) Community assembly and shifts in plant trait distributions across an environmental gradient in coastal California. *Ecological Monographs*, **79**, 109-126.

Díaz, S., Lavorel, S., de Bello, F., Quétier, F., Grigulis, K. *et al.* (2007) Incorporating plant functional diversity effects in ecosystem service assessments. *Proceedings of the National Academy of Sciences of the United States*, **104**, 20684-20689.

Harms, K.E., Condit, R., Hubbell, S.P. & Foster, R.B. (2001) Habitat associations of trees and shrubs in a 50-ha neotropical forest plot. *Journal of Ecology*, **89**, 947-959.

HilleRisLambers, J., Adler, P.B., Harpole, W.S., Levine, J.M. & Mayfield, M.M. (2012) Rethinking community assembly through the lens of coexistence theory. *Annual Review of Ecology, Evolution and Systematics.*, **43**, 227-248.

Hubbell, S.P. & Foster, R.B. (1986) Canopy gaps and the dynamics of a neotropical forest. *Plant Ecology* (ed. M.J. Crawley), pp. 77-96. Blackwell Science, Oxford, UK.

Hubbell, S.P. (1979) Tree dispersion, abundance, and diversity in a tropical dry forest. *Science*, **203**, 1299-1309.

Hubbell, S.P. (2001) *The Unified Neutral Theory of Biodiversity and Biogeography*. Princeton Univ. Press. Princeton, NJ.

Hubbell, S.P., Condit, R. & Foster, R.B. (2005) Barro Colorado Forest Census Plot Data. Available at: http://ctfs.arnarb.harvard.edu/webatlas/datasets/bci/. Last accessed: 12-May-2011.

Hubbell, S.P., Foster, R.B., O'Brien, S.T., Harms, K.E., Condit, R., Wechsler, B. *et al.* (1999) Light gap disturbances, recruitment limitation, and tree diversity in a neotropical forest. *Science* **283**, 554-557.

John, R., Dalling, J.W., Harms, K.E., Yavitt, J.B., Stallard, R.F., Mirabello, M. *et al.* (2007) Soil nutrients influence spatial distributions of tropical tree species. *Proceedings of the National Academy of Sciences of the United States*, **104**, 864-869.

Kembel, S.W. & Hubbell, S.P. (2006) The phylogenetic structure of a neotropical forest tree community. *Ecology*, **87**, S86–S99.

Kraft, N.J.B. & Ackerly, D.D. (2010) Functional trait and phylogenetic test of community assembly across spatial scales in an Amazonian forest. *Ecological Monographs*, **80**, 401-422.

Kraft, N.J.B., Valencia, R. & Ackerly, D.D. (2008) Functional traits and niche based tree community assembly in an Amazonian forest. *Science*, **322**, 580-582.

Laliberté, E. & Legendre, P. (2010) A distance-based framework for measuring functional diversity from multiple traits. *Ecology*, **91**, 299-305.

Lohbeck, M., Poorter, L., Paz, H., Pla, L., van Breugel, M., Martínez-Ramos, M. *et al.* (2012) Functional diversity changes during tropical forest succession. *Perspectives in Plant Ecology, Evolution and Systematics*, **14**, 89-96.

Loosmore, N.B. & Ford, E.D. (2006) Statistical inference using the G or K point pattern spatial statistics. *Ecology*, **87**, 1925-1931.

Mayfield, M.M., Bonser, S.P., Morgan, J.W., Aubin, I., McNamara, S. & Vesk, P.A. (2010) What does species richness tell us about functional trait diversity? Predictions and evidence for responses of species and functional trait diversity to land-use change. *Global Ecology and Biogeography*, **19**, 423-431.

McGill, B.J., Enquist, B.J., Weiher, E. & Westoby, M. (2006) Rebuilding community ecology from functional traits. *Trends in Ecology and Evolution*, **21**, 178-185.

McIntire, E.J.B. & Fajardo, A. (2009) Beyond description: the active and effective way to infer processes from spatial patterns. *Ecology* **90**, 46-56.

Mouillot, D., Culiolib, J.M., Pelletierc, D. & Tomasinia, J.A. (2008) Do we protect originality in protected areas? A new index and an application to the Bonifacio Strait Natural Reserve. *Biological Conservation,***141**: 1569-1580.

Paine, C.E.T., Baraloto, C., Chave, J. & Hérault, B. (2011) Functional traits of individual trees reveal ecological constraints on community assembly in tropical rain forests. *Oikos*, **120**, 720–727.

Pakeman, R.J. (2013) Functional trait metrics are sensitive to the completeness of the species' trait data?. *Methods in Ecology and Evolution*, **5**, 9-15.

Petchey, O.L. & Gaston, K.J. (2006) Functional diversity (FD), species richness and community composition. *Ecology Letters*, **5**, 402-411.

Plotkin, J.B., Potts, M.D., Leslie, N., Manokaran, N., LaFrankie, J. & Ashton, P.S. (2000) Species-area curves, spatial aggregation, and habitat specialization in tropical forests. *Journal of Theoretical Biology*, **207**, 81-99.

Purves, D.W. & Pacala, S.W. (2005) Ecological drift in niche-structured communities: neutral pattern does not imply neutral process. In: Burslem, D., Pinard, M. & Hartley, S. (eds.) *Biotic Interactions in the Tropic.* Their role in the maintenance of species diversity. Cambridge University Press. New York.

Royal Botanic Gardens Kew. (2008) Seed Information Database (SID). Version 7.1. Available at: http://data.kew.org/sid/ Last accessed: 25-February-2014.

Schemera, D., Podani, J. & Eros, T. (2009) Measuring the contribution of community members to functional diversity. *Oikos*, **118**, 961-971.

Schreeg, L.A., Kress, W.J., Erickson, D.L. & Swenson, N.G. (2010) Phylogenetic analysis of local-scale tree soil association in a lowland moist tropical forest. *PLoS ONE*, **5**, e13685.

Smith, A.B., Sandel, B., Kraft, N.J.B. & Carey, S. (2013) Characterizing scale-dependent community assembly using the functional-diversity–area relationship. *Ecology*, **94**, 2392-2402.

Swenson, N.G. (2011) The role of evolutionary processes in producing biodiversity patterns, and the interrelationships between taxonomic, functional and phylogenetic biodiversity. *American Journal of Botany*, **98**, 472-480.

Weiher, E. & Keddy, P.A. (1995) Assembly rules, null models, and trait dispersion - new questions front old patterns. *Oikos*, **74**, 159-164.

Westoby, M. & Wright, I.J. (2006) Land-plant ecology on the basis of functional traits. *Trends in Ecology and Evolution*, **21**, 261-268.

Wiegand, T. & Moloney, K. (2004) Rings, circles and null-models for point pattern analysis in ecology. *Oikos*, **104**, 209-229.

Wiegand, T., Gunatilleke, C.V.S., Gunatilleke, I.A.U.N. & Huth A. (2007) How individual species structure diversity in tropical forests. *Proceedings of the National Academy of Sciences of the United States*, **104**, 19029-19033.

Wright, I.J., Reich, P.B., Westoby, M., Ackerly, D.D., Baruch, Z., Bongers, F. *et al.* (2004) The worldwide leaf economics spectrum. *Nature*, **428**, 821-827.

Wright, S.J., Kitajima, K., Kraft, N.J.B., Reich, P.B., Wright, I.J., Bunker, D.E. *et al.* (2010) Functional traits and the growth–mortality trade-off in tropical trees. *Ecology*, **91**, 3664-3674.

CONCLUSIONES GENERALES

CONCLUSIONES GENERALES

Muchos estudios teóricos y empíricos se han centrado en el papel rol complejo de los patrones espaciales en los procesos ecológicos con el propósito de descubrir la información contenida en la organización interna de los sistemas ecológicos. Desentrañar estas señales a partir de los patrones espaciales sigue siendo aun un reto importante. La investigación detallada en la presente disertación, muestra aplicaciones potenciales para entender los procesos ecológicos que ocurren en la estructuración de poblaciones o comunidades vegetales. Por un lado, mediante se han desarrollasdo herramientas nuevas para comprobar hipótesis sobre la dispersión de plantas parásitas (Cap. 1), y para evaluar el efecto de factores abióticos y su interacción, sobre la estructura poblacional de un arbusto dominante, con datos basados en patrones replicados (cap. 2). Por otro lado, se ha evaluado la relación entre el síndrome de dispersión y el patrón espacial en una comunidad de bosque tropical, considerando el efecto de la limitación de la dispersión y heterogeneidad del hábitat (Cap. 3); y finalmente, se construyó un índice que evalúa, a nivel de individuo, la diversidad funcional en la comunidad y, que incluye el patrón espacial de distribución de cada especie y cuatro rasgos funcionales clave de las especies presentes en la comunidad. Como consecuencia de esta investigación, podemos concluir que:

1. Modelos mulos basados en funciones kernel, son efectivos para explicar la dispersión. La elección adecuada de la función kernel, es importante para describir un proceso de dispersión. En el caso de *A. oxycedri*, la función kernel bi-dimensional t de Student (2Dt), fue la que explicó mejor el comportamiento de dispersión de la especie parásita.
2. Entre las funciones kernel Gaussiano y bi-dimensional t de Student, ésta última resultó menos afectada por la denso-dependencia espacial.
3. La forma de dispersión balística de *A. oxycedri*, así como la densidad de los árboles hospedantes definen el agrupamiento de los árboles infectados, a cortas distancias (r<10m). Al comparar el modelo empírico con los modelos simulados, se observó que existen otros factores que están influyendo en la dispersión del muérdago enano, a distancias más largas. Esto se ratificó con la fuerte dependencia espacial del patrón de árboles afectados versus el patrón de árboles no-afectados, revelada a todas las escalas.

4. La topografía del terreno presentó efecto principal observado significativo sobre la estructura espacial de la población de *Croton sp.*, de forma similar la interacción entre los dos factores altitud vs topografía, resultó también significativa. Es decir, la diferencia entre llano y pendiente observada en altitud baja (1400-1550m), no es igual a una altitud mayor (1700-1900m).
5. A pequeñas distancias (r<1m), en altitud baja, *Croton sp.* presentó patrón más agregado en topografía plana, mientras que en pendiente se observó fuerte agregación a distancias grandes; en consistencia con los efectos predominantes de facilitación. Las parcelas ubicadas a mayor altitud y fuerte pendiente, mostraron en promedio menor agregación.
6. Abaja altitud, la agregación espacial en topografía plana se vió afectada por el incremento en el tamaño medio del parche (13.01 m) y una disminución del número de agregados por parcela (18 en promedio).
7. Nuestro método ANOVA-like, en combinación con patrones de puntos replicados y con adecuado diseño muestral, sugiere posibles procesos y mecanismos subyacentes al patrón espacial. Estos difícilmente se podría identificar mediante un patrón singular, y además los resultados obtenidos son interpretables en términos ecológicos.
8. La altitud por sí sola no resultó significativa en la formación del patrón espacial de *Croton sp* Sin embargo, se ha visto que en asociación con otros factores ecológicos, es capaz de modificar su distribución. La capacidad de respuesta de este arbusto asegura la supervivencia y dominancia en el matorral seco al sur del Ecuador; siendo además una especie facilitadora para otras especies herbáceas propias del ecosistema seco.
9. Utilizando cuatro modelos teóricos de procesos espaciales de puntos (HPP, IPP, HPCP y IPCP), hemos verificado que el efecto conjunto de la limitación a la dispersión y la heterogeneirad ambiental se reveló como más influyente en la formación del patrón espacial de la mayoría de las especies (63% de las especies, 114 especies); mientras que la quinta parte de las especies (45 especies) presentaron un patrón espacial consistente con el efecto único de la dispersión limitada.
10. No se identificaron especies cuya distribución espacial obedeciera únicamente al azar. Si embargo casi la quinta parte de las especies (40 especies) presentó

patrones congruentes con un proceso de Poisson heterogéneo, sugiriendo que tales patrones pueden ser explicados únicamente por la heterogeneidad de hábitat, esto sugiere que una buena parte de la comunidad se beneficia de crecer en hábitats favorables.

11. No se observó relación significativa entre el grado de agrupamiento de las especies y el síndrome de dispersión, sin embargo se identificó prevalencia de mayor agregación en las especies anemócoras y autodispersadas. que las dispersadas por animales, manteniéndose este comportamiento a todas las escalas.
12. La inclusión de la heterogeneidad ambiental como un factor explicativo del ensamblaje de la comunidad es tan importante como la dispersión limitada, así el patrón espacial del 80% de las especies de la parcela de BCI se ajustó mejor al incluirse a heterogenidad ambiental.
13. Las predicciones sobre los patrones espaciales de especies de bosque tropical y su relación con el síndrome de dispersión puedes mejorarse escogiendo el mejor modelo para cada especie a partir de un conjunto de modelos que involucren diferentes mcanismos causales, en lugar de forzar el ajuste de un tipo único de models para todas las especies.
14. El índice de dispersión funcional local (IFDAR) que se ha desarrollado en este estudio, es capaz de detectar variaciones positivas o negativas de la diversidad funcional de la comunidad respecto de cada especie individual, y presenta una rápida estabilidad asintótica, en relación a otros índices especie-área.
15. Se observó un alto porcentaje de especies acumuladoras de diversidad funcional para escalas superiores a 20m, lo que sugiere la presencia de mecanismos que limitan a semejanza entre especies y que fomentan la co-existencia de especies con estrategias diferenciadas. La ausencia de esta señal a pequeña escala puede obedecer al espacio insuficiente para la acumulación de las especies.
16. Fuertes diferencias significativas entre especies neutrales vs acumuladoras y neutrales vs repulsoras, se encontró respecto a la abundancia, dominancia local y agrupamiento. Esto se atribuye a la baja abundancia que presentaron las especies neutrales; sin embargo esto no fue significativo entre repulsoras y acumuladoras.
17. La presencia de especies funcionalmente próximas, o más alejadas respecto a la comunidad completa, dependiendo del nivel de competencia que ejercen sobre la

comunidad, son indicadoras del efecto de hábitat y denso-dependencia. Las especies denominadas competidores superiores, pueden ser insensibles a la limitación de la dispersión.

18. Al contrario de lo postulado por la teoría neutral, los resultados de este estudio indican que el ensamblaje de la comunidad está influido tanto por limitaciones de similitud como por heterogeneidad ambiental a diferentes escalas.

APÉNDICES

APPENDIX 1. Mathematical details about dispersal kernels

Null Models

Null models are used to determine whether observed properties of a spatial pattern, such as the extent of clustering, can be explained by making an explicit hypothetical assumption (Law et al. 2009). The choice of a null model needs more careful thought (Goreaud & Pélissier 2003). For instance, suppose the question is about spatial locations of individuals with different qualitative marks, such as infected and uninfected host. Null model could be that there are independent spatial point processes responsible for location of plants with different marks.

Kernel functions for smoothing

When estimating second-order radial statistics that assume stationarity (pattern is translation invariant) and isotropy (pattern is rotation invariant), it is usual to apply some kernel function k(x) over a distance x, to make the statistics smooth functions of distance.

Spatially explicit models inevitably require the use of functions called kernels, which describe the dispersion in space (Clark et al. 1998, Chesson and Lee 2005). The intensity functions are estimated by means of nonparametric methods based on kernel The density at each grid intersection is the average density for all of the kernels that overlap at each point (Erran-Seaman and Powell 1996), equivalent to determining risk elevations around each event point process and based on the aggregation of these elevations (Martinez-Beneito 2005). The kernel is a probability density and (Worton 1989), and unimodal (Silverman 1986), and all kernels have a volume that integrates to 1, satisfying the property:

$$\int_{R^2} K(x)dx = 1$$

Theoretically, the kernel estimator of the intensity function for bivariate data is defined as (Erran-Seaman and Powell 1996):

$$\hat{\lambda}_K(x) = \frac{1}{nh^2}\sum_{i=1}^{n} K\left(\frac{x-x_i}{h}\right)$$

where n is the number of points, h > 0 represents half the bandwidth of the kernel, also known as the amount of smoothing (Lloyd 2007), K is the kernel density function, x is a

vector of coordinates (x, y) that describe the location where the function is being evaluated, and x_i is a set of vectors whose coordinates describe the location of each observation i.

Since kernel estimates of density near the border of the study area tend to be distorted and as there may be neighboring points outside the border, a kernel estimator includes edge correction.

The concept of a "fat-tailed" kernel can best be demonstrated by a density function that is expressed in terms of two parameters, a "distance parameter" α, and a "shape parameter" c, that determines higher moments (including kurtosis):

$$k(x) = \frac{c}{2\alpha\Gamma(\frac{1}{c})} exp\left[-\left|\frac{x}{\alpha}\right|^c\right]$$

where Γ() is the gamma function with argument 1/c. This density includes several familiar density functions, including exponential (c=1) and Gaussian (c=2). Fat tailed distributions are ones with kurtosis larger than the exponential distribution or c parameters less than 1, and characterized by accelerating spread (Kot et al. 1996).

Gaussian kernel

If c=2 for k(x) expression, this density is called Gaussian kernel smoothing:

$$K(x) = (2\pi)^{-1} exp\left(-\frac{1}{2}\left(\frac{x - x_i}{h}\right)\right)$$

where bandwidth h is the standard deviation of the normal distribution..

The kernel estimation performed by a simple Nadaraya-Watson type kernel smoother can be specified as a probability function (Diggle 2003). This probability estimation can be written as:

$$\hat{p}_h(x) = \frac{\sum_{i=1}^{n} K_h(x - x_i) y_i}{\sum_{i=1}^{n} K_h(x - x_i)}$$

where K_h represents the radially symmetric kernel function described below, and bandwidth h was chosen by cross-validation method, motivated by maximum -likelihood principle (Kelsall and Diggle 1998).

Two-dimensional (2Dt) kernel

Proposed by Portnoy and Wilson (1993), who argued that the tail of the dispersal kernel could be approximated by the following relationship, exposed by Turchin (1998):

$$V(r) = ar^{-\emptyset} \exp\left[-br^{\theta}\right]$$

where r is the dispersal distance from the seed source. This model include many mechanistic and phenomenological dispersal distance curves as negative exponential (ϕ=0, θ=1), the Gaussian (ϕ=0, θ=2), among other. Later, Levin (2003) proposed a general parametric formulation as from Turchin (1998). This model is

$$P(r) = \frac{a}{r^{\beta}} \exp(-br^{\alpha}) = a \exp(-br^{\alpha} - \beta\, ln(r))$$

where a, b, α y β are parameters.

Modifying Gaussian kernel and assuming that it varies with prevailing conditions, for example that alpha value describe the kernel for different conditions and solving for marginal conditioned density. Thus, fat-tailed distributions (2Dt function) is expressed as (Clark et al. 1999):

$$f(r) = p \,/\, \pi u \left[1 + \frac{r^2}{u}\right]^{p+1}$$

Equivalently, Levin (2003) expressed this function as:

$$P(r) = a(1 + br^2)^{-\alpha}$$

where a, b and α are parameters, and r is the dispersal distance. For α=1 the distribution is Cauchy, a dispersal kernel that is strongly leptokurtic (centrally peaked and long-tailed).

REFERENCES

Chesson, P.; Lee, Ch.T., 2005: Families of discrete kernels for modeling dispersal. *Theoretical Population Biology* 67, 241-256.

Clark, J.S.; Silman, M.; Kern, R.; Macklin, E.; HilleRisLambers, J., 1999: Seed Dispersal Near and Far: Patterns Across Temperate and Tropical Forests. *Ecology* 80(5), 1475-1494.

Diggle, P.J., 2003: *Statistical analysis of spatial point patterns*. Second edition. Arnold. London. UK.

Erran Seaman, D.; Powell, R.A., 1996: An Evaluation of the Accuracy of Kernel Density Estimators for Home Range Analysis. Ecological Society of America. *Ecology* 77(7), 2075-2085.

Goreaud, F.; Pélissier, R., 2003: Avoiding misinterpretation of biotic interactions with the intertype K12-function: population independence vs. random labelling hypotheses. *Journal of Vegetation Science* 14, 681-692.

Kot, M.; Lewis, M.A.; van den Driessche, P., 1996: Dispersal data and spread of invading organisms. *Ecology* 77(7), 2027-2042.

Kelsall, J.; Diggle, P., 1998: Spatial Variation in Risk of Disease: A Nonparametric Binary Regression Approach. *Appl. Statist.* 47(4), 559 – 573.

Law, R.; Illian, J.; Burslem, D.F.R.P.; Gratzer, G.; Gunatilleke, C.V.S; Gunatilleke, I.A.U.N., 2009: Ecological information from spatial patterns of plants: insights from point process theory. *Journal of Ecology* 97, 616-628.

Levin, S.A.; Muller-Landau, H.C.; Nathan, R.; Chave, J. 2003: The ecology and evolution of seed dispersal: a theoretical perspective. *Annual Review of Ecology, Evolution, and Systematics* 34, 575-604.

Lloyd, Ch., 2007: *Local Models for Spatial Analysis.* Queen's University Belfast. Edit. CSC Press.

Martínez Beneito, MA., 2005: *Métodos estadísticos en la detección de focos de riesgo en brotes epidémicos*. Disertación. Facultad de Matemáticas - Universidad de Valencia.

Portnoy, S.; Wilson, M.F., 1993: Seed dispersal curves - behavior of the tail of the distribution. *Evolutionary Ecology* 7, 25-44.

Silverman, B.W., 1986: *Density Estimation for Statistics and Data Analysis*. CHAPMAN & HALL/CRC. New York.

Turchin, P. 1998. *Quantitative analysis of movement: measuring and modeling population redistribution in animals and plants*. Sinauer Associates, Sunderland, Massachusetts, USA.

Worton, B.J., 1989: Kernel Methods for Estimating the Utilization Distribution in Home-Range Studies. *Ecology* 70, 164 – 168.

APPENDIX 2. Estimation of the K function for replicated point patterns and between-groups comparison for unifactorial designs.

When spatial data consist of *m* replicated point patterns, and we can assume that each pattern arises from the same underlying process, an estimator of the overall K function is (Diggle et al. 1991; Diggle 2003):

$$\widehat{K}(r) = \sum_{i=1}^{m} n_i \widehat{K}_i(r) \Big/ \sum_{i=1}^{m} n_i$$

where $\widehat{K}_i(r)$ are the individual estimates and n_i the number of points in each of the *m* replicates. To assess the sampling variance of $\widehat{K}(r)$, Diggle et al. (1991) proposed using a method based on the bootstrap (Efron and Tibshirani 1994). For this, they first defined residual K functions as:

$$R_i(r) = n_i^{0.5}\left[\widehat{K}_i(r) - \widehat{K}(r)\right], \;\; i = 1, \dots, m.$$

When the underlying processes are identical, these residual functions $R_i(r)$ are exchangeable even if the processes differ in their intensity. So, one could build a bootstrap sample of K functions as:

$$K_i^*(r) = \widehat{K}(r) + n_i^{-0.5} R_i^*(r), \;\; i = 1, \dots, m,$$

where the $R_i^*(.)$ are randomly extracted, with replacement, from the set $\{R_1(.), \dots, R_m(.)\}$. Finally, the resampled $\widehat{K}(r)$ is computed as:

$$\widehat{K}^*(r) = \sum_{i=1}^{m} n_i \widehat{K}_i^*(r) \Big/ \sum_{i=1}^{m} n_i.$$

Repeating this procedure many times, the sampling variance of all the $\widehat{K}^*(r)$ can be considered a bootstrap approximation to the sampling variance of $\widehat{K}(r)$.

When there are two or more groups of replicates, it is possible to test the hypothesis that the three groups are generated by the same underlying processes, with a non-parametric method analogous to analysis of variance (Diggle et al. 1991, Diggle 2003). For this, if n_{ij} is the number of points in the *jth* plot within the *ith* group, and $\widehat{K}_{ij}(r)$ is its estimated K-function, compute the overall K function for each group i $\widehat{K}_i(r)$. Then,

compute $\widehat{K}_0(r)$, a weighted average of all $\widehat{K}_i(r)$ functions, with weights proportional to the total number of points in each group (i.e., $n_i = \sum_{j=1}^{m_i} n_{ij}$).

If $K_i(r)$ denotes the expectation of $\widehat{K}_{ij}(r)$ under repeated sampling, the null hypothesis for the test is that $K_i(r) = K(r)$, i.e., that $K_i(r)$ is the same for all the groups.

Finally, compute this statistic:

$$BTSS = \sum_{i=1}^{g} n_i \int_0^{r_0} w(r)\{\widehat{K}_i(r) - \widehat{K}_0(r)\}^2 dr$$

where g is the total number of groups, r_0 is the larger scale (i.e., the maximum r) for which we are interested in spatial differences, and $w(r)$ is a function to normalize large scale variation in the differences between K functions.

BTSS is analogous to a between-treatment sum of squares in the analysis of variance (Diggle et al. 1991; Diggle 2003). Its null sampling distribution must be estimated with bootstrap resampling. For this, residual K-functions for each plot j within each group i are defined as:

$$R_{ij}(r) = n_{ij}^{0.5}\left\{\widehat{K}_{ij}(r) - \widehat{K}_i(r)\right\}$$

These residuals are exchangeable under the null or alternative hypothesis (Diggle et al. 1991; Diggle 2003) so, if $R_{ij}^*(r): j = 1, \ldots, m_i : i = 1, \ldots, g$ are obtained from the original Rij(r) by sampling with replacement, a set of resampled K-functions under the null hypothesis can be built as:

$$\widehat{K}_{ij}^*(r) = \widehat{K}_0(r) + n_{ij}^{-0.5} R_{ij}^*(r)$$

Each resample is a complete set of K-functions (e.g., $g \cdot m$ K-functions if all the groups have m replicates), and is used to compute a resampled BTSS value.

The test consists in comparing the observed BTSS value with the distribution of s resampled BTSS values.

REFERENCES

Diggle, P .J. et al. 1991. Analysis of Variance for Replicated Spatial Point Patterns in Clinical Neuroanatomy. - J. Am. Stat. Assoc. 86(415): 618-625.

Diggle, P.J. 2003. Statistical analysis of spatial point patterns. Second edition. – Arnold, London.

Efron, B. and Tibshirani, R.J. 1994. An Introduction to the Bootstrap. - Chapman & Hall/CRC. New York.

APÉNDICE 3: Detalles matemáticos de los modelos ajustados

Proceso homogéneo de Poisson (HPP)

Considerado como la base de los procesos espaciales de puntos (Diggle 2003), es el más sencillo de los procesos estocásticos y empleado como modelo teórico para probar la aleatoriedad espacial completa. El HPP es caracterizado por dos propiedades fundamentales: Distribución de Poisson de un conjunto discreto de puntos, y dispersión independiente (Illian et al. 2008). Su parámetro λ denota la intensidad del patrón y describe el número medio de los puntos localizados en una unidad de superficie, es decir, la densidad media de árboles por unidad de área para cada especie (Plotkin et al. 2000, Shen et al. 2009). λK(r) es el número esperado de puntos en un círculo de radio r alrededor de un punto arbitrario. La función K para un patrón de puntos homogéneo es estimada como:

$$\widehat{K}(r) = \frac{1}{A}\sum_{i=1}^{n}\sum_{j\neq i}\frac{w_{ij}}{\lambda^2} I(d_{ij} < r)$$

donde A y n son el área y el número de puntos en la parcela respectivamente, w_{ij} es un factor de corrección de borde, y la función indicador I. El HPP tiene una intensidad constante a lo largo del área de estudio y la distribución de los puntos es independiente, por lo que el valor esperado es $K(r) = \pi r^2$ (Illian et al. 2008).

Proceso heterogéneo de Poisson (IPP)

Es una clase de proceso de puntos no estacionario que comparte la independencia de los puntos, en relación a un HPP y la intensidad constante (λ) es reemplazada por una función de intensidad λ(x) con valores que varían respecto a la ubicación x (Diggle 2003), y en estudios ecológicos se asume que depende de la heterogeneidad ambiental (Wiegand et al. 2007, Getzin et al. 2008, Wiegand y Moloney 2014). Esta función de intensidad λ(x) sirve para describir la correlación entre la densidad de árboles y los factores de hábitat como la topografía del terreno, propiedades físicas del suelo entre otros (Shen et al. 2009). Para caracterizar los IPPs, utilizamos la función K heterogénea que es una generalización de la función K de Ripley, donde se asume estacionariedad ponderada de segundo orden (Baddeley et al. 2000). Un estimador insesgado de la función K heterogénea está dado por:

$$\widehat{K}_I(t) = \frac{1}{A}\sum_i \sum_j \frac{w_{ij}}{\lambda(x_i)\lambda(x_j)} I(d_{ij} \le r)$$

donde x={x_1,…,x_n}⊂A, w es el factor de corrección de borde (Ripley 1977, Baddeley 1999).

El valor esperado de la función K heterogénea para un IPP es $\widehat{K_I}(r) = \pi r^2$. La función de intensidad λ(x) puede ser estimada en diferentes formas. Aquí utilizamos el método basado en "kernel smoothing" (Baddeley 2010), que estima la intensidad en la ubicación u como $\hat{\lambda}(u) = e(u)\sum_{i=1}^{n} \kappa(u - x_i)$, donde k(u) es una función kernel arbitraria y e(u) es término de corrección de borde. Utilizamos kernel Gaussiano bidimensional como función de suavizamiento.
El IPP supone la formación del patrón en dos etapas, primero se genera un patrón de Poisson homogéneo, luego los puntos del patrón son retenidos con una probabilidad proporcional a la superficie λ(x), la cual describe la heterogeneidad ambiental. En ausencia de valores de variables ambientales, esa superficie es estimada con una función kernel. Este proceso puede ser utilizado para examinar los efectos de interacción entre la densidad de árboles y los factores ambientales (Shen et al. 2009).

Proceso de Poisson cluster homogéneo (HPCP)

Un caso especial del proceso Poisson cluster fue introducido por Neyman (1939) en aplicaciones a la entomología y bacteriología, como una generalización del modelo de Poisson de Student (1907). Luego el modelo fue aplicado a problemas de cosmología por Neyman y Scott (1958). El HPCP genera puntos no-independientes (agrupados) en un proceso de dos pasos. Primero, se genera un HPP de puntos "padres" con intensidad ρ. Luego cada "padre" produce un número aleatorio de "descendientes" que se distribuyen de acuerdo a una ley de Poisson, con media μ=λ/ρ, donde λ representa la intensidad de los descendientes; y sus ubicaciones son independientes, isotrópica y normalmente distribuidos alrededor de cada árbol padre, con media cero y desviación estándar σ (Stoyan y Stoyan 1994). La función K esperada para un HPCP se estima por:

$$\widehat{K}(r) = \pi r^2 + \frac{1 - e^{(-r^2/4\sigma^2)}}{\rho}$$

Los parámetros ρ y σ son usualmente ajustados comparando la función K empírica con la función K teórica, mediante el método de mínimo contraste (Stoyan y Stoyan 1994,

Diggle 2003). De esta forma, la agregación del patrón es cuantificada por ρ (número medio de grupos), y el tamaño medio de los grupos está dado por σ.

El HPCP considera la distribución de descendientes como una función de dispersión limitada y asume homogeneidad, sin embargo las características que conlleva esta condición podrían no cumplirse por muchas especies debido a la heterogeneidad ambiental y asociación de hábitat (Gunatilleke et al. 2006, Wiegand et al. 2007b, Morlon et al. 2008).

Proceso de Poisson cluster heterogéneo (IPCP)

Como una alternativa al IPP, es considerado también una extensión del HPCP, donde la distribución de los puntos además de ser agrupada es heterogénea. Waagepetersen (2007) considera un proceso cluster $X=X_{c\in Y}$ donde X_c son los cluster de los "descendientes" asociados a los puntos "padres" c en un proceso de Poisson estacionario Y con intensidad $\rho > 0$. La función de intensidad de X tiene forma log-lineal, y el valor esperado para la función K heterogénea tiene la misma forma que para el HPCP.

Este proceso es adecuado para evaluar el efecto conjunto de heterogeneidad de hábitat y dispersión limitada (Diggle 2003, Illian et al. 2008), de forma similar al HPCP, excepto por el número de descendientes por padre, el cual ya no es una constante, sino que debe ser estimado a través de una función de intensidad espacialmente heterogénea (Waagepetersen 2007, Yi-Ching Lin et al. 2011).

Proceso de Modelamiento

Descripción del patrón espacial.

Para describir el patrón espacial de cada especie empleamos la función K de Ripley (Ripley 1977, Illian et al. 2008). Para un patrón homogéneo de intensidad λ, $\lambda K(r)$ es el número de puntos esperado dentro de un círculo de radio r alrededor de un punto cualquiera del patrón. En el caso de patrones heterogéneos, empleamos la función K-heterogénea (Baddeley et al. 2000). De manera resumida se puede definir la función $K_I(r)$ como el valor esperado, para un punto arbitrario u, de la suma de todos los términos $1/\lambda(x_j)$ correspondientes a todos los puntos x_j separados de u por una distancia $\leq r$, siendo $\lambda(x_j)$ el valor de la intensidad en el punto x_j. Para λ=constante, $K_I(r) = K(r)$

(Baddeley y Turner 2005). Tanto para el IPP como para el IPCP, la función de intensidad fue estimada utilizando la función density.ppp() del paquete spatstat. Esta función implementa un suavizado del kernel de un patrón de puntos, basado en un kernel Gaussiano. En estudios ecológicos, elegir el ancho de banda del kernel para estimar la superficie de intensidad, se basa en criterios biológicos, es decir, elegir un ancho de banda mayor a la escala a la cual los efectos de segundo orden ocurren (Wiegand et al. 2007, Getzin et al. 2008).

Selección del modelo de mejor ajuste

Para evaluar la idoneidad de los diferentes modelos ajustados estimamos para cada especie un conjunto de 56 superficies de intensidad diferentes con ancho de banda Epanechnikov variando desde 30 hasta 250m, para los procesos de Poisson y Poisson cluster heterogéneos. Con cada superficie se calculó la función K heterogénea y para cada una la suma de cuadrados de las diferencias entre la función teórica y esperada en cada caso. De entre todas las funciones heterogéneas se ha elegido aquella con menor suma de cuadrados. Finalmente, comparamos las sumas de cuadrados de todos los procesos heterogéneos frente a los procesos homogéneos, y empleamos el AIC basado en la suma de los residuales y el número de parámetros en cada modelo (Webster y McBratney 1989, Shen et al. 2009, Wang et al. 2011), para selecciona el modelo que mejor se ajustó al patrón espacial de cada especie.

REFERENCIAS

Baddeley, A.J. 1999. Spatial sampling and censoring. In:Barndorff-Nielsen, O.E., Kendall, W.S., and van Lieshout, M.N.M. (eds.) *Stochastic geometry: Likelihood and Computation*. Chapman and Hall/CRC, London pp. 37-78.

Baddeley, A.J., MØller, J. y Waagepetersen, R. 2000. Non- and semi –parametric estimation of interaction in inhomogeneous point patterns. Statistica Neerlandica 54(3): 329-350.

Baddeley, A.; Turner, R., 2005: Spatstat: an R package for analyzing spatial point patterns. *Journal of Statistical Software* 12(6), 1-42.

Baddeley, A.J. 2010. Analysing spatial point patterns in R. CSIRO and University of Western Australia, Workshop notes, version 4.1.

Diggle, P. J. 2003. *Statistical analysis of spatial point patterns*. Second edition. - Arnold, London.

Getzin, S.; Wiegand, T.; Wiegand, K.; Fangliang, He. 2008: Heterogeneity influences spatial patterns and demographics in forest stands. *Journal of Ecology* 96, 807-820.

Gunatilleke, C. V. S., Gunatilleke, I. A. U. N., Esufali, S., Harms, K. E., Ashton, P. M. S., Burslem, D. F. R. P. y Ashton, P. S. 2006. Species-habitat associations in a Sri Lankan dipterocarp forest. *Journal of Tropical Ecology* 22: 371-384.

Illian, J., Penttinen, A., Stoyan, H. y Stoyan, D. 2008. *Statistical Analysis and Modeling of Spatial Point Patterns*. John Wiley & Sons Ltd. England.

Morlon, H., Chuyong, G., Condit, R., Hubbell, S. Kenfack, D., Thomas, D., Valencia, R. y Green, J. L. 2008. A general framework for the distance-decay of similarity in ecological communities. Eco*logy Letters* 11: 904-917.

Neyman, J. 1939. On the new class of "contagious" distributions, applicable in entomology and bacteriology. *The Annals of Mathematical Statistics* 10(1): 35-57.

Neyman, J. y Scott, E.L. 1958. Statistical approach to problems of cosmology. *Journal of the Royal Statistical Society. Series B.* 20(1): 1-43.

Plotkin, J.B., Potts, M.D., Leslie, N., Manokaran, N., LaFrankie, J. y Ashton, P. 2000. Species-area curves, spatial aggregation, and habitat specialization in tropical forest. *Journal of Theoretical Biology* 2007: 81-99.

Ripley, B.D. 1977. Modeling spatial patterns. *Journal of the Royal Statistical Society. Series B (Methodological)* 39(2): 172-212.

Shen, G., Yu, M., Hu, X-S., Mi, X., Ren, H., Sun, I-F., y Ma, K. 2009. Species-area relationship explained by the joint effects of dispersal limitation and hábitat heterogeneity. *Ecology* 90(11): 3033-3041.

Stoyan, D. y Stoyan, H. 1994. Fractals, Random Shapes and Point Fields. Wiley, Chichester.

Waagepetersen, R. P. 2007. An Estimating Function Approach to Inference for Inhomogeneous Neyman–Scott Processes. *Biometrics* 63: 252–258.

Wang, X., Wiegand, T., Wolf, A., Howe, R., Davies, S. J. y Hao, Z. 2011. Spatial patterns of tree species richness in two temperate forests. *Journal of Ecology* 99: 1382-1393.

Webster, R. y Mcbratney, A.B. 1989. On the Akaike information criterion for choosing models for variograms of soil properties. *Journal of Soil Science* 40: 493–496.

Wiegand, T., Gunatilleke, S. y Gunatilleke, N. 2007. Species associations in a heterogeneous Sri Lankan Dipterocarp forest. *The American Naturalist* 170: E77–E95.

Wiegand, T, y Moloney, K.A. 2014. *Handbook of Spatial Point-Pattern Analysis in Ecology*. Chapman & Hall/CRC. Iowa, USA.

Yi-Ching, L., Chang, L-W., Yang, K-Ch., Wang, H-H. y Sun, I-F. Point patterns of tree distribution determined by habitat heterogeneity and dispersal limitation. *Oecologia* 165: 175-184.

Apéndice 4. Análisis bivariado de los patrones espaciales de *C. wagneri* en cuatro niveles de altitud (1400, 1550, 1700 y 1900m), y dos niveles topográficos (plane, slope). La línea continua representa la función L(r), la línea discontinua es el modelo de proceso de Poisson, y la región gris conformada por las envolturas de 99 simulaciones Monte Carlo del modelo nulo.

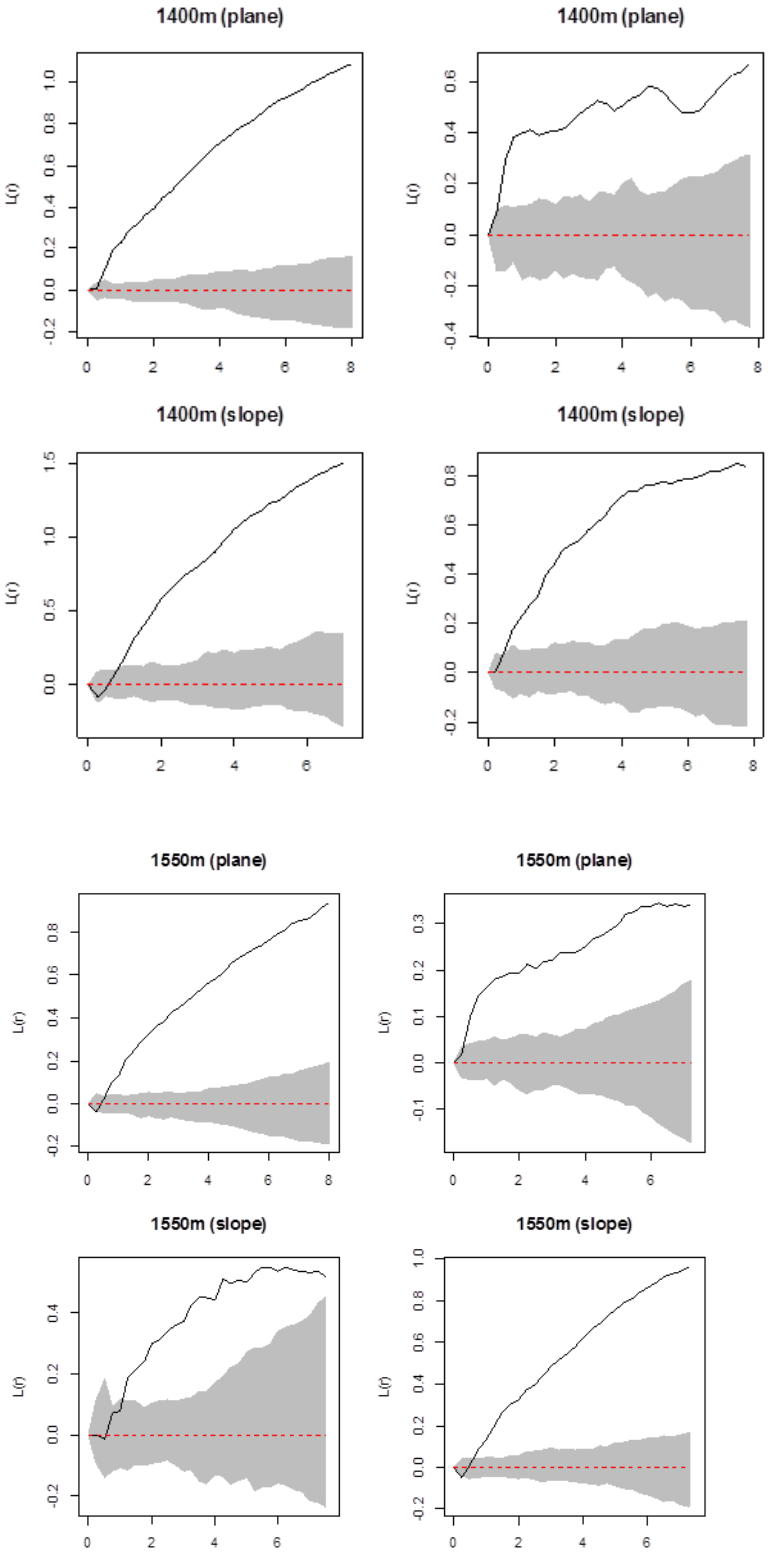

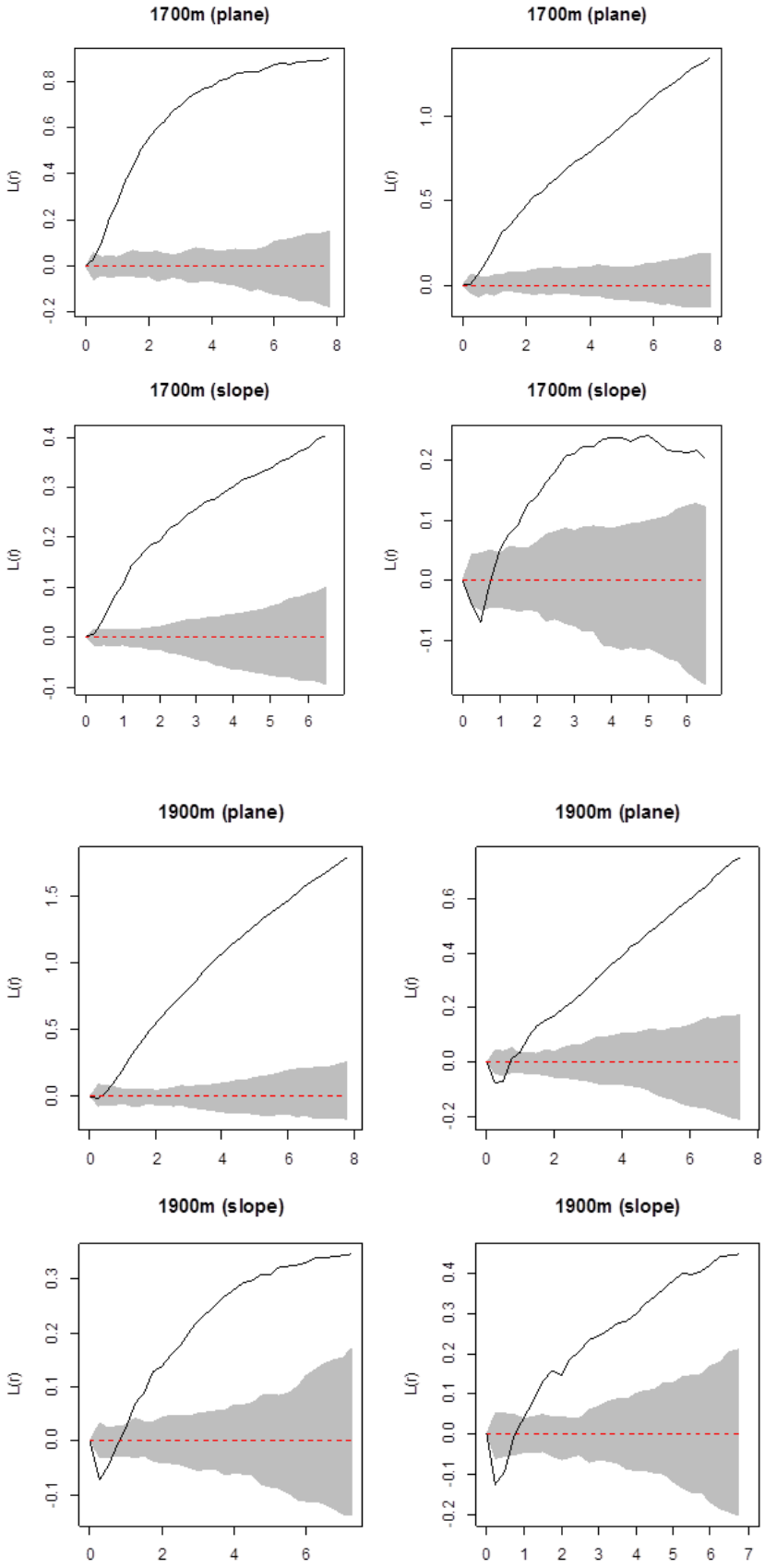
1700m (plane)
1700m (plane)
1700m (slope)
1700m (slope)
1900m (plane)
1900m (plane)
1900m (slope)
1900m (slope)
L(r)

Apéndice 5. (Table S1.4 - Cap. 2)

Properties of the nominal p values from 1000 replicate simulations of the bootstrap procedure under the null hypotheses of no interaction and no effect of individual factors. Numbers indicate proportion of simulations where p-values smaller than the nominal values were reported.

	Nominal p value		
Factor	<=0.10	<=0.05	<=0.01
Altitude	0.199	0.103	0.042
Slope	0.203	0.113	0.031
Altitude:Slope	0.179	0.094	0.015

Apéndice 5. (Table S2.4 - Cap. 2)

Empirical power estimates for the interaction term Altitude:Slope when plots of low altitude with steep slope topography and high altitude with flat slope are assigned a Poisson cluster process with ρ= 0.39, and the other groups (plots in low altitude with flat slope and high altitude with steep slope) are assigned another Poisson cluster process with ρ= 0.39 - Δρ.

	Significance Level (p-value)		
Δρ	> 0.10	> 0.05	> 0.01
0.04	0.16	0.05	0.00
0.08	0.25	0.11	0.03
0.12	0.21	0.14	0.03
0.16	0.17	0.07	0.01
0.19	0.23	0.08	0.01
0.23	0.19	0.14	0.06
0.27	0.18	0.03	0.00
0.31	0.41	0.26	0.08
0.35	0.74	0.47	0.18
0.38	1.00	1.00	0.78

Apéndice 5. (Figure S1 - Cap. 2)

Figure S1. Differences of short scale spatial inhibition between plots. Red boxes: plots in flat slopes; white boxes: plots in steep slopes. Here, "spatial inhibition" is measured for each plot as the absolute of the sum of negative values of the L(r) function [$L(r) = \sqrt{K(r)/\pi} - r$]; for all plots K(r) was computed for r=0 to r=8 with 0.05 m intervals. The expected value of the empirical L-function respect to complete random process is L(r)=0,whereas negative values indicate inhibition. The "range of spatial inhibitions" indicates the range of r distances for which L(r)<0.

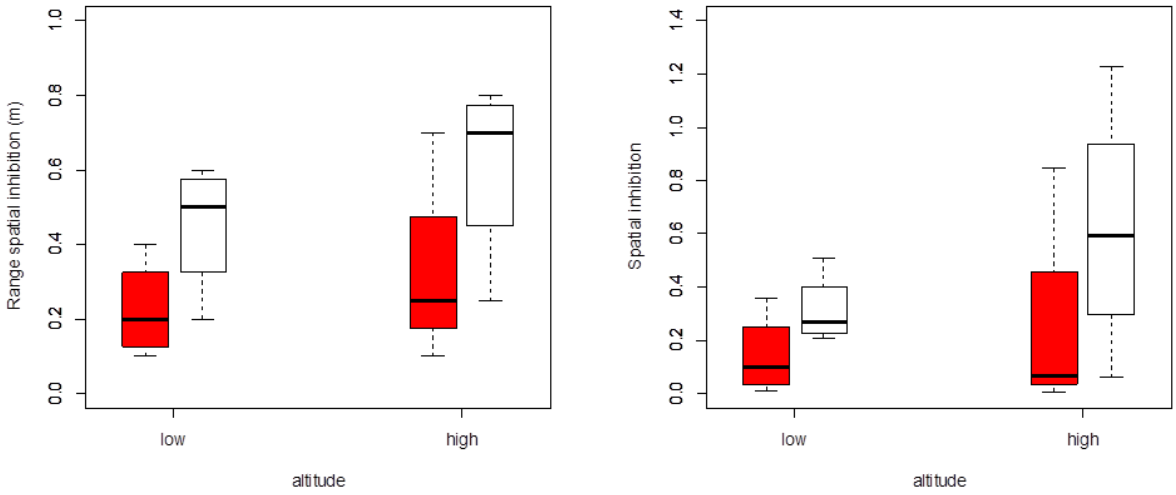

Apéndice 6. (Table S1-Cap 4)

Goodness-of–fit tests. Proportion of species with significant ($p < 0.01$ and $0.01 \leq p < 0.05$) and no significant ($p \geq 0.05$) deviations from the expected IFDAR functions for the heterogeneous null models.

Significance	Spatial range for GoF test		
	1 - 50m	1 – 10m	11 – 50m
$p < 0.01$	0.48	0.14	0.67
$0.01 \leq p < 0.05$	0.22	0.03	0.19
$p \geq 0.05$	0.30	0.83	0.14

This test assessed the overall fit of the empirical IFDAR curves to the heterogeneous model over the range of spatial scales when significant point-wise departures were observed in the simulation envelopes. This test computes the sum of squared deviations from the theoretical IFDAR for each of the observed and simulated IFDAR curves. If the statistic for the observed IFDAR was larger than the fifth largest value of the statistics computed for each simulated IFDAR, the observed IFDAR was considered significantly different from the expected IFDAR with an α level of 0.05.

Apéndice 7. (Table S2-Cap. 4). Functional and spatial characteristics of the studied species

Species	Accumulator	Repeller	Normal	N	Character	$M_{tt}(10)$	$M_{tt}(20)$	$M_{t0}(10)$	$M_{t0}(20)$	Δ_{tt} (10)	Δ_{tt} (20)	D(10)	D(20)
Apeiba membranacea	46	0	4	237	accumulator	0.15	0.63	12.88	52.51	0.00	0.04	0.01	0.01
Astrocaryum standleyanum	31	0	19	217	accumulator	0.32	1.29	12.45	50.00	0.19	0.74	0.03	0.03
Beilschmiedia pendula	46	0	4	296	accumulator	0.57	2.45	12.70	51.85	0.39	1.71	0.04	0.05
Brosimum alicastrum	40	0	10	185	accumulator	0.08	0.45	12.32	51.84	-0.04	-0.01	0.01	0.01
Casearia arborea	29	0	21	119	accumulator	0.18	0.57	13.95	56.12	0.11	0.27	0.01	0.01
Cecropia insignis	38	0	12	257	accumulator	1.28	2.75	15.22	56.15	1.11	2.10	0.08	0.05
Chrysophyllum argenteum	25	0	25	86	accumulator	0.02	0.09	13.24	51.22	-0.03	-0.12	0.00	0.00
Cordia bicolor	40	0	10	285	accumulator	0.60	1.80	13.60	53.69	0.42	1.08	0.04	0.03
Cordia lasiocalyx	42	0	8	444	accumulator	0.47	1.43	13.07	52.01	0.19	0.32	0.03	0.03
Eugenia coloradoensis	32	0	18	83	accumulator	0.07	0.34	12.55	51.99	0.02	0.13	0.01	0.01
Eugenia oerstediana	34	0	16	159	accumulator	0.28	0.88	13.12	54.43	0.18	0.48	0.02	0.02
Faramea occidentalis	48	0	2	1649	accumulator	1.61	5.54	13.21	52.32	0.57	1.40	0.11	0.10
Garcinia intermedia	33	0	17	82	accumulator	0.07	0.20	12.48	51.10	0.02	-0.01	0.01	0.00
Guapira standleyana	33	0	17	101	accumulator	0.00	0.28	13.11	52.27	-0.06	0.02	0.00	0.01
Guarea guidonia	40	0	10	376	accumulator	0.39	1.53	12.51	51.71	0.16	0.58	0.03	0.03
Guatteria dumetorum	42	0	8	278	accumulator	0.25	1.01	13.13	52.25	0.08	0.31	0.02	0.02
Guettarda foliacea	30	0	20	80	accumulator	0.03	0.33	13.26	53.44	-0.03	0.12	0.00	0.01
Hasseltia floribunda	39	0	11	248	accumulator	0.34	0.93	12.94	52.01	0.18	0.30	0.03	0.02
Heisteria concinna	43	0	7	274	accumulator	0.32	1.10	12.10	50.00	0.15	0.41	0.03	0.02
Hirtella triandra	44	2	4	618	accumulator	0.80	2.89	12.06	50.30	0.41	1.33	0.06	0.05
Hura crepitans	31	0	19	101	accumulator	0.10	0.53	12.16	49.77	0.04	0.28	0.01	0.01
Inga marginata	33	0	17	88	accumulator	0.48	1.20	13.47	53.97	0.42	0.98	0.03	0.02

Inga nobilis	34	1	15	53	accumulator	0.08	0.23	12.08	51.47	0.04	0.09	0.01	0.00
Jacaranda copaia	44	0	6	241	accumulator	0.76	1.89	14.17	53.99	0.60	1.29	0.05	0.03
Lindackeria laurina	36	0	14	69	accumulator	0.17	0.35	12.75	49.32	0.13	0.17	0.01	0.01
Lonchocarpus heptaphyllus	43	0	7	125	accumulator	0.10	0.45	13.24	51.24	0.02	0.13	0.01	0.01
Luehea seemannii	34	0	16	93	accumulator	0.04	0.41	12.48	51.72	-0.02	0.17	0.00	0.01
Maquira guianensis	45	0	5	177	accumulator	0.18	0.52	12.99	52.85	0.07	0.07	0.01	0.01
Miconia argentea	34	0	16	57	accumulator	0.39	0.81	13.74	52.68	0.35	0.66	0.03	0.02
Ocotea whitei	35	2	13	172	accumulator	0.81	2.07	12.76	50.98	0.71	1.64	0.06	0.04
Oenocarpus mapora	46	1	3	752	accumulator	0.81	2.60	12.61	51.14	0.34	0.71	0.06	0.05
Platymiscium pinnatum	29	0	21	61	accumulator	0.03	0.20	13.15	50.98	-0.01	0.04	0.00	0.00
Poulsenia armata	46	0	4	801	accumulator	1.65	5.78	12.99	51.82	1.15	3.76	0.11	0.10
Pouteria reticulata	38	0	12	191	accumulator	0.13	0.54	12.65	51.51	0.01	0.06	0.01	0.01
Prioria copaifera	45	1	4	335	accumulator	0.46	1.96	12.42	50.43	0.25	1.12	0.04	0.04
Socratea exorrhiza	48	0	2	336	accumulator	1.51	4.33	13.77	53.53	1.29	3.48	0.10	0.07
Virola surinamensis	11	0	39	162	accumulator	0.20	0.74	12.53	51.10	0.10	0.33	0.02	0.01
Alchornea costaricensis	0	0	50	158	normal	0.87	2.08	13.19	53.45	0.77	1.68	0.06	0.04
Cassipourea elliptica	0	1	49	77	normal	0.05	0.47	12.13	50.61	0.00	0.27	0.00	0.01
Croton billbergianus	0	0	50	75	normal	0.77	1.44	12.59	49.88	0.73	1.25	0.06	0.03
Dendropanax arboreus	0	0	50	93	normal	0.13	0.47	12.54	51.98	0.07	0.24	0.01	0.01
Drypetes standleyi	4	1	45	263	normal	0.61	2.14	11.99	49.35	0.44	1.48	0.05	0.04
Inga sapindoides	0	0	50	77	normal	0.03	0.21	13.27	53.51	-0.02	0.01	0.00	0.00
Randia armata	3	0	47	241	normal	0.44	1.39	12.87	52.92	0.29	0.79	0.03	0.03
Simarouba amara	3	0	47	269	normal	0.58	1.61	13.46	52.93	0.41	0.94	0.04	0.03
Sloanea terniflora	0	0	50	81	normal	0.12	0.30	12.56	49.72	0.07	0.09	0.01	0.01
Unonopsis pittieri	0	1	49	160	normal	0.21	0.70	13.24	53.19	0.11	0.30	0.02	0.01
Xylopia macrantha	8	0	42	128	normal	0.61	2.11	12.02	47.97	0.53	1.79	0.05	0.04
Zanthoxylum ekmanii	0	5	45	140	normal	0.79	1.57	13.61	53.10	0.70	1.22	0.05	0.03

Adelia triloba	0	38	12	106	repeller	0.75	2.34	13.29	55.59	0.69	2.07	0.05	0.04
Alseis blackiana	3	42	5	936	repeller	1.06	4.28	13.69	55.72	0.47	1.92	0.07	0.07
Gustavia superba	0	44	6	649	repeller	4.64	17.26	16.12	63.79	4.24	15.63	0.22	0.21
Protium costaricense	0	24	26	106	repeller	0.11	0.38	12.86	51.16	0.05	0.11	0.01	0.01
Protium tenuifolium	0	42	8	358	repeller	0.32	1.20	12.14	50.00	0.09	0.30	0.03	0.02
Pterocarpus rohrii	0	17	33	83	repeller	0.02	0.34	13.19	53.29	-0.03	0.13	0.00	0.01
Quararibea asterolepis	1	43	6	699	repeller	0.69	2.49	12.55	50.99	0.25	0.74	0.05	0.05
Swartzia simplex	0	33	17	336	repeller	0.35	1.35	12.57	51.46	0.14	0.51	0.03	0.03
Tabernaemontana arborea	0	41	9	304	repeller	0.36	1.28	12.44	51.20	0.17	0.51	0.03	0.02
Tachigali versicolor	0	38	12	88	repeller	0.02	0.25	12.86	51.07	-0.03	0.03	0.00	0.00
Tetragastris panamensis	0	41	9	362	repeller	0.45	1.44	12.14	49.37	0.22	0.53	0.04	0.03
Trichilia pallida	0	40	10	79	repeller	0.18	0.66	12.72	51.53	0.13	0.46	0.01	0.01
Trichilia tuberculata	0	47	3	1783	repeller	2.07	6.90	12.84	51.77	0.95	2.42	0.14	0.12
Triplaris cumingiana	1	34	15	145	repeller	0.44	1.63	13.50	53.54	0.35	1.26	0.03	0.03
Virola sebifera	0	39	11	605	repeller	0.50	1.85	13.08	52.75	0.12	0.33	0.04	0.03

Accumulator: number of *r* spatial scales (radii *r*) where each species' *IFDAR(r)* was significantly higher than expected for the heterogeneous Poisson null model. **Normal**: number of *r* scales where *IFDAR(r)* wasn't significantly different from the expected value. **Repeller:** number of *r* scales where *IFDAR(r)* was significantly smaller than expected. **N:** species abundance. **Character:** "global" IFDAR behavior of each species. Accumulator or repeller behavior was assigned to species having more than 10 IFDAR(r) values higher or lower than expected, respectively.

$M_{to}(r)$*:** average number of stems of all other species within circles with radius *r* around the stems of the target species. ***$M_{tt}(r)$*:** average number of stems of each target species within circles with radius *r* around the stems of the target species (not counting the focal stem). ***$\Delta_{tt}(r)$: clustering tendency at scale *r*. It is computed as $\Delta_{tt}(r) = M_{tt}(r) - \lambda_t a(r)$, where λ_t is the intensity of the target species. Positive and negative values indicate respectively a tendency to aggregate and regular patterns. ***D(r)*:** local dominance of the focal species, computed as $D(r) = M_{tt}(r)/[M_{tt}(r) + M_{to}(r)]$. Larger values indicate a dominance of target's over other species' stems at scale *r*. Average number of stems, clustering tendency and local dominance are shown for r= 10 and 20 m.

Apéndice 8. (Figure S3-Cap. 4)

Relationships between Individual Functional Diversity-Area Relationships [*IFDAR(r)*] and Individual Species-Area Relationships [*ISAR(r)*] values for *r* = 10 m. Letters indicate species' character for IFDAR at this scale: accumulator (A), repeller (R) or normal (N). Note that at this scale some repeller species have larger ISAR values (i.e., inhabit local assemblages with larger taxonomic diversity) than some normal or accumulator species.